HYPERTHERMOPHILIC HYDROGEN PRODUCTION BY *GEOGLOBUS ACETIVORANS* IN MICROBIAL ELECTROLYSIS CELLS

A THESIS SUBMITTED TO
THE GRADUATE SCHOOL OF NATURAL AND APPLIED SCIENCES
OF
MIDDLE EAST TECHNICAL UNIVERSITY

BY

AYKUT KAŞ

IN PARTIAL FULFILLMENT OF THE REQUIREMENTS
FOR
THE DEGREE OF MASTER OF SCIENCE
IN
ENVIRONMENTAL ENGINEERING

SEPTEMBER 2021

Approval of the thesis:

HYPERTHERMOPHILIC HYDROGEN PRODUCTION BY *GEOGLOBUS ACETIVORANS* IN MICROBIAL ELECTROLYSIS CELLS

submitted by **AYKUT KAŞ** in partial fulfillment of the requirements for the degree of **Master of Science** in **Environmental Engineering, Middle East Technical University** by,

Prof. Dr. Halil Kalıpçılar
Dean, Graduate School of **Natural and Applied Sciences** _____

Prof. Dr. Bülent İçgen
Head of the Department, **Environmental Engineering** _____

Assist. Prof. Dr. Yasemin Dilşad Yılmazel Tokel
Supervisor, **Environmental Engineering, METU** _____

Examining Committee Members:

Prof. Dr. Filiz Bengü Dilek
Environmental Engineering, METU _____

Assist. Prof. Dr. Yasemin Dilşad Yılmazel Tokel
Environmental Engineering, METU _____

Prof. Dr. Bülent İçgen
Environmental Engineering, METU _____

Prof. Dr. İpek İmamoğlu
Environmental Engineering, METU _____

Assist. Prof. Dr. Bilgin Taşkın
Agricultural Biotechnology, Van Yüzüncü Yıl Uni. _____

Date: 10.09.2021

I hereby declare that all information in this document has been obtained and presented in accordance with academic rules and ethical conduct. I also declare that, as required by these rules and conduct, I have fully cited and referenced all material and results that are not original to this work.

Name Last name : Aykut Kaş

Signature :

ABSTRACT

HYPERTHERMOPHILIC HYDROGEN PRODUCTION BY *GEOGLOBUS ACETIVORANS* IN MICROBIAL ELECTROLYSIS CELLS

Kaş, Aykut
Master of Science, Environmental Engineering
Supervisor: Assist. Prof. Dr. Yasemin Dilşad Yılmazel Tokel

September 2021, 147 pages

Utilization of hyperthermophilic microorganisms was suggested to improve reaction rates and insoluble pollutant degradation and minimize the risk of contamination in bioelectrochemical systems (BESs). So far only a small group of hyperthermophilic microorganisms were identified, which show the ability to donate electrons to solid electrodes in BESs and here we present a new culture that fits to this description. The iron reducing archaeal culture *Geoglobus acetivorans*, originally isolated from a hydrothermal structure, produced 1.53 ± 0.24 A/m^2 peak current density in microbial electrolysis cells (MECs) operated at 80 °C. This current density value is 2.5 – 3 times higher than the previously reported electro-active behavior of closely related archaeal species of *Ferroglobus placidus* and *Geoglobus ahangari* with the exact reactor configuration. Maximum hydrogen production rate (Q_{H_2}) was found as 0.57 ± 0.06 m^3 H_2/m^3*d in the 5 mL Mini-MEC reactors fed with 10mM acetate. There was a visible biofilm formation on the anode and minimum 6 cycles of biohydrogen generation coupled with high current generation was observed. Upon longer operation of reactors, biofilm started to detach from the electrode surface and both hydrogen and current production were decreased. Cyclic voltammetry (CV) analysis produced a sigmoidal catalytic wave with a mid-point potential of −0.40 V (vs.

Ag/AgCl). Direct electron transfer (DET) capability by *G. acetivorans* was shown with peak separation analysis, rapid current density recovery after media replacement and thick biofilm formation on the anode electrode. *G. acetivorans* was able to utilize complex organic waste in hyperthermophilic MECs, after initial biofilm formation with acetate.

Keywords: Microbial electrolysis cell, electrohydrogenesis, hyperthermophiles, iron-reducer archaea, biohydrogen production, *Geoglobus acetivorans*

ÖZ

GEOGLOBUS ACETIVORANS İLE MİKROBİYAL ELEKTROLİZ HÜCRELERİNDE HİPERTERMOFİLİK HİDROJEN ÜRETİMİ

Kaş, Aykut
Yüksek Lisans, Çevre Mühendisliği
Tez Yöneticisi: Dr. Öğr. Üyesi Yasemin Dilşad Yılmazel Tokel

Eylül 2021, 147 sayfa

Biyoelektrokimyasal sistemlerde (BESler) reaksiyon hızlarını arttırmak, zor çözünen kirleticiler arıtılmasını iyileştirmek ve kontaminasyon riskini en aza indirmek için hipertermofilik mikroorganizmaların kullanılması önerilmektedir. Şimdiye kadar, katı elektrotlara elektron verme yeteneğine sahip küçük bir grup hipertermofilik mikroorganizma tespit edilmiştir ve bu çalışmada bu gruba giren yeni bir kültür sunmaktayız. Demir indirgeyici arke kültürü *Geoglobus acetivorans*, daha önce hidrotermal bir yapıdan izole edilmiş olup, 80 °C'de çalıştırılan Mikrobiyal Elektroliz Hücrelerinde (MEH) 1,53 ± 0,24 A/m^2 pik akım yoğunluğu üretmiştir. Bu akım yoğunluğu değeri, *Geoglobus acetivorans* ile yakından ilişkili olan *Ferroglobus placidus* ve *Geoglobus ahangari* arke kültürleri ile, tamamen aynı reaktör konfigürasyonuna sahip reaktörlerde elde edilen sonuçtan 2,5 - 3 kat daha yüksektir. 10mM asetat ile beslenen 5 mL Mini-MEH reaktörlerinde maksimum hidrojen üretim hızı (Q_{H_2}) 0,57 ± 0,06 m^3 H_2/m^3*gün olarak tespit edilmiştir. Anot elektrot üzerinde gözle görülür biyofilm oluşumu dışında 6 döngü boyunca biyohidrojen üretimi ve yüksek akım üretimi gözlemlenmiştir. Reaktörlerin daha uzun işletilmesinden sonra biyofilm elektrot yüzeyinden soyulmaya başlamış ve hem hidrojen hem de akım üretimi azalmıştır. Döngüsel voltametri (CV) analizi, orta noktası -0,40 V (vs.

Ag/AgCl) potansiyelinde olan bir sigmoidal katalitik dalga üretmiştir. *Geoglobus acetivorans* kültürünün doğrudan elektron transferi (DET) yapabilme yeteneği, pik ayırma analizi, medya değişiminden sonra hızlı akım yoğunluğu geri kazanımı ve anot elektrotunda kalın biyofilm oluşumu ile gösterilmiştir. *Geoglobus acetivorans*, asetat ile ilk biyofilm oluşumundan sonra hipertermofilik MEH'lerde kompleks organik atık malzeme kullanabildiğini göstermiştir.

Anahtar Kelimeler: Mikrobiyal elektroliz hücreleri, elektrohidrojenesis, hipertermofiller, demir-indirgeyen arkeler, biyohidrojen üretimi, *Geoglobus acetivorans*

To my family

ACKNOWLEDGMENTS

Firstly, I wish to express my sincere gratitude to my supervisor Assist. Prof. Dr. Yasemin Dilşad Yılmazel Tokel for her guidance, discussions and insight throughout the research. I would like to thank Examining Committee Members Prof. Dr. Filiz B. Dilek, Prof. Dr. Bülent İçgen, Prof. Dr. İpek İmamoğluand Assist. Prof. Dr. Bilgin Taşkın for their valuable contributions to this thesis.

I also gratefully acknowledge the financial support provided to this research by the; Scientific and Technological Research Council of Turkey (TÜBİTAK) grant number 119C113, METU Office of Sponsored Research Career grant number 10273 and the World Academy of Sciences (TWAS) grant number 18-302 RG/REN/AS_C – FR3240305798.

I would like to express my gratefulness to Prof. Dr. Bülent İçgen and Prof. Dr. İpek İmamoğlu for allowing me to use the facilities of their laboratories.

I am deeply indebted to the members of our research group BIOERG; Amin Ghaderi Kia, Mert Şanlı, Yasin Odabaş, Berivan Tunca, and Ece Kutlar for their comments, friendship and support.

I want to exclusively thank you my parents and my siblings who have supported me throughout this journey. Finally, I would like to thank Begüm Başer who provided ever-constant support and sincerely encouraged me even at most difficult times.

TABLE OF CONTENTS

LIST OF TABLES

TABLES

LIST OF FIGURES

FIGURES

LIST OF ABBREVIATIONS

ABBREVIATIONS

AD: Anaerobic digestion

BES: Bioelectrochemical system

BSA: Bovine serum albumin

CEM: Cation exchange membrane

COD: Chemical oxygen demand

CoV: Coefficient of variation

CV: Cyclic voltammetry

DET: Direct electron transfer

DF: Dark fermentation

DSMZ: Deutsche Sammlung von Mikroorganismen und Zellkulturen (German Collection of Microorganisms and Cell Cultures)

EET: Extracellular electron transfer

FID: Flame ionization detector

GC: Gas chromatography

HER: Hydrogen evolution reaction

LSV: Linear sweep voltammetry

MEC: Microbial electrolysis cell

MES: Microbial electrosynthesis

MET: Mediated electron transfer

MFC: Microbial fuel cell

PES: Polyethersulfone

PFA: Paraformaldehyde

SHE: Standard hydrogen electrode

SEM: Scanning electron microscopy

SMR: Steam methane reforming

SS: Stainless steel

TCD: Thermal conductivity detector

TKN: Total Kjeldahl nitrogen

TS: Total solids

VFA: Volatile fatty acids

VS: Volatile solids

CHAPTER 1

INTRODUCTION

1.1 Background Information

The fast depletion of fossil fuels and the increase in environmental problems associated with pollution loads caused by waste materials is promoting the search for alternative energy sources. These alternative sources are not limited to traditional renewable sources such as solar and wind, also bioenergy production from wastes offer a promising alternative energy source (Rittmann, 2008). Bioelectrochemical systems (BESs) have been intensely studied and improved in the past decade to provide such an alternative and a number of different applications have been discovered. A common principle shared in the BES is at the electro-active microorganisms called exoelectrogens interact with the electrode and enable producing different forms of energy depending on the configuration (Logan et al., 2019; Logan & Rabaey, 2012).

By using microbial fuel cells (MFCs) energy is produced in the form of direct electrical current, while with microbial electrolysis cells (MECs) hydrogen and methane gas could be produced (Lin et al., 2016; Logan et al., 2019; Wang & Ren, 2013). BESs provide new opportunities for the sustainable production of energy and they can be operated with different carbohydrates as well as complex substrates originating from waste materials such as wastewater (Feng et al., 2008; Patil et al., 2009; Tenca et al., 2013; Wagner et al., 2009) and wastewater sludge (Lu et al., 2012; Scott & Murano, 2007) . Working principle of MFCs is that microorganisms growing on the anode oxidize organic matter and the electrons produced from these substrates are transferred to anode and flow to the cathode and meet with oxygen the terminal electron acceptor, and due to the potential difference electricity is produced (Logan

et al., 2006). MFCs offer a biotechnological process where organic waste is degraded with simultaneous electricity production (Rabaey & Verstraete, 2005). MECs resemble to MFCs in terms working principle, however, surface catalytic hydrogen gas production occurs at the cathode as protons are electron acceptors and they operate under completely anaerobic conditions (Logan et al., 2008). It was also found that microorganisms that grow on the cathode of MECs are capable of consuming the electrons to produce methane in a process called electromethanogenesis and the microorganisms involved in this process are called electrotrophs (Cheng et al., 2009). Microbial Electrosynthesis (MES) is another example of the many configurations of BES that is used for converting electricity and carbon dioxide to biofuels including acetate, formate, ethanol and butanol (Nevin et al., 2010; Rabaey & Rozendal, 2010).

Most applications were conducted at mesophilic (25-35 °C) temperatures. Yet there are also thermophilic or hyperthermophilic microorganisms that have stable protein and membrane structures and they can be used even at high temperatures in BES applications. Thermophilic processes can offer significant advantages for industrial applications, in terms of higher reaction rates, improvement of insoluble pollutant degradations, applications with wider substrate ranges, minimal risk of contamination and maintaining anaerobic conditions with the lower solubility of oxygen in high temperatures (Sekar et al., 2017).

Effluents of fermentative processes generally have high VFA content including acetate as a major end product (Thauer et al., 1977) and various exoelectrogens were reported to have the ability to donate electrons to anode by utilizing acetate (Logan et al., 2019). Incorporating MECs for extracting remaining energy in the waste stream of fermentative process was proposed to increase overall efficiency of these two biohydrogen production processes.

1.2 Aim of the Study

Aim of this thesis study is to assess whether pure culture hyperthermophilic archaea *Geoglobus acetivorans* has electro-active properties and could be used for hydrogen production in MEC fed with acetate. Dissimilatory iron reducer *G. acetivorans* is closely related to *Ferroglobus placidus* and *Geoglobus ahangari* previously used in hyperthermophilic MECs (Yilmazel et al., 2018). Further, *G. acetivorans* was reported to have largest number of *c*-type multiheme cytochrome genes for electron transfer to insoluble iron among hyperthermophilic iron reducer archaea (Mardanov et al., 2015). Therefore, *G. acetivorans* was identified as a potential candidate that could be utilized in MECs for hydrogen production from relevant feedstock. In the eventual scaling-up and widespread adaptation of BESs, waste organic matters are expected to be utilized more (Logan & Rabaey, 2012) compared to simple substrates that are commonly used in laboratory experiments. *G. acetivorans* has been reported to anaerobically oxidize various organic substrates including acetate, formate, pyruvate, fumarate, malate, propionate, butyrate, succinate, glycerol and peptone coupled to its iron reduction (Slobodkina et al., 2009). Therefore, this iron reducer, if electro-active, could also potentially metabolise fermentation effluents consisting these organic matters and enable their use for further hydrogen production. Based on this consideration, the objectives of this research can be summarized as:

- to show electro-active capabilities of *G. acetivorans* in MECs fed with simple substrate (acetate)
- to investigate extracellular electron transfer mechanisms of *G. acetivorans* in MECs
- to investigate the potential of utilizing dark fermentation effluent by *G. acetivorans* in hyperthermophilic MECs, which in turn will shed a light on the potential of series application of the two biohydrogen production processes: dark fermentation + MECs

1.3 Scope of the Study

The experimental work consists of three sets. In the first experimental set, MECs were constructed as small-scale reactors fed with simple substrate, acetate, to show electro-active capabilities of this microorganism, which has not been tested in BESs so far. In the second experimental set, reactors sizes were doubled with the objective to better understand the electron transfer mechanisms of *G. acetivorans*. Additionally, in the second set after a certain period in acetate-fed operation, reactors were fed with the effluent of dark fermentation process that has high content of acetic acid, to show the potential of utilization of fermentation effluents. In the final set, MECs were started with dark fermentation effluent instead of acetate, and the potential of growing hyperthermophilic electro-active microorganisms directly with dark fermentation effluent was assessed to investigate the potential series application of dark fermentation and MECs.

CHAPTER 2

LITERATURE REVIEW

2.1 Biohydrogen Production

Energy density of the hydrogen gas is almost 3 times of the gasoline (around 120 MJ per kg compared to 42 MJ per kg) but it is not considered as a carbon-neutral fuel due to its current most common production methods (Ding et al., 2016). Currently hydrogen gas is produced mainly from fossil fuels (96%) and water electrolysis (4%) (Rittmann & Herwig, 2012). Hydrogen gas production using fossil fuel related processes from steam methane reforming (SMR) produces significant amount of greenhouse gasses and water electrolysis is being energy intensive, both are not considered renewable or green production methods (Chandrasekhar et al., 2015; Muradov & Veziroğlu, 2005). Hydrogen production through various biological routes, on the other hand, is a promising alternative, since it provides a way for biofuel production with renewable characteristics (Ding et al., 2016). These biological routes can be categorized as fermentative hydrogen production, biophotolysis and electrochemically assisted biohydrogen production (electrohydrogenesis) (Figure 2.1).

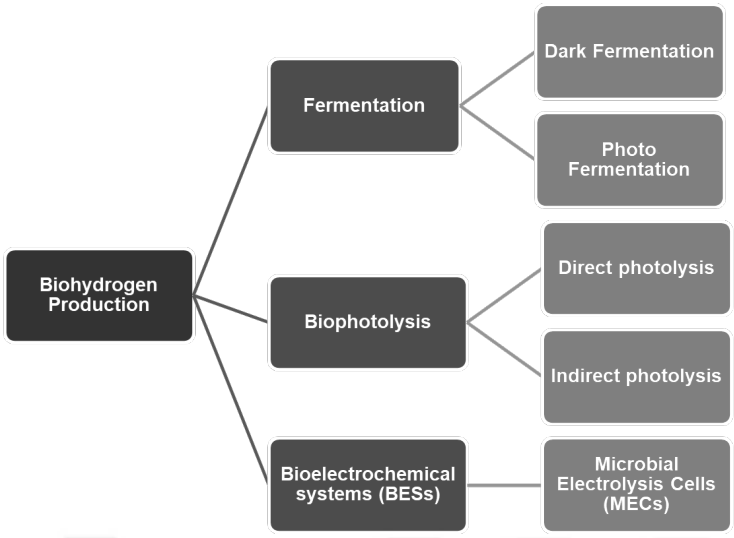

Figure 2.1. Processes for biohydrogen production

2.1.1 Fermentative Biohydrogen Production

Photofermentation is the light dependent fermentation of organics to hydrogen gas. Hydrogen yield and production rate is considered too low for any practical applications (Chandrasekhar et al., 2015).

Dark fermentation (DF) is fermentative conversion of organic substrates in the absence of light and biohydrogen production is achieved through this process similar to the two stages of anaerobic digestion (AD); hydrolysis and acidogenesis (Figure 2.2) (Chong et al., 2009). Facultative anaerobe or obligate anaerobe bacteria, grown in the dark on carbohydrate rich substrates carry out hydrogen production (S. Rittmann & Herwig, 2012). DF is usually carried out in acidic pH, since neutral pH enables methanogenic activity in mixed cultures (Nath & Das, 2011). During the exponential growth phase of fermentative bacteria, the substrate is converted into organic acids (mostly acetic acid), H_2 and CO_2 (Schröder et al., 1994).

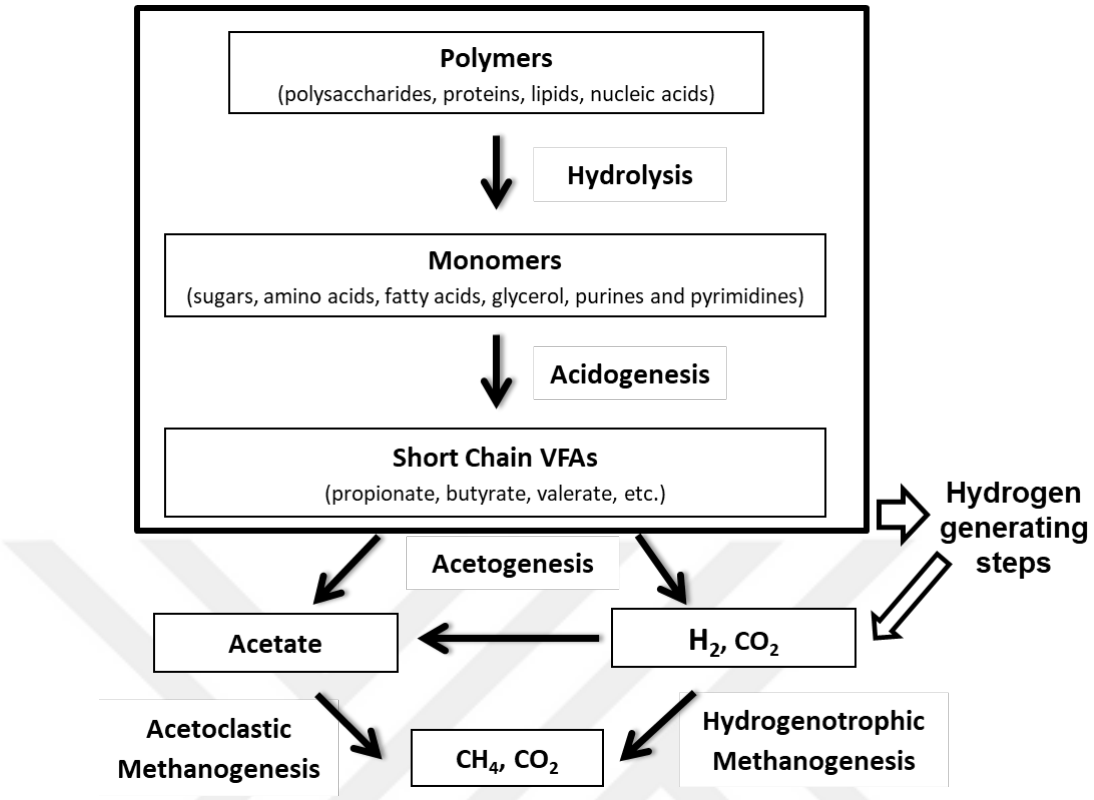

Figure 2.2. Stages of anaerobic digestion

Formation of acetate through dark fermentation is correlated to the net production of hydrogen gas (Cappai et al., 2015). Theoretically, catabolism of one mole of glucose could yield 12 mole of H_2 gas but through dark fermentation maximum obtainable yield is limited to (also known as Thauer Limit) 4 mole of H_2 per mole of glucose (Thauer et al.,1977) as shown in Equation 2-1. Production of H_2 gas lower than stoichiometric balance comes from the energy necessary for cell growth (Jackson & McInerney, 2002).

$$C_6H_{12}O_6 + +2H_2O \rightarrow 2CH_3COOH + 2CO_2 + 4H_2 \qquad \text{(Equation 2-1)}$$

Only hyperthermophiles such as the members of the *Caldicellilusiruptor* genus that could grow on various substrates including recalcitrant biomasses at high conversion rates could reach biohydrogen production yields close to Thauer limit (Zurawski et

al., 2014) and this yield drops to a lower value for mesophilic systems (Dessì et al., 2018). Bioconversion of organics through DF cannot provide a complete conversion of the wastes to energy (Chandrasekhar et al., 2015) because the effluent stream contains fermentation by products such as acetic acid and lactic acid. These products may still be used for further hydrogen production in microbial electrochemical reactors (Osman et al., 2020) . Along with the low yield this is another drawback of DF systems (Chandrasekhar et al., 2015). At the end of DF process, a mixed biogas containing CO_2, and lesser amounts of CH_4, CO and H_2S is produced and thus purification is typically needed for collecting H_2 gas. (Levin & Chahine, 2010). As for the advantages of the process; the high production rate in comparison to some other competing processes such as photofermentation and photolysis and simpler reactor design and operation can be listed (Rittmann & Herwig, 2012)

2.1.2 Biophotolysis

In the presence of light, solar energy is converted to hydrogen gas by microorganisms such as green algae and cyanobacteria in a photobiological hydrogen production process (J. Yu & Takahashi, 2007). Direct biophotolysis uses light energy directly to power activity of hydrogenase enzyme to produce hydrogen gas (Equation 2-2).

$$2H_2O + light \rightarrow 2H_2 + O_2 \quad \text{(Equation 2-2)}$$

Indirect biophotolysis refers to a process consists two stages: carbohydrates synthesis in presence the light (Equation 2-3) and fermentation of carbohydrates for H_2 production (Equation 2-4).

$$6H_2O + 6CO_2 + light \rightarrow C_6H_{12}O_6 + 6O_2 \quad \text{(Equation 2-3)}$$

$$C_6H_{12}O_6 + +6H_2O \rightarrow 12H_2 + 6CO_2 \quad \text{(Equation 2-4)}$$

Disadvantages of photobiological hydrogen production was listed as the low oxygen tolerance of hydrogenase enzymes and low energy efficiency of light conversion (Ding et al., 2016).

2.1.3 Electrochemically Assisted Hydrogen Production

Electrochemically assisted hydrogen production (also called electrohydrogenesis) is another and hydrid biohydrogen production method that is combining electrochemisty and microbiology. Microbial electrolysis cells (MECs) are used during this process are a part of bioelectrochemical system (BES) technology that utilizes electro-active microorganisms. Thermodynamics of hydrogen production in MECs is summarized below.

Electrohydrogenesis can be used for hydrogen production from a wide range of organic materials present in wastewaters such as acetate, glucose and glycerol (Rozendal et al., 2006). Yet, in most studies acetate has been used as substrate in MECs (Logan et al., 2019). Acetate is unsuitable for hydrogen production through fermentative pathways (Equation 2-5) due to being thermodynamically unfavorable ($\Delta G = +104.6\ kJ/mol > 0$) and is among those present in the effluent of a DF process (Logan et al., 2008).

$$CH_3COO^- + 4H_2O \rightarrow 2HCO^- + H^+ + 4H_2 \quad \text{(Equation 2-5)}$$

Electrochemically assisted hydrogen production in MECs follows the reactions shown on Equation 2-6 for anode and Equation 2-7 for cathode. Bioelectrochemical oxidation of acetate on anode produces a potential around -0.279 V and hydrogen evolution reaction at the cathode required a potential around -0.414 V (Logan et al., 2008). Overall cell potential to produce hydrogen in MEC is shown on Equation 2.8.

$$CH_3COO^- + 4H_2O \rightarrow 2HCO^- + 9\,H^+ + 8\,e^- \quad E_{anode} \cong -0.28\,V \quad \text{(Equation 2-6)}$$

$$8\,H^+ + 8\,e^- \rightarrow 4\,H_2 \quad E_{cathode} \cong -0.42\,V \quad \text{(Equation 2-7)}$$

$$E_{cell} = E_{cathode} - E_{anode} \cong -0.14\,V \quad \text{(Equation 2-8)}$$

In other words, at least 0.14 V of external potential needs to be applied to produce hydrogen gas in MECs. Considering the electrode overpotentials and ohmic losses due to reactor materials, this requirement becomes at least 0.5 V in practice

(Geelhoed et al., 2010). Compared to the water electrolysis process which requires 1.23 V in theory and 1.8 V in practice (Li et al., 2020), the energy requirement is significantly lower in electrohydrogenesis (Rozendal et al., 2006).

There are some other applications of BESs and these are explained in more detail in the following section.

2.2 Bioelectrochemical Systems (BESs)

An electrochemical cell is a device that uses the energy released by a spontaneous redox reaction to generate electrical current. Two conductive electrodes are present in electrochemical cells where oxidation and reduction reactions takes place at anode and cathode respectively (Bard & Faulkner, 2008) . The electrodes can be made of a variety of conductive materials including metals, graphite or polymers (Bard & Faulkner, 2008).

Bioelectrochemical systems (BESs) utilizes electro-active microorganisms which can take place in redox reactions of chemicals and conduct electron transfer to an electrode (Logan et al., 2019). Ever since the discovery of insoluble metal-reducing microorganisms, which have the ability to transport electrons out of the cell (Lovley & Phillips, 1988) with a process that is called extracellular electron transfer later (Kim et al., 1999), various research groups have shown that microorganisms capable of reducing these metals often can donate electrons to anodes in BES (Gorby et al., 2006; Parameswaran, et al., 2009; Mathis et al., 2008; Wrighton et al., 2008).

The most commonly studied microorganisms in BESs are various *Geobacter spp.* and *Shewanella spp.* (Logan & Rabaey, 2012) . These species and other exoelectrogens mostly isolated at mesophilic temperatures (Wrighton et al., 2008) but thermophilic or hyperthermophilic microorganisms have been known to possess exoelectrogenic abilities as well (Fukushima et al., 2015; Kobayashi et al., 2017; Lusk et al., 2015; Marshall & May, 2009; Mathis et al., 2008; Parameswaran et al.,

2013; Pillot et al., 2018; Sekar et al., 2017; Yilmazel et al., 2018; Yu et al., 2017). However, numbers of studies with thermophilic or hyperthermophilic BESs are scarce in comparison to the abundance of mesophilic BES studies (Figure 2.3).

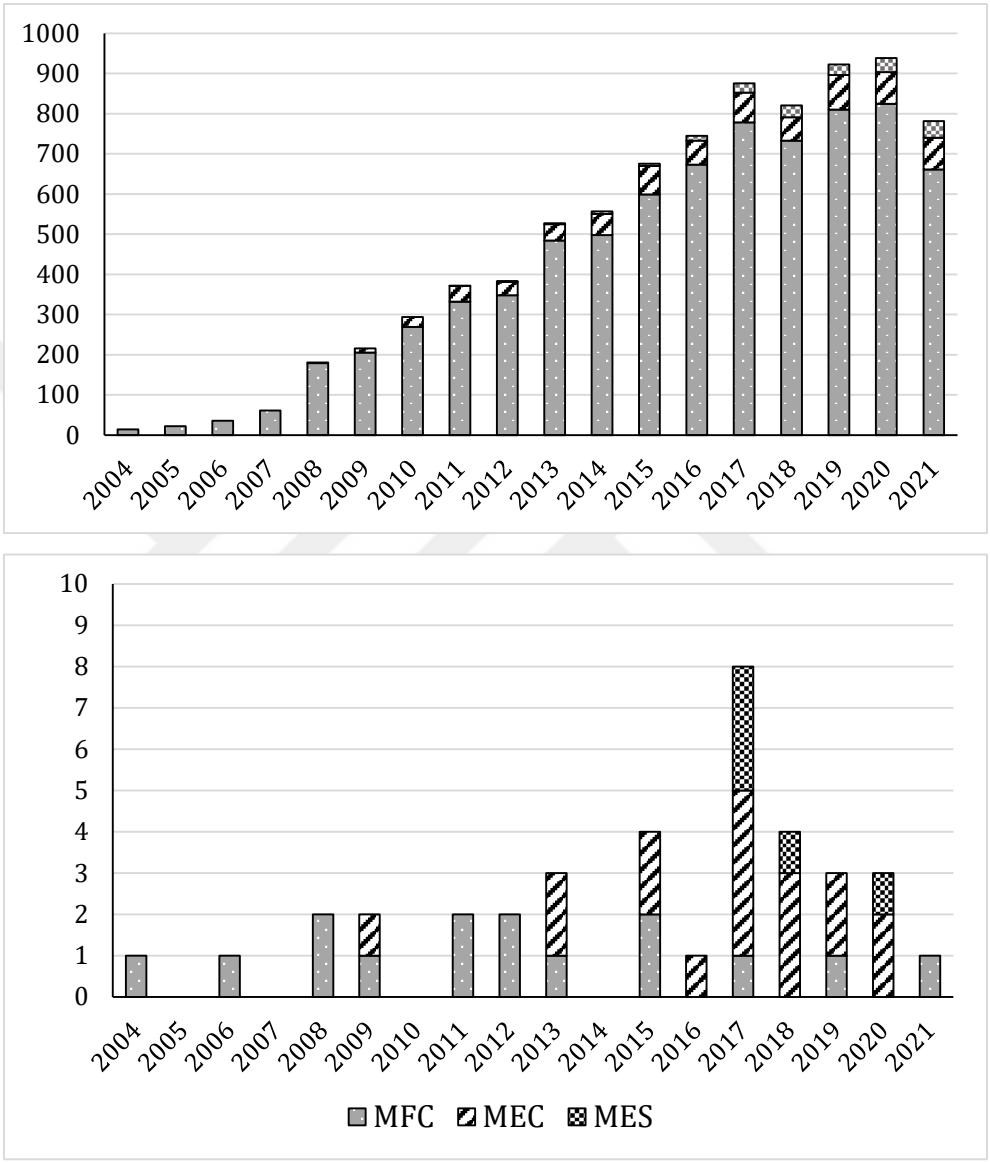

Figure 2.3. Number of mesophilic (top) and thermophilic/hyperthermophilic (bottom) and studies conducted between 2004 and 2021 (search method explained at Appendix A)

2.2.1 Reactor Materials

Performance of BESs are affected by factors such as inoculum source, electrode material and the configuration of reactors (Logan et al., 2019). However, most of the costs associated with the BESs stems from to electrodes/catalysts or membranes in double chamber BESs. Typical electrode materials are carbon based materials such as graphite for anode (Cheng & Logan, 2007; Gorby et al., 2006) and stainless steel, Pt electrodes or Pt coated metals for cathode (Choi et al., 2019; Logan et al., 2006). Initial cost of cation exchange membranes (CEM) in double chamber BESs are high (Zuo et al., 2007) and also possible biofouling of membranes can cause operational problems and additional expenses (Chu & Li, 2005).

2.2.2 Exoelectrogens

Microorganisms that can donate electrons to solid anode electrodes and produce current in BESs are called exoelectrogens (Logan, 2009). This group of microorganisms are diverse and includes various bacteria and archaea (Logan et al., 2019). Even microorganisms that can thrive in extreme conditions including high temperatures, high salinity or extreme pH environment were shown to possess exoelectrogenic ability (Logan et al., 2019). Electron transfer capability of *Geobacter sulfurreducens* and *Shewanella oneidensis* was known for a long period of time (Bond & Lovley, 2003; Kim et al., 2002). Both species are considered to be among the most important and model exoelectrogens and former is the most commonly identified in mixed culture inoculated BESs at mesophilic temperatures (Logan et al., 2019). Identifying new exoelectrogenic species is an important aspect of BES research, since based on different capabilities of the microorganisms involved a variety of applications can be developed. However, there are no molecular tools available that can target exoelectrogenic species as a group yet (Logan et al., 2019). The following section describes the electron transfer mechanism of exoelectrogenic microorganisms.

2.2.2.1 Extracellular Electron Transfer

The extracellular electron transfer (EET) mechanism is an important aspect of the energy production in BES which can be done in two ways (i) by direct electron transfer (DET) over membrane-bound *c*-type cytochromes and long-range electron transfer via microbial nanowires (Caccavo et al., 1994; Ehrlich, 2008; Lovley & Phillips, 1988; Lovley, 2008; Myers & Myers, 1992), (ii) mediated electron transfer (MET) via external electron carriers (Y. Choi et al., 2004). The illustration of these mechanisms is shown on Figure 2.4. Studies showed that both bacteria and archaea have the ability to perform EET and they can be utilized in BES in various configurations (Fu et al., 2013; Lusk, Khan, et al., 2015; Sekar et al., 2017; Yilmazel et al., 2018).

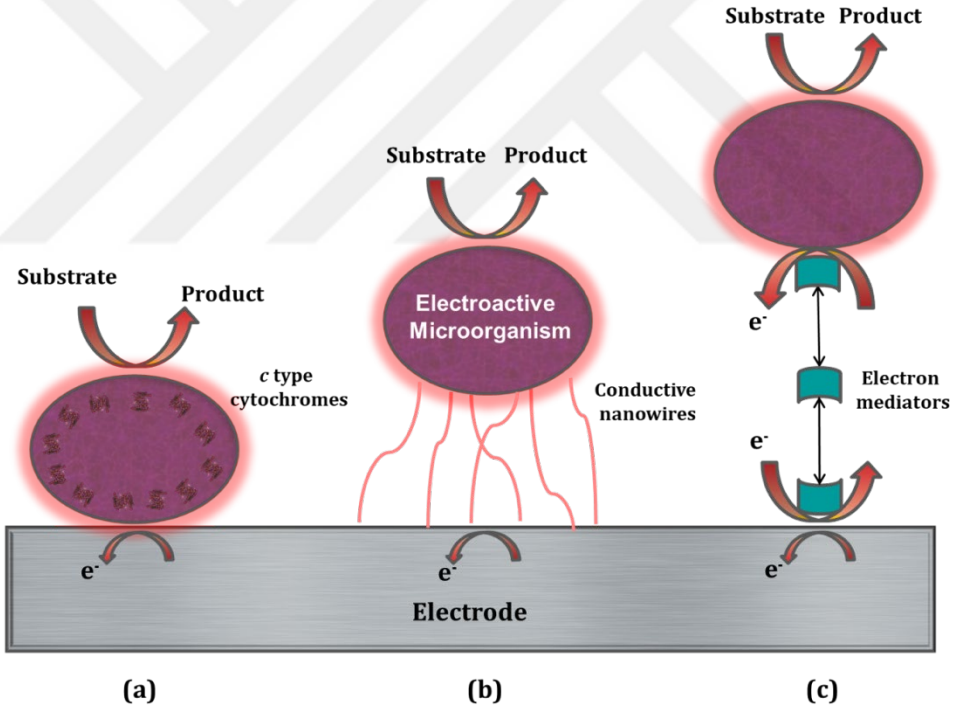

Figure 2.4. Electron transfer mechanism on anode (a) DET over membrane-bound *c*-type cytochromes (b) DET via microbial nanowires (long-range electron transfer) (c) MET via external electron carriers

2.2.2.1.1 Direct Electron Transfer (DET) in Bioelectrochemical Systems

Evidence for DET capabilities of electro-active microorganisms in BESs are of highest importance, since DET capable microorganisms are required for scaling-up BESs. Electrochemical methods such as cyclic voltammetry (CV) analysis and linear sweep voltammetry (LSV) are often used to investigate the mechanism of electron transfer of the microorganisms (Fu et al., 2013; Fu, Kuramochi, et al., 2015; Hara et al., 2013). Through the comparative analysis of voltammograms, the presence of electron shuttles *i.e.* MET or use of cytochromes/nanowires *i.e.* DET could be determined. For example, the presence of peaks in the CV when there is biofilm and the lack of similar peaks with spent medium (reactor content) in the absence of biofilm would be an indicator of DET (Yilmazel et al., 2018). Scanning Electron Microscopy (SEM) images of the electrode surfaces could show complex structures (*e.g.* conductive pili) and thick biofilm formation which could be attributed to DET capability. Another indication of DET is the rapid recovery of current after feeding with fresh medium (Marshall & May, 2009; Parameswaran et al., 2013). Further, high protein content in electrode surface in comparison to reactor content are accepted as other signs of a biofilm formation on the electrodes which in turn implies the presence of DET (Yilmazel et al., 2018).

2.2.2.1.2 Mediated Electron Transfer (MET) in in Bioelecrochemical Systems

Mediated electron transfer (MET) occurs when microorganisms use either self-produced or externally added electron shuttles during the electron transfer process (Schröder, 2007) . Electron transfer via external electron carriers (*e.g.* neutral red, AQDS) is expected to be more problematic during operation of large scale reactors for several reasons: (i) because most are reported to be ecotoxic (Kastury et al., 2015), (ii) their disposal after consumption may introduce an environmental challenge, (iii) costs associated with these mediators are expected to be higher and

(iv) this may put the long-term stability of the reactor systems in jeopardy compared to DET utilizing systems. (Kim et al., 1999; Steinbusch et al., 2010; Thrash & Coates, 2008). Only mediators produced by the microorganisms were said to be of interest since there is no need for external mediators (Logan et al., 2019). The problem associated with this may be due to washout, which may happen as a result of sudden change in operational conditions.

During experimental studies, attention must be paid to exclude external mediators to the BES reactors. In the case of introducing electron mediators unintentionally through the feedstock or growth mediums of microorganisms used in BES studies, results must be reproduced with excluding the mediators to clearly observe the capability of DET.

2.2.3 Reactor types

2.2.3.1 Microbial Fuel Cell (MFC)

Microbial Fuel Cells (MFCs) are developed to produce electricity while organic materials are degraded (Logan et al., 2006). MFCs utilize exoelectrogenic microorganisms that oxidize organic or inorganic matter. During this oxidation process, exoelectrogens donate electrons to the anode and electrons flows to the cathode connected through conductive wiring. A resistor is placed in series to the this conductive wiring and electrical current is produced (Logan et al., 2006). MFCs are expected to provide higher conversion efficiency compared to other bioconversion methods, since it converts organic matters directly into electricity where oxygen is the terminal electron acceptor at the cathode chamber (Rabaey & Verstraete, 2005). Configuration of a typical double chamber MFC is shown on Figure 2.5. MFCs are usually built in double chamber systems (H-Cells) with a cation exchange membrane (CEM) in between the chambers (Logan et al., 2006). This membrane prevents oxygen leakage to the anode chamber and allows protons

to pass to the cathode chamber where they react with oxygen to produce water (Logan et al., 2006)

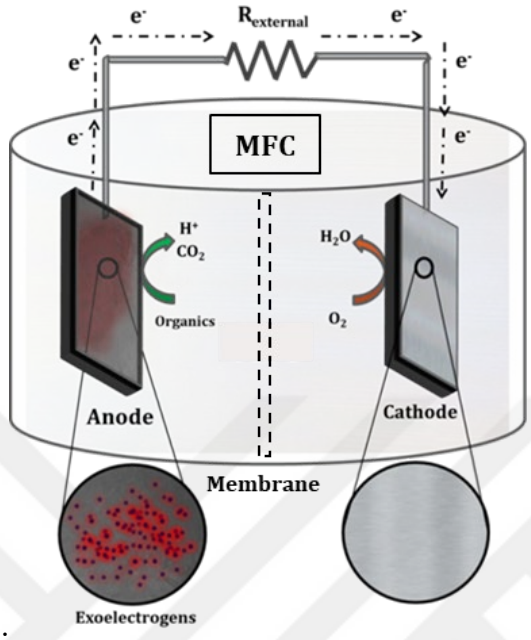

Figure 2.5. A typical double chamber MFC (oxygen is provided to the cathode chamber)

2.2.3.2 Microbial Electrolysis Cell (MEC)

Microbial Electrolysis Cells (MECs) are modified reactors of MFCs used for production of hydrogen gas (Logan et al., 2008). In MECs both chambers are free of oxygen to support anaerobic microorganism growth (Chae et al., 2008). Aim of MECs are to produce biofuels either in the form of hydrogen gas or methane gas (Logan et al., 2019). Hydrogen production in MECs (Figure 2.6) is made possible thermodynamically with the addition of small external voltage (around 0.14 V in theory, Equation 2-8) for abiotic hydrogen production at the cathode. This process is also called electrohydrogenesis and the reactions are discussed previously on Chapter 2.1.3.

MECs may also include (Figure 2.5) biocathodes. For example, there are biocathodes present in methane producing MECs. In these reactors methanogenic archaea is grown as biofilm on cathode and produce methane by consuming electrons in a process called electromethanogenesis (Cheng et al., 2009). Similar reactor configurations and materials of MFCs are also used in MECs with the necessary modification for gas collection. (Luque et al., 2016).

Most MEC applications use a double chamber system with CEM in between (Cheng & Logan, 2007; Ditzig et al., 2007; Liu et al., 2005; Rozendal et al., 2008). Yet there are also a number of single chamber applications studied (Call & Logan, 2008; Hu et al., 2008; Yilmazel et al., 2018). Presence of a membrane in MECs were reported to increase acidity in anode chamber and cause a pH gradient that increases the external voltage requirement (Luque et al., 2016).

Hydrogen production efficiencies reported in MECs were higher than fermentation process using glucose (Call & Logan, 2008). MECs are showing immense potential for biohydrogen production and can be used to utilize wide range of complex wastes (Cusick et al., 2011; Lu et al., 2012; Tenca et al., 2013; Wagner et al., 2009). To scale up MEC reactors an important factor to consider is to identify cost effective materials and reactor configurations. Single-chamber MECs usually produce higher current density and construction is more simple compared to the double chamber MECs (Call & Logan, 2008). Cost effective cathode materials such as stainless steel can be used in MECs since it was argued at applied voltage of 0.7 V high cost cathode materials such as Pt showed no appreciable increase in hydrogen generation (Chae et al., 2009).

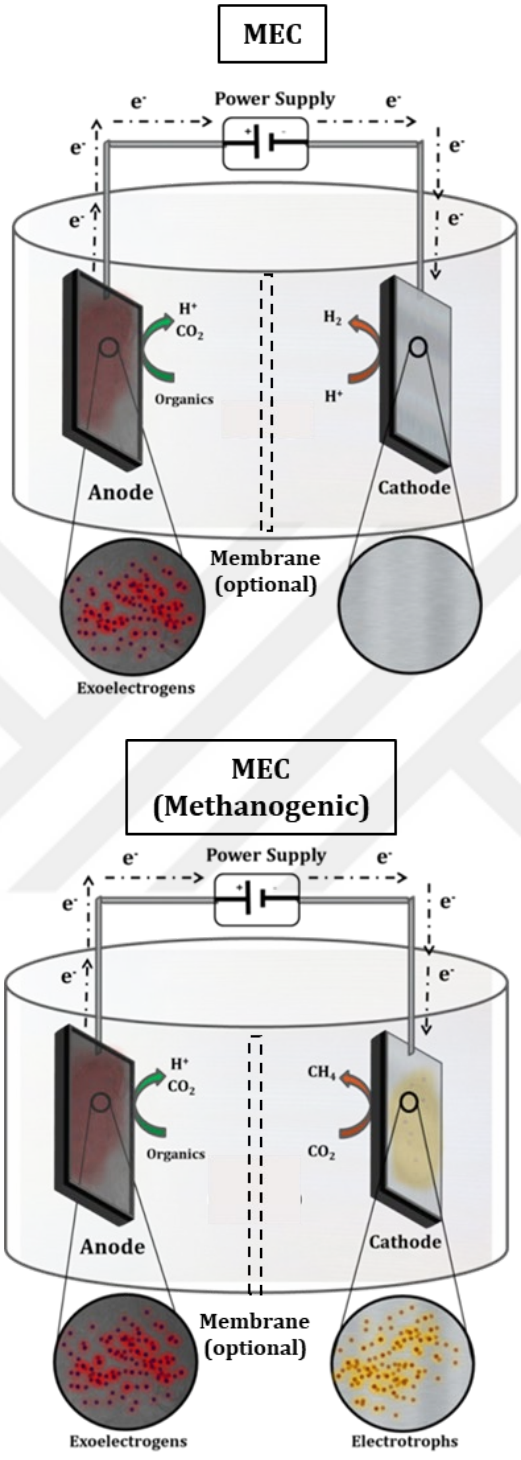

Figure 2.6. A typical hydrogen producing MEC (top) and methane producing MEC (bottom)

2.2.3.3 Microbial Electrosynthesis (MES)

Microbial Electrosynthesis (MES) is also one of the many configurations of BES (Figure 2.7) that is used for converting electricity and carbon dioxide to biofuels including acetate, formate, ethanol and butanol (Nevin et al., 2010; Rabaey & Rozendal, 2010). In MES systems where electrotrophs grow on the cathode as they accept electrons from the electrode, mechanism of organic compound production is not completely understood and it was suggested that either extracellular enzymes catalyzed the electrosynthesis or biofilms can directly uptake the electrons from the cathode for autotrophic metabolism (L. Yu et al., 2017). Limiting factors in microbial electrosynthesis were listed as CO_2 uptake, proton transfer, electron transfer and enzyme catalyzed synthesis rates (L. Yu et al., 2017).

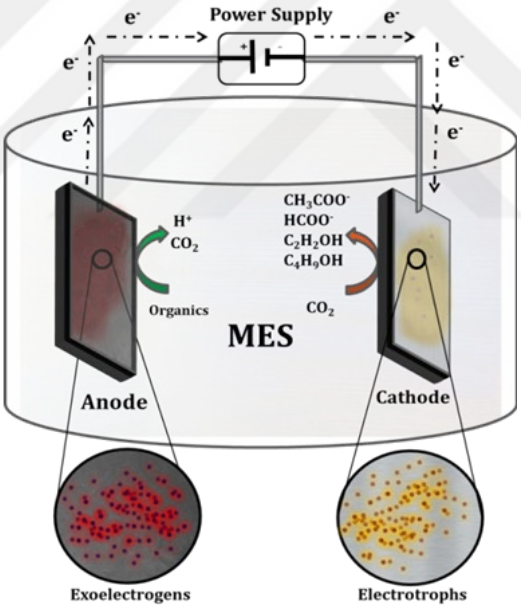

Figure 2.7. Typical configuration of MESs

2.3 High Temperature Bioelectrochemical Systems

In high temperature BES studies only a small fraction is working with pure culture microorganisms that are known to possess electron transfer capabilities. Knowledge

on the factors effecting the reactor operations is limited and identified electro-active species and operation temperature of the reactors vary significantly. In some cases, for mixed culture operations, bioelectrochemical activity is attributed to certain isolates without concrete evidence. Identification of electro-active microorganisms that is capable of DET compared to the ones that utilize mediators could be the first step in scaling up approach. In order to study the DET capabilities, elimination of potential external electron mediators is needed for systematic approach. Isolation from dominant species in mixed culture applications or studies with the closely related species could be the way to discover new electro-active microorganisms for novel BES applications. High temperature applications of BESs were grouped with respective to their electro-active species and their taxonomic rank of order in this review chapter.

2.3.1 Thermophilic and Hyperthermophilic Electro-active Microorganisms

2.3.1.1 Electro-active Bacteria

Since the earliest studies searching for the electron transfer capable microorganism and their use in BESs mesophilic gram negative bacteria such as *Geobacter sulfurreducens* (Bond & Lovley, 2003; Caccavo et al., 1994) and *Shewanella oneidensis* (Kim et al., 2002; Myers & Myers, 1992) were used in the BES studies. Differences in membrane structures divide bacteria into two category as gram negative and gram positive (Figure 2.8) and membrane characteristics play an important role in electrochemical activity for domain bacteria (Matsunaga & Nakajima, 1985). Gram positive bacteria differs from gram negative bacteria in a way that they have a thicker cell wall mainly constituted of peptidoglycan and an external lipoteichoic acid layer that enhances formation of biofilms (on electrodes) and their electron transfer abilities were expected to be different than gram negative

bacteria (Ehrlich, 2008; Modestra & Mohan, 2014). On the other hand thin layer of peptidoglycan and selective outer membrane in gram negative bacteria is expected to enable easier secretion of permeable metabolites, which could be the exogenous electron mediators in BESs (Modestra & Mohan, 2014).

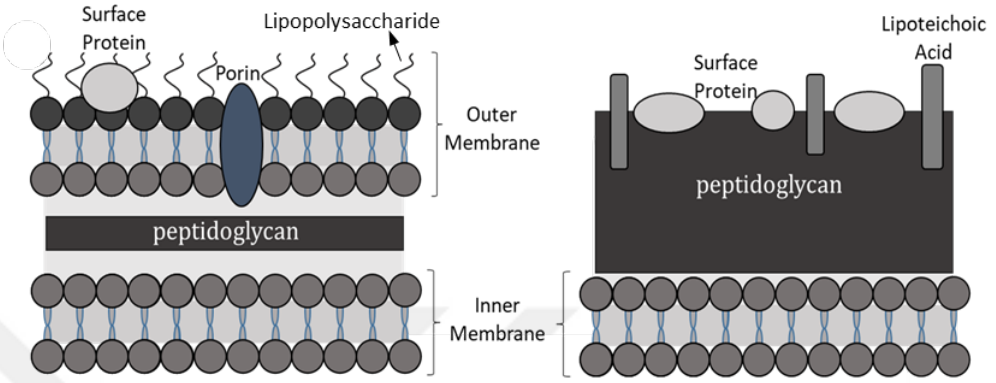

Figure 2.8. Cell membrane structures of gram-negative (left) and gram-positive (right) bacteria

Depending on the classification according to the cell wall structure (i.e. gram positive or gram negative), factors such as growth, EET mechanisms and substrate utilization processes might differ for electro-active bacteria (Borole et al., 2011; Modestra & Mohan, 2014). In the earlier studies of BESs, gram positive bacteria were thought to have an interaction role rather than a direct involvement in EET (Rabaey et al., 2007). Due to the presence of thick non-conductive cell envelope, gram positive bacteria is mostly considered as incapable of DET and required shuttling mediators to perform EET (Modestra & Mohan, 2014).

Yet, among the various thermophilic members of the bacteria domain (Table 2.1) gram positive genus of *Thermincola* were commonly used in thermophilic BES studies and their ability to produce current without using electron shuttles were reported in a number of studies (Lusk et al., 2015; Marshall & May, 2009; Mathis et al., 2008; Wrighton et al., 2008).A recent study hypothesized that improving the cell permeability in peptidoglycan layer can enhance electron transfer gram positive

bacteria (Chen et al., 2018). There is evidence indicating membrane characteristics of bacteria affect bioelectrochemical system performance through changes in DET capability (Parameswaran et al., 2013; Wrighton et al., 2008) and processes such as proton transfer but the extent of these effects is unknown and needs to be further investigated.

Table 2.1. Thermophilic and hyperthermophilic exoelectrogenic bacteria in BES

Exoelectrogenic Bacteria	Isolation/ Inoculum Source	BES Type	T (°C)	References
Thermincola ferriacetica	From a terrestrial hydrothermal spring	MEC	60	(Lusk et al., 2016, 2018; Marshall & May, 2009; Parameswaran et al., 2013)
Thermincola potens	MFC reactors inoculated with thermophilic AD sludge	MFC	55	(Wrighton et al., 2008)
Thermoanaerobacter pseudethanolicus	Algal-bacterial mat in Octopus Spring	MEC	60	(Lusk, Khan, et al., 2015)
Calditerrivibrio nitroreducens	Terrestrial hot spring	MFC	55	(Fu et al., 2013)
Calditerrivibrio nitroreducens related specie	Thermophilic digester sludge from a WWTP	MFC	55	(Fu et al., 2013)
Thermincola sp.	Marine sediment from temperate waters	MFC	60	(Mathis et al., 2008)
Ureibacillus sp.	MFCs acclimated with thermophilic sewage sludge digestate	MFC	55	(Dessì et al., 2019)
Thermodesulfobacterium commune related isolate	Formation water produced at a petroleum reservoir from an oil field	MFC	95	(Fu, Kuramochi, et al., 2015)
Bacteroides genus	Brine pool sample from Red Sea	MEC	70	(Shehab et al., 2017)
Carboxydothermus ferrireducens	Mixed sample of sediment, water and biomass of hot spring	MFC	65	(Gavrilov et al., 2021)

2.3.1.1.1 Clostridiales

In the ecologically diverse order of the *Clostridiales* (also known as *Eubacteriales*) both gram positive and gram negative organisms are present (Rainey, 2015). So far only the gram-positive species of the *Thermincola* genus were utilized in the thermophilic BES studies. In the earliest study investigating thermophilic BES application, anode of MFC reactors were transferred from a sediment MFC operated in temperate waters (Mathis et al., 2008). Although the sediment is acquired at mesophilic temperatures, thermophiles including *Thermincola sp. ,*closely related to the *Thermincola carboxydophila* (99% similarity of 16S rRNA genes) were found as dominant in microbial community analysis after reactor operation (Mathis et al., 2008). It could be argued that although the sediment was expected to provide better conditions for mesophilic community to grow, thermophilic community were present in a non-ideal conditions and could prosper with adjusted conditions. MFCs operated at higher temperatures (60 °C) produced higher electric currents than low temperatures (22 °C) showing that the thermophilic population acquired from the sediment had greater effectiveness in generating electrical current reaching to 0.25 A/m^2 (Mathis et al., 2008).

A different study a year later from the first thermophilic BES investigation reports the earliest operation with pure cultures of *Thermincola sp.* strain *JR* and *Geobacillus sp.* strain *S2E* (of *Bacillales* order). These microorganisms were isolated from the scrapings of MFC electrodes inoculated with thermophilic anaerobic digester sludge (Wrighton et al., 2008). Pure cultures of *Thermincola sp.* strain *JR* and *Geobacillus sp.* strain *S2E* were isolated with a selective media for iron reducing – acetate oxidizing capabilities. *Thermincola sp.* strain *JR* was proven to be superior in MFC operation in terms of current generation with 0.67 A/m^2 (originally reported as 0.42 mA). *Geobacillus sp.* strain *S2E* MFCs even with the presence of mediators produced an insignificant electrical current (0.03 mA) (Wrighton et al., 2008). This study on *Thermincola* genus (Wrighton et al., 2008) did not include the investigation of mechanisms behind the EET. In a later study 16S rRNA gene sequence identity

showed that *Thermincola sp.* strain *JR* (later renamed as *Thermincola potens*) shares 99% similarity with the two known members of the *Thermincola* genus *Thermincola carboxdophilia* and *Thermincola ferriacetica* (Byrne-Bailey et al., 2010) where latter is used in a number of times in thermophilic BES studies in follow-up work (Lusk et al., 2016; Marshall & May, 2009; Parameswaran et al., 2013).

In a thermophilic single chamber MFC study with pure culture of *T. ferriacetica* another member of *Thermincola* genus proved similar results for the case of exoelectrogenic capabilities of gram positive bacteria and produced a current density of 0.4 A/m^2 (Marshall & May, 2009). It is hypothesized that due to the results such as rapid recovery of current when MFC is washed with fresh medium, presence of thick biofilms and complex connective structures on anode similar to conductive pili (*e.g.* nanowires) and CV data with no peaks detected in cell-free spent medium DET capability of *T. ferriacetica* was shown (Marshall & May, 2009).

A thermophilic MEC operation consolidated previous findings for DET through a solid conductive matrix for *T. ferriacetica;* with results including high current density, SEM showing a thick biofilm with multiple layers of active cells and rapid recovery of current density when medium is replaced (Parameswaran et al., 2013). CV results of *T. ferriacetica* at peak current density were compared to the electrochemical behavior of *Geobacter sulfurreducens* (capable of DET) reported earlier (Lee, Torres, & Rittmann, 2009) and it shows a good fitting which was argued to be an indicator of DET capability (Parameswaran et al., 2013). Peak current density reached up to 12 A/m^2 and sustainable current densities of 7.5 A/m^2 and 8 A/m^2 are reported for the 2 sets of operation conducted at different times (Parameswaran et al., 2013).

Previous study with this culture produced much lower current density (0.4 A/m^2) during single chamber operation of *T. ferriacetica* (Marshall & May, 2009) against this study with 8 A/m^2 (Parameswaran et al., 2013) produced by the double chamber operation. Even with the use of same exoelectrogen depending on the operation conditions performance of the BES could significantly change as it can be seen for *T. ferriacetica* MECs. High current density values recorded with *T. ferriacetica* in

this optimized reactors operation were comparable to the model exoelectrogens producing current density around 9 A/m^2 (Katuri et al., 2012; Peng et al., 2010). Reactor conditions such as changes in bulk pH and proton gradients caused by high current productions were argued to be the most important contributor to the changes in electrochemical activity of *T. ferriacetica* biofilms (Lusk et al., 2018). Proton transfer mechanism defined as the diffusion of protons from the biofilm formed on the electrode to bulk solution after the substrates are utilized by the biofilms and electrons are transferred to anode (Lusk et al., 2016). Production of protons in biofilm could create a pH gradient and a low pH value in the biofilm is a limiting factor for both the microbial growth and EET (Franks et al., 2009) (Figure 2.9).

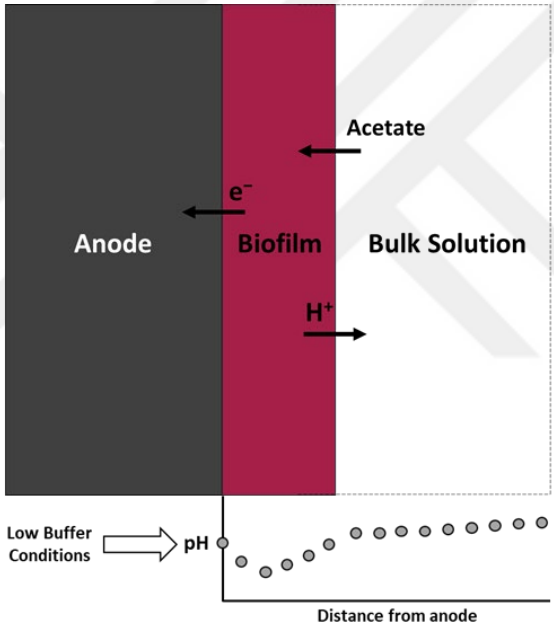

Figure 2.9. Graphical illustration of pH gradient in biofilms of BESs

It was reported that the thermophilic operations provide an advantage for the proton transport, but could still be a major limitation in current production and biofilm thickness (Lusk et al., 2016). Addition of buffers can both prevent major pH shifts and also it could help proton transfer with following Equation 2.9 where protons binding into bicarbonate (HCO_3^-) and produce carbonic acid (H_2CO_3) to transfer protons out of the biofilm. This aided transport is significantly faster than the proton

transfer on its own due to the concentration gradient at neutral pH usually required by exoelectrogens (Lusk et al., 2016).

$$HCO_3 + H^+ \leftrightarrow H_2CO_3 \quad \text{(Equation 2-9)}$$

T. ferriacetica could be offering a number of operational advantages when the environmental conditions are adjusted since it is reported to have the ability to metabolize a wide range of substrates (Zavarzina et al., 2007). For this reason, *T. ferriacetica* has been suggested to be used to treat low-alkalinity waste streams in BESs (Lusk et al., 2016). Investigations unraveling the conditions that yield high current densities and the mechanisms of DET performed by this thermophilic exoelectrogen provided helpful information for scaling-up high temperature BES reactors.

2.3.1.1.2 *Thermoanaerobacterales*

A member of the *Firmicutes* phylum *Thermoanaerobacter pseudethanolicus* (ATCC 33223) that is capable of both Fe(III)-reduction and fermentation, used in a thermophilic MEC operation and its ability to produce current from xylose, glucose, cellobiose, and acetate was investigated (Lusk, Khan, et al., 2015). High current density values were obtained with *T. pseudethanolicus* for glucose-fed (4.3 ± 1.9 A/m^2), cellobiose-fed (5.2 ± 1.6 A/m^2) and xylose-fed reactors (5.8 ± 2.4 A/m^2) (Lusk, Khan, et al., 2015). Current production was started after acetate build up due to fermentation of sugars, meanwhile acetate-fed reactor did not produce any significant current. (Lusk, Khan, et al., 2015). This result indicates favorable growth conditions might be required before exoelectrogenic activity on anode is demonstrated. Implications of using a pure culture with the ability to utilize both sugars and fermentation end products could be an important step to generate new possible applications for BES applications especially in the bioconversion of wastes with high sugar content.

2.3.1.1.3 Bacillales

An unidentified member of the *Bacillales* order of gram-positive bacteria, *Ureibacillus sp.* was found to be the dominant specie in flow-through and up-flow MFCs (Dessì et al., 2019). Up-flow reactor was inoculated with sewage sludge digestate from a thermophilic biogas plant and the flow-through reactor was inoculated by taking sample from the up-flow MFC operated for a long period of time (Dessì et al., 2019). Flow-through thermophilic MFC performed significantly better than the up-flow thermophilic MFC in terms peak current densities resulted that was around 0.43 A/m^2 and 0.12 A/m^2, respectively (Dessì et al., 2019). Also *Symbiobacterium sp.* was abundant in the community and the researchers suggested that it formed a syntrophic relation with the *Ureibacillus sp.* (Dessì et al., 2019). A similar note was also made by Pillot and others (2018) when deep-sea hydrothermal vents were used to inoculate BES reactors in their study (Pillot et al., 2018). In the growth medium used in this study (Dessì et al., 2019) some electron mediators such as EDTA and resazurin was excluded but some such as sodium sulfide were still present and therefore may enable mediated EET pathways (Yilmazel et al., 2018). Therefore, the capability of DET by *Ureibacillus sp.* is unknown.

2.3.1.1.4 Deferribacterales

Thermophilic MFC operation used thermophilic digester sludge as inoculum showed that dominating specie (clone named as TA-B1) in the anodic biofilm was closely related to the *Calditerrivibrio nitroreducens* str. Yu37-1 of the *Deferribacteres* phylum (Fu et al., 2013) that is originally isolated from a terrestrial hot spring in Japan (Iino et al., 2008). Reactors inoculated with sludge were operated both at thermophilic (55 °C) and mesophilic (25 °C) conditions in two-chamber MFC reactors. Their results show that maximum power density in the thermophilic MFC was more than 8 times higher than the mesophilic MFC, and also it was shown that dominant specie is capable of DET by rapid current recovery and CV analysis of the

spent medium (Fu et al., 2013). Any external effect due to electron mediators in the inoculum was prevented by centrifuging the inoculum and discarding the supernatant (Fu et al., 2013). Additional tests with the pure culture of *C. nitroreducens* str. Yu37-1 were produced a current density of 0.6 A/m^2 (originally reported as 2.5 mA) compared to 0.8 A/m^2 (originally reported as 3.45 mA) for the thermophilic MFC operation and 0.3 A/m^2 (originally reported as 1.4 mA) for mesophilic MFC operation (Fu et al., 2013). Identifying the capabilities of the inoculum and relating this capability to the dominant specie with further investigation could be a precise way to discover alternative electro-active microorganisms to be used in BES studies.

2.3.1.1.5 Bacteroidales

First investigation of both thermophilic (70 °C) and hypersaline conditions (25 % salinity) were done in MEC reactors inoculated with brine pool samples acquired at the Red Sea and operated with a 405 mV vs. SHE anode potential application (Shehab et al., 2017). This set potential was chosen since it would help interactions with the electrode by preventing the use of sulfate or ferric iron naturally present in the brine pool samples (Shehab et al., 2017). One of the 3 sets inoculated with brine pool samples reported to produce a stable current density of 6.8 ± 2.1 A/m^2 (Shehab et al., 2017). Brine pool sample resulted in higher current density was acquired at mesophilic temperatures (34.2 °C) and still it produced higher current densities than a different sample acquired at high temperatures (68 °C) (Shehab et al., 2017). A similar observation was reported by Mathis and others (2008); sample acquired at the mesophilic temperatures performed better under the thermophilic conditions with a marine sediment MFC anode. In the study, with Read Sea pool samples, microbial community analysis at genus level showed bacteria belonging to *Bacteroides* genus of *Bacteroidales* order which was enriched during MEC operation and was not detected with open circuit controls (Shehab et al., 2017). Therefore, bioelectrochemical activity is attributed to this dominant group while CV analysis

with cell-free media showed no redox peaks (Shehab et al., 2017) indicating capability of DET by this electro-active group.

2.3.1.1.6 Thermodesulfobacteriales

In a research study that used hyperthermophilic mixed culture in MFC operation inoculum was acquired from formation water produced at a petroleum reservoir from an oil field in Niigata, Japan and it was the first study to report hyperthermophilic microorganisms' ability to oxidize organic substrates and transfer electrons to anode for the first time (Fu, Fukushima, et al., 2015). In the operated MFC, power density was highest at 95 °C among different operational temperatures (75 °C to 98 °C) reaching to 165 mW/m^2 (with current density 0.8 A/m^2 at this point) (Fu et al., 2015). In this study, archaeal growth was not detected this is the highest operational temperature reported with a bacterial community in a BES. Microbial community analysis showed one isolate closely related to the *Thermodesulfobacterium commune* of *Thermodesulfobacteriales* order to be dominant in the system and exoelectrogenic activity is attributed to this isolate (Fu, Fukushima, et al., 2015). This sulfate-reducing microorganism group was known to form a distinct lineage among bacteria (Hatchikian et al., 2015) as it is evident in the phylogeny tree constructed by using thermophilic and hyperthermophilic bacteria used in BESs (Figure 2.10). Single-layer biofilm formation on the anode observed with SEM and limited system performance was attributed to inadequate biofilm formation (Fu, Fukushima, et al., 2015). However, due to system quickly recovering the current production when media was replaced it was argued that *T. commune* related isolate did not require shuttling mediators to perform EET (Fu, Fukushima, et al., 2015). So far *T. commune* related isolate used in this study (Fu, Fukushima, et al., 2015) is the only hyperthermophilic bacteria to be shown to possess exoelectrogenic activity.

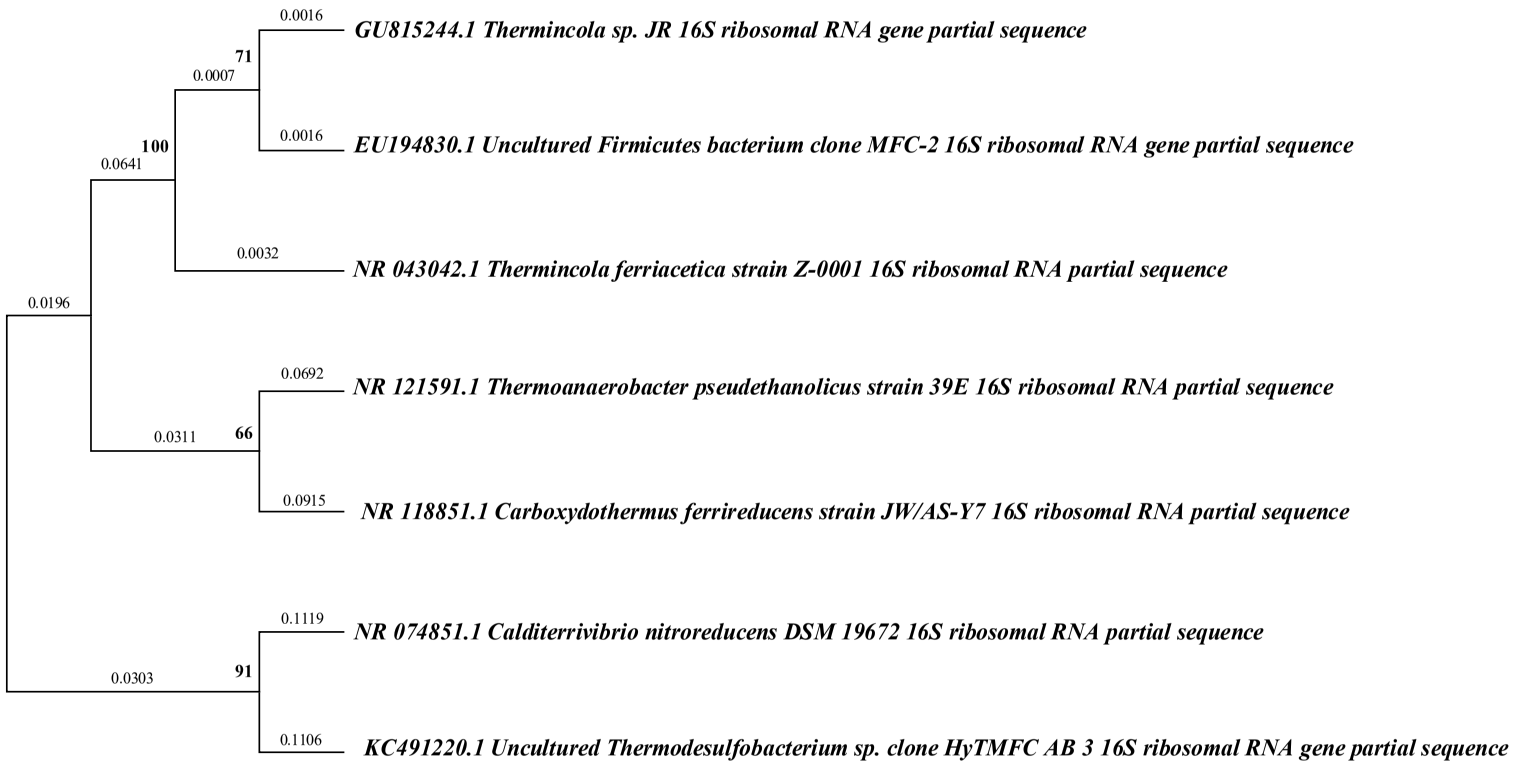

Figure 2.10. Phylogenetic tree constructed by using the Maximum Likelihood method (results described in Appendix A) based on the partial 16S rRNA gene analysis of pure culture exoelectrogenic thermophilic/hyperthermophilic bacteria used in BESs. The percentage of trees (≥50%) in which the associated taxa clustered together is shown next to the branch nodes on the basis of 2,000 bootstrap replications. GenBank accession numbers are given in brackets.

2.3.1.2 Electro-active Archaea

Besides the bacteria used for the purpose of EET, archaea have also been used in BESs. Similar to bacteria, exoelectrogenic archaea similarly have the ability to donate electrons to the anode and there are also electrotrophic archaea (such as methanogens) that can accept electron from cathode (Logan et al., 2019).

Archaeal cell wall structure contains an outer surface S-layer consisted of glycoproteins typically covers the surface (Figure 2.11 left) and certain methanogenic archaea also have an intermediate layer called pseudopeptidoglycan (Figure 2.11 right) consisted from polymers (Sleytr et al., 2014). Cell wall structure of archaeal species of *Geoglobus* and *Ferroglobus* genus shows typical single S-layer structure and these species were shown to possess EET capability previously (Hafenbradl et al., 1996; Kashefi et al., 2002). Members of *Methanothermobacter* genus was described for having an intermediate pseudopeptidoglycan layer (Visweswaran et al., 2011) and *M. thermautotrophicus* was also shown to be capable of EET (Hara et al., 2013). In short, there are microorganisms that could perform EET regardless of the type of cell wall structures in the archaea domain, and similar results was also observed for the gram-positive and gram-negative bacteria.

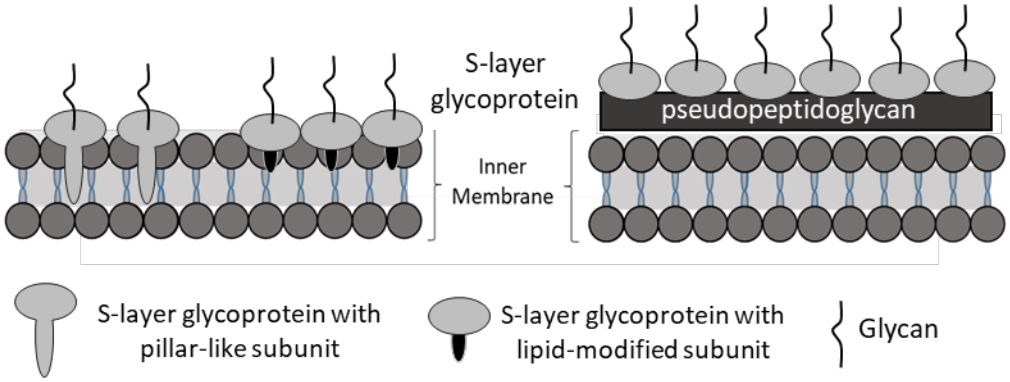

Figure 2.11. Typical cell membrane structures of archaea with single outer surface S-layer (left) or S-layer combined with intermediate pseudopeptidoglycan (pseudomurein) layer (right)

Electrotrophic archaea were only used in thermophilic studies (Fu, Kuramochi, et al., 2015; Hara et al., 2013; Kobayashi et al., 2017). On the other hand, so far only a small number of pure culture hyperthermophilic exoelectrogenic archaea were utilized in BESs (Table 2.2). They include closely related 2 species in the *Archaeaoglobales* order and one in *Thermococcales* order (Figure 2.12). Use of hyperthermophilic archaea have been suggested to possess immense potential in various industrial biotechnology applications due to the extremozymes that can act as biocatalysts (Egorova & Antranikian, 2005). In spite of this distinctive advantage, only small scale BESs that utilize hyperthermophilic archaea as exoelectrogens were reported so far. The number of studies and knowledge on using hyperthermophilic archaea is quite limited.

Table 2.2. Hyperthermophilic exoelectrogenic archaea in BES

Exoelectrogenic Archaea	Isolation/ Inoculum Source	BES Type	T (°C)	References
Pyrococcus furiosus	Geothermally heated marine sediment	MFC	90	(Sekar et al., 2017)
Ferroglobus placidus	Submarine hydrothermal vent	MEC	85	(Yilmazel et al., 2018)
Geoglobus ahangari	Hydrothermal system at a depth of 2000 m	MEC	80	(Yilmazel et al., 2018)
Archaeoglobales and *Thermocccales*	Deep-sea hydrothermal vents	MEC	80	(Pillot et al., 2018)

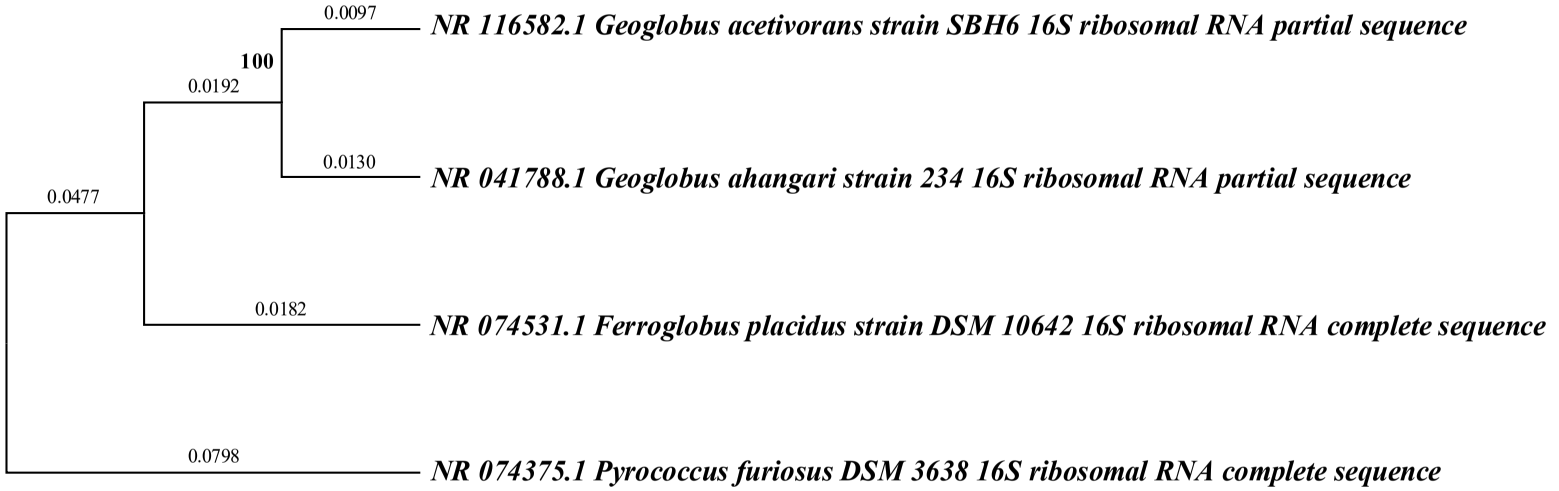

Figure 2.12. Phylogenetic tree constructed by using the Maximum Likelihood method (results described in Appendix A) based on the partial 16S rRNA gene analysis of pure culture exoelectrogenic hyperthermophilic archaea used in BESs. The percentage of trees (≥50%) in which the associated taxa clustered together is shown next to the branch nodes on the basis of 2,000 bootstrap replications. GenBank accession numbers are given in brackets.

2.3.1.2.1 Thermococcales

Pyrococcus furiosus, a hyperthermophilic archaea belonging to the order of *Thermococcales* was utilized in a two chamber MFC operated at 90 °C (Sekar et al., 2017). *P. furiosus* culture was originally isolated from a geothermally heated marine sediment (Fiala & Stetter, 1986). Tests were done with *P. furiosus* actively growing on a defined medium produced peak current density reaching to 0.67 A / m^2 (Sekar et al., 2017). Biofilm formation on the anode observed with SEM imagery, quick recovery of the peak currents after medium replenishment and no redox peaks in spent medium CV analysis that can be attributed to electron shuttles indicated *P. furiosus* is capable of DET (Sekar et al., 2017). Despite of the evidence supporting the DET capability of *P. furiosus* potential electron shuttles such as cysteine and sodium sulfide in the growth medium might have enabled mediated EET (Yilmazel et al., 2018) and the extent of current generation by DET is unknown. Suspension buffer fed reactors (pelleted and resuspended) produced a peak much faster than the actively growing reactors indicating that *P. furiosus* were using endogenous reducing equivalents produced during cultivation that it could not replace later (Sekar et al., 2017) Although the peak current was significantly lower, suspension buffer fed reactors produced a peak much faster than the actively growing reactors indicating that *P. furiosus* were using endogenous reducing equivalents produced during cultivation that it could not replace later (Sekar et al., 2017). This situation shows the first cycles during a BES operation with exoelectrogens might produce misleading results since such interfering chemicals might be produced during inoculation.

2.3.1.2.2 Archaeoglobales

Pure cultures of hyperthermophilic archaea of *Ferroglobus placidus* and *Geoglobus ahangari* are members of the *Archaeoglobales* order and isolated from submarine hydrothermal vent (Hafenbradl et al., 1996) and hydrothermal system at a depth of

2000 m (Kashefi et al., 2002) respectively. These hyperthermophilic archaea were utilized in single chamber MECs at the temperatures of 85 °C and 80 °C, respectively (Yilmazel et al., 2018). In order to test the reactor set-up and observe the impact of operational conditions a separate set with model exoelectrogen *G. sulfurreducens* were operated at 30 °C which produced current densities (1.9 A/m^2) that was consistent with an earlier study (Call et al., 2009). Current density of 0.68 ± 0.11 A/m^2 was achieved with *F. placidus* and 0.57 ± 0.10 A/m^2 with *G. ahangari* (Yilmazel et al., 2018). Low current generation with hyperthermophilic archaea when compared to *G. sulfurreducens* may be due to the lack the stress-related enzymes in hyperthermophiles which model exoelectrogen possesses (Yilmazel et al., 2018). Proton transfer and pH change was listed among the stresses on the anode surface that could have been resulted in low current generation similar to the challenges observed with *T. ferriacetica* operations (Lusk et al., 2016, 2018). CV analysis with sterile or spent medium suggested that no endogenous or external mediators were used in current production (Yilmazel et al., 2018). Although it was not proven, it was highly probable that both of the hyperthermophilic archaea are able to perform DET through *c*-type cytochromes since they have multiple genes for coding for putative *c*-type cytochrome proteins (30 for *F. placidus*, and 21 for *G. ahangari*) (Manzella et al., 2015; Smith et al., 2015). Also 3 times higher protein concentration at the anode biofilm compared to the surrounding medium was related to the electron transfer proteins (Yilmazel et al., 2018) such as *c*-type cytochromes. Members of *Archaeoglobales* and *Thermococcales* orders that showed taxonomic similarity to *G.ahangari* (99% and 95% respectively) enriched from the deep-sea hydrothermal vents showed higher current density reaching a maximum of 5.9 A/m^2 within a microbial organization similar to trophic chain (Pillot et al., 2018). It was suggested that rather than a hyperthermophilic pure culture BES application as previously done (Yilmazel et al., 2018), mixed culture inoculation with conditions that enriches the exoelectrogens would improve the current generation due to syntrophic activities of electro-active microorganisms (Pillot et al., 2018). Yeast extract included in the media were expected to be converted into acetate by

heterotrophic microorganisms (Pillot et al., 2018) but its presence might have induced mediated electron transfer through flavin-type compounds (Sayed et al., 2012). Therefore, the extent of the current production that could be attributed to DET mechanisms is not clear.

2.3.1.2.3 Geoglobus acetivorans

Geoglobus acetivorans SBH6 is a obligate anaerobic, hyperthermophilic, ferric iron reducing archaeal specie isolated from a hydrothermal vent at a depth of 4100 m (Slobodkina et al., 2009). *G. acetivorans* is the one of the two members of *Geoglobus* genus (Kashefi et al., 2002; Slobodkina et al., 2009) and both species are dependent on dissimilatory iron reduction. This specie can utilize various substrates including acetate, aromatic compounds or molecular hydrogen with this Fe(III) reduction (Mardanov et al., 2015).

Dissimilatory iron reducers were suggested to perform EET (Kim et al., 1999) were seen to apply to most exoelectrogens so far (Logan et al., 2019) including thermophilic bacteria *T. ferriacetica* (Lusk et al., 2015; Parameswaran et al., 2013) and hyperthermophilic archaea *F. placidus* (Hafenbradl et al., 1996; Yilmazel et al., 2018), *G. ahangari* (Kashefi et al., 2002; Yilmazel et al., 2018) and *P. furiosus* (Sekar et al., 2016; Sekar et al., 2017). There are also some exceptions to iron reducers such as *Pelobacter carbinolicus* which was unable to produce current in MFCs (Richter et al., 2007).

F. placidus and *G. ahangari* of *Archaeaglobales* order was used in hyperthermophilic MECs successfully and two new hyperthermophilic exoelectrogenic species were introduced in a recent study (Yilmazel et al., 2018). Together with *P. furiosus*, they consist of all known hyperthermophilic exoelectrogens to date.

G. acetivorans, is another member of *Archaeoglobales* order. This specie shares significant similarities with *G. ahangari* (97% identical in 16S rRNA genes)

(Manzella et al., 2015) and with *F. placidus* share more than half (57%) of the *c*-type cytochrome sequences used in dissimilatory Fe(III) reduction (Smith et al., 2015). Additionally, this specie was known to possess pili-like appendages for binding to insoluble iron particles during dissimilatory iron reduction (Mardanov et al., 2015) (Figure 2.13). Because of these similarities, pure culture of *G. acetivorans* were studied in this thesis as it provided a high potential to show exoelectrogenic activity in hyperthermophilic MECs.

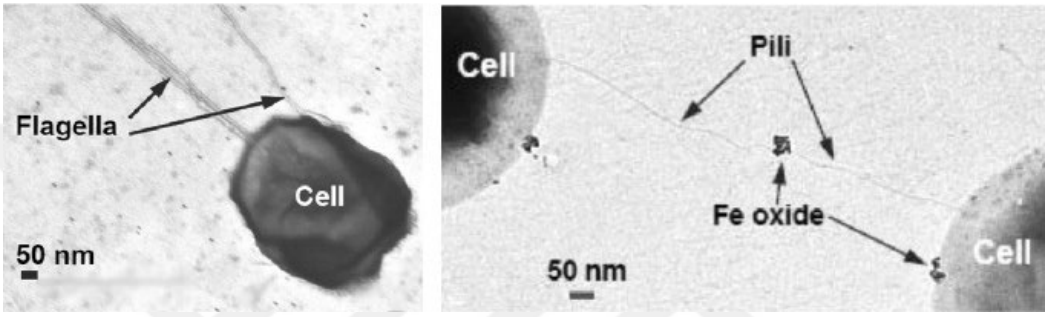

Figure 2.13. Electron micrographs of *G. acetivorans* cells; cell morphology and flagella (left) and pilus-like appendages used in dissimilatory iron reduction (right) (adopted from Mardanov et al., 2015)

2.3.2 Fermentative Process Effluent as Electron Donor Source at High Temperature BESs

Use of any complex waste or process effluent materials in high temperature MECs are a rare occurrence in the literature. There are only 3 studies reporting complex wastes utilization in high temperature MECs to the best of our knowledge. These applications were done exclusively in the thermophilic temperature range and at hyperthermophilic conditions no studies were carried out yet. Details of the implementation and the outcomes are summarized in Table 2.3.

Various exoelectrogens were reported to have the ability to donate electrons to anode by utilizing acetate (Call & Logan, 2011; Fu et al., 2013; Lusk, Khan, et al., 2015; Sekar et al., 2017; Yilmazel et al., 2018). During DF, hydrogen gas and effluents

with high organic acid content including acetate as a major end product are produced from organic substrates (Thauer et al., 1977). Implementing BES to DF, especially an MEC system into this well-known process can provide many operational advantages since they share common goal of hydrogen production. Therefore, using complex organic substrates such as effluent of dark fermentation process could provide significant advantages. Incorporating other treatment methods for extracting remaining energy in the waste stream otherwise that would be discarded, could decrease the costs associated with the disposal and improve overall efficiency compared to use of different systems separately.

In the first report of two-stage DF and MEC system *Clostridium thermocellum* was used as the fermentative bacterium to degrade the corn-stover lignocellulose and cellobiose (Lalaurette et al., 2009). Electrodes used in MEC reactors were acclimated for 2 months. During acclimation in MFC reactors, a wastewater inoculum was either fed with single pure substrates or their mixture representing a synthetic fermentative effluent (54% acetate, 29% ethanol, 12% succinic acid , 4% lactic acid, 1% formic acid) in 5 different MFC sets (Lalaurette et al., 2009). Although the fermentative reactors included electron mediators such as resazurin and yeast extract, highest current density of 0.146 A/m^2 (originally reported as 1.15 ± 0.05 A/m^3) was observed with an MEC using a synthetic effluent (Lalaurette et al., 2009) that excluded such mediating compounds. Hydrogen yield for cellobiose fed fermentative reactors and MEC reactors utilizing this effluent were reported as 1.64 and 8.31 mole H_2 / mole glucose respectively and the overall yield of the DF and MEC integrated system was significantly increased to 9.95 mole H_2/ mole glucose (Lalaurette et al., 2009). According to these results, it could be argued for the treatment of recalcitrant lignocellulosic materials combining DF and MEC at thermophilic temperatures could be an effective alternative.

Another study that shows the utilization of fermentation effluent in MECs, fed cassava starch processing wastewater into a DF reactor inoculated with a pure culture fermentative bacteria, *Thermoanaerobacterium thermosaccharolyticum PSU-*

(Khongkliang et al., 2017). This fermentative bacteria was previously reported for its ability to utilize various types of substrates and acid tolerance (O-Thong et al., 2008). MEC reactors were fed with the effluent of the DF operation and inoculated with a thermophilic mixed culture enriched from peatland soil (Khongkliang et al., 2017). Comparison between only MEC and DF followed up by MEC operation showed that; MEC reactor in the successive operation (205 ml H_2 / g COD) performed slightly better than the single-stage MEC (185 ml H_2 / g COD) (Khongkliang et al., 2017). Hydrogen generated at DF stage was 260 mL H_2 / g COD resulting in a total of 465 mL H_2 / g COD from cassava starch wastewater (Khongkliang et al., 2017). Even with an external voltage application of 0.1 V a significant amount of hydrogen gas was produced 106 mL H_2 / g COD (Khongkliang et al., 2017) where production through HER at the cathode is not possible at this potential. Hence, a significant portion of the hydrogen gas production could be a result of further fermentative activity by the mixed culture inoculum. *Geobacillus sp.*, *Caloranaerobacter sp.* and *Brevibacillus sp.* were the dominant bacteria where exoelectrogenic activity at the anode were attributed to these unidentified species (Khongkliang et al., 2017). It was argued that all of these bacteria contributed to current generation to certain extent (Khongkliang et al., 2017) but EET capable species for this mixed culture or the EET mechanisms were not investigated. Contribution by *Brevibacillus sp.* could be limited since in a MFC study that was operated with a member of *Brevibacillus sp.* genus in their anodes resulted in weak electricity generation and needed to be supplemented with the electron mediators produced by the MFCs operated with a *Pseudomonas sp.* (Pham et al., 2008). Meanwhile one of the two known members of the *Caloranaerobacter* genus; *Caloranaerobacter ferrireducens* was said to use Fe (III) reduction pathway for various substrates (Zeng et al., 2015) and exoelectrogens are said to be typically from iron- reducing microorganisms (Logan et al., 2019). Similar configuration of DF-MEC integrated system was used to treat palm oil mill wastewater effluent with external voltages applied between 0.2 V to 0.9 V to MEC reactor at 55 °C (Khongkliang et al., 2019). Although the current densities, EET mechanisms were

not investigated in this study, hydrogen yield increased from 73 ml H_2 / g COD produced only from DF to 236 ml H_2 / g COD with the DF-MEC integrated system at 0.7 V external voltage application (Khongkliang et al., 2019). A group of microorganisms including *Shewanalla sp.* and *Geobacillus sp.* were dominant in the anodic biofilm depending on the elapsed operation time and exoelectrogenic ability was attributed to these unidentified species (Khongkliang et al., 2019).

One case of DF-MFC application showed that overall yield or high rates of utilization of DF effluents is not the case for every application. MFCs operated at mesophilic temperatures and fed directly with wastewater performed better than the MFCs fed with DF effluent of same wastewater (Vemuri et al., 2021). Although this study used BESs operated at mesophilic temperatures, it was argued that during the thermophilic DF process easily degradable organics were utilized steadily and the effluent was left with only recalcitrant organic material at much lower COD values (Vemuri et al., 2021). Therefore, adjusting the dosage and the compatibility with the electron donors resulting from the DF process should be taken into serious account also in high temperature BES applications.

Implementing the well-studied bioconversion technology of AD with a newly emerging MFC system was also suggested at the early stages of bioelectrochemical studies (Pham et al., 2006) and ever since then there are many instances of integrated systems operated at mesophilic temperatures (Ge et al., 2013; Liu et al., 2011; Xiao et al., 2011). However, interactions between the DF-MEC or the use of similar process effluents high in organic acids require more work to understand the benefits of integrating BES to other bioconversion methods especially at high temperatures.

Table 2.3. Configuration and outcome summary for high temperature process effluent utilization in BES

MEC/MFC Substrate	MEC/MFC Inoculum	T (°C)	Outcomes	Reference
DF effluent of corn-stover feedstock	Bioelectrodes acclimated in MFCs to individual substrates within DF effluent	50	Highest current density with synthetic effluents without electron mediators. Overall hydrogen yield increased 6 times with MEC implementation.	(Lalaurette et al., 2009)
DF effluent of cassava starch processing wastewater	Peat soil sample	55	MECs used after DF performed better than MECs fed directly with the process effluent. Overall yield increased more than 2.5 times.	(Khongkliang et al., 2017)
DF effluent of palm oil mill effluent	Peat soil sample	55	Overall hydrogen yield increased more than 3 times. External voltage optimization studies found 0.7 V for optimum hydrogen production.	(Khongkliang et al., 2019)

2.4 Remarks

Direct comparison between the performance indicators are not possible without same reactor configuration, materials and operational conditions in BESs (Logan et al., 2019). Nonetheless visualizing performances of these applications could provide information on the progress with their respective electro-active species in BESs. The most commonly studied microorganisms in BESs are various *Geobacter* spp. and *Shewanella* spp. These species and other exoelectrogens mostly isolated at mesophilic temperatures but thermophilic or hyperthermophilic microorganisms have been known to possess exoelectrogenic abilities. Scarcity of high temperature BES studies produces a significant gap in terms of identifying the model exoelectrogenic microorganisms. Hyperthermophilic electro-active microorganisms were almost exclusively identified in the archaea domain including the species from *Archaeoglobales* and *Thermococcales* orders. Effective electrochemical interaction between living cells and electrodes is a complex event, which leads to creation of a strong basis for optimization and rational use of materials and an improved performance of bioelectrochemical systems and implementation into real-life applications. Similar to other alternative energy technologies, ultimate goal of high temperature BESs would be to enable widespread adaptation of the technology and larger scale operations. With that in mind, how thermophiles and hyperthermophiles could provide desirable advantages for industrial applications that are cost-effective and offer simplified design for larger scale should be investigated. In order to have a successful large scale application, cost of operating at higher temperatures should be compensated with well optimized systems that can compete with other bioenergy technologies. Currently treatment starting from a waste feed or complex substrate is common practice for mesophilic integrated systems while thermophilic and hyperthermophilic single-stage BESs mostly work with easily degradable substrates such as acetate. There is a need for research on the capability of using process effluents or complex wastes in (hyper)thermophilic applications. So far, factors affecting the BES operation in these integrated systems were not investigated

thoroughly. Further research on the thermophilic or hyperthermophilic BESs are needed to suggest efficient system designs. Identification of optimum operational conditions is required for larger scale applications and eventually widespread adaptation of high temperature BES technologies.

CHAPTER 3

MATERIALS AND METHODS

3.1 Microorganisms and growth mediums

Geoglobus acetivorans SBH6 (DSM 21716), *Ferroglobus placidus* strain AEDII12DO^{T} (DSM10642) and *Geobacter sulfurreducens* strain PCA (DSM 12127) were obtained from the Leibniz Institute DSMZ-German Collection of Microorganisms and Cell Cultures in the actively growing culture form (Figure 3.1). Hyperthermophiles used in this study were isolated from hydrothermal vents; *G. acetivorans* was originally isolated from fragment of hydrothermal structure, 4100 m depth (Slobodkina et al., 2009) and *F. placidus* was originally isolated from a shallow submarine hydrothermal system located in Vulcano, Italy (Hafenbradl et al., 1996). The mesophilic bacteria, *G. sulfurreducens* was isolated from surface sediments of a hydrocarbon-contaminated ditch (Caccavo et al., 1994).

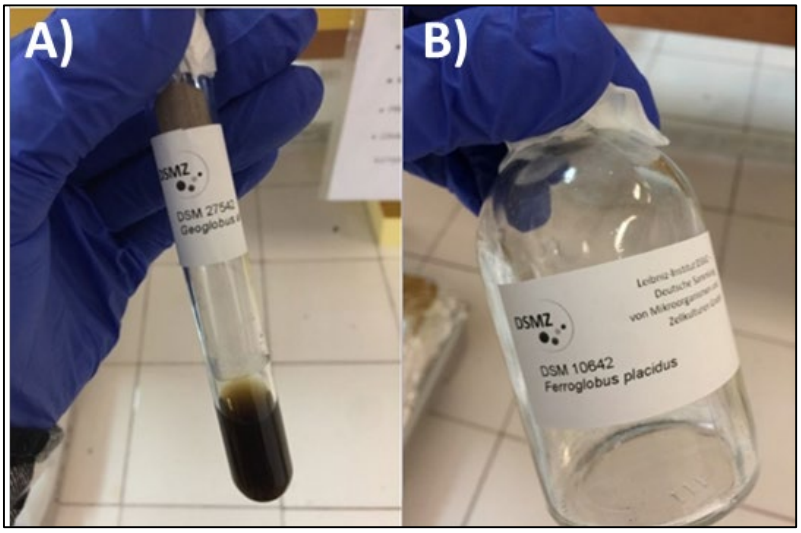

Figure 3.1. Actively growing cultures of *G. acetivorans* (A) and *F. placidus* (B) acquired from DSMZ

G. acetivorans and F. placidus were initially grown with 10 mM acetate as electron donor and 56 mM Fe(III)-citrate (Part number: F3388, Sigma, US) as electron acceptor. Hyperthermophilic growth medium contained $MgCl_2 \cdot 6H_2O$, 4.3 g; NaCl, 18 g; $CaCl_2 \cdot 2H_2O$, 0.14 g; KCl, 0.34 g; KH_2PO_4, 0.4 g; NH_4Cl, 0.24 g; $NaHCO_3$, 5 g; vitamin solution, 10 mL; and trace element solution, 10 mL per liter of medium (Table 3.1). Initially, deionized water was heated to 95 °C to ensure complete dissolution of ferric citrate then solution was placed in an ice bath and the other components were added at room temperature (Figure 3.2).

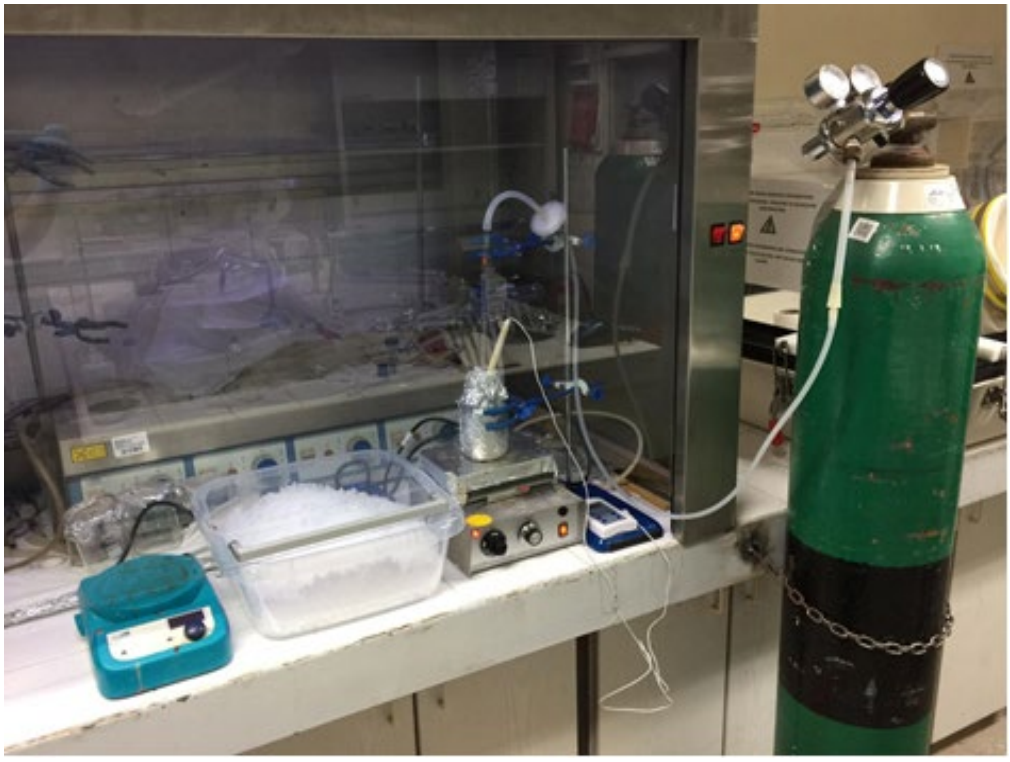

Figure 3.2. Setup for the hyperthermophilic electro-active archaea growth medium (ferric citrate solution) preparation

G. sulfurreducens was initially grown in slightly modified DSMZ Medium 826 containing 10 mM sodium acetate as electron donor, 50 mM sodium fumarate (Part number: F1506, Sigma, US) as electron acceptor and 30 mM sodium bicarbonate as

buffer. Trace element and vitamin solutions were used from the stocks previously prepared for the hyperthermophilic microorganisms (Table 3.1). Concentration of other chemicals for *G. sulfurreducens* growth are NH_4Cl, 1.5 g; Na_2HPO_4, 0.6 g; KCl, 0.1 g; vitamin solution, 10 mL; and trace element solution, 10 mL per liter of medium.

Table 3.1. Hyperthermophilic electro-active archaea growth medium

Salts		**Buffer**		**Electron Donor**		**Electron Acceptor**	
NH_4Cl	0.24 g/L	$NaHCO_3$	5 g/L	Na-Acetate	8.2 g/L	Ferric Citrate	13.7 g/L
KH_2PO_4	0.4 g/L						
$MgCl_2•6H_2O$	4.3 g/L						
$CaCl_2•2H_2O$	0.14 g/L						
NaCl	18 g/L						
KCl	0.34 g/L						

Vitamins		**Trace Elements**	
		Nitriloacetic Acid	1.5 g/L
		$MgSO_4.\ 7H_2O$	3 g/L
		NaCl	1 g/L
Pyridoxine-HCl	10 mg/L	$MnSO_4.\ 7H_2O$	0.5 g/L
Thiamin-HCl	5 mg/L	$NiCl_2.\ 6H_2O$	0.2 g/L
Riboflavin	5 mg/L	$FeSO_4.\ 7H_2O$	0.1 g/L
Nicotinic Acid	5 mg/L	$CoCl_2$	0.1 g/L
Calcium Pantothenate	5 mg/L	$CaCl_2.\ 2H_2O$	0.1 g/L
Vitamin B12	5 mg/L	$ZnSO_4$	0.1 g/L
p-Aminobenzoic Acid	5 mg/L	$CuSO_4.\ 5H_2O$	0.1 g/L
Lipoic (Thioctic) Acid	5 mg/L	$AlK\ (SO_4)_2$	0.01 g/L
Biotin	2 mg/L	H_3BO_3	0.01 g/L
Folic Acid	2 mg/L	$Na_2MoO_4.\ 2H_2O$	0.01 g/L
		Na_2SeO_3	0.01 g/L
		Na_2WO_4	0.01 g/L

All glassware was sterilized via autoclaving at 121 °C for 15 minutes prior to use. Solutions were sparged and the headspace of the media bottles were purged from oxygen using N_2:CO_2 gas mixture (80%:20%). Liquid transfers for merging of the growth medium and inoculations were done inside an anaerobic chamber (model no: 818-GB, Plas Labs, MI, USA, Figure 3.3) that had an inner atmosphere of high purity nitrogen gas. All liquids were sterilized with either autoclaving at 121 °C for 15 minutes or with the use of 0.22 µm pore size polyethersulfone (PES) syringe filters. All culture tubes were incubated in dark; *G. acetivorans* at 80 °C, *F. placidus at* 85 °C and *G. sulfurreducens* at 35 °C. Strict anaerobic culturing and sampling techniques were used throughout the experiments. The pH of the growth mediums was measured with a pH meter (model number: HQ11D, Hach, USA) and recorded as 7.0 ± 0.1. To make the solutions neutral, HCl (1N) or NaOH (10% w/v) solutions was used for pH adjustments. All solutions were stored at 4 °C in the dark until they were used.

Figure 3.3. Anaerobic chamber used throughout the experiments

3.2 Initial Growth of Pure Culture Exoelectrogens

3.2.1 Oxygen Leakage Tests

In order to ensure that the hyperthermophilic archaea, which are obligate anaerobes, can grow in a suitable environment and to prevent oxygen penetration to the reactors, oxygen leakage tests were conducted for both culture tubes and fabricated MECs. In these leakage tests, a redox sensitive chemical resazurin (part number: R7017, Sigma-Aldrich, USA) was used. The working mechanism of this indicator can be briefly summarized as follows; it shows blue-violet color in inactive form and shows pink color in the presence of oxygen and takes a transparent form (no color) in anaerobic environment (Wagner et al., 2019). Liquid transfers were conducted inside the anaerobic chamber, all bottles were flushed from oxygen with N_2:CO_2 gas mixture (80%:20%). Butyl rubber stoppers were recommended by DSMZ and shown to be effective against any oxygen leakage in the culturing of obligate anaerobic microorganisms (DSMZ, 2002). To make the liquid transfers, repeated piercing of the butyl stoppers (Part Number: CLS 4209-14, Chemglass, USA) using sterile needle and direct pipette transfer of liquid without using syringes were tested (Figure 3.4). Results showed that liquid transfer between anaerobic bottles inside the anaerobic chamber is mandatory and it is important to use syringes while avoiding repeated puncturing. In the case of repeated puncturing is absolutely necessary (*e.g.* during reactor operation) reactors were purged with anoxic gases to remove any oxygen from the headspace.

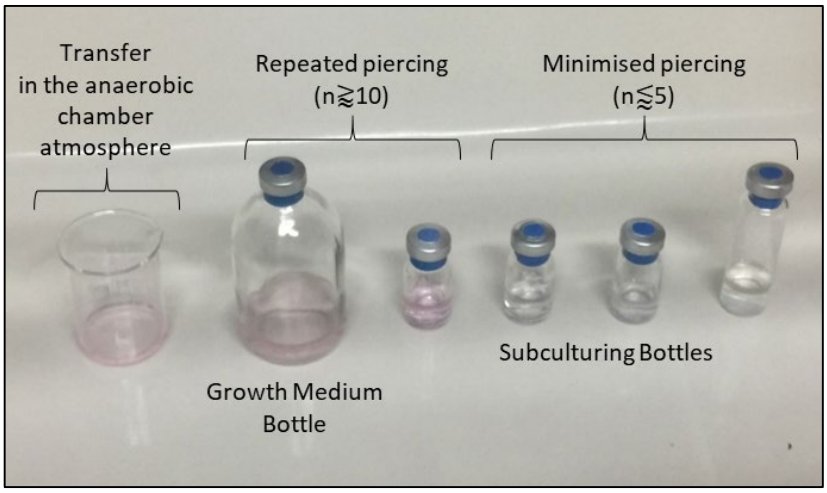

Figure 3.4. Oxygen leakage tests inside the anaerobic chamber using resazurin indicator

3.2.2 Initial Growth of Hyperthermophilic Electro-active Archaea

Actively growing exoelectrogen pure culture samples supplied by DSMZ were grown by ensuring anaerobic and sterile conditions, taking into account the special instructions published by this organization (DSMZ, 2002). Some modifications to the growth mediums recommended by DSMZ for the cultures were made. The reason is that the recommended DSMZ medium contains possible electron mediators such as nitrate, cysteine and sodium sulfide and eliminating such potential mediators is required to investigate the mechanism of EET (Yilmazel et al., 2018). For hyperthermophilic exoelectrogenic archaea, *F. placidus* were successfully grown with the same growth media in a previous study (Yilmazel et al., 2018) and *G. acetivorans* was successfully grown with the same solution during this study. Inoculated *G. acetivorans* bottles were placed into a high temperature incubator (model no: 51028717, ThermoFisher Scientific, USA) set to 80 °C. The growth solution used was prepared shortly before the cultures were acquired. It is known that these exoelectrogens can also use hydrogen as an electron donor coupled with CO_2 utilization as carbon source (Hafenbradl et al., 1996; Kashefi et al., 2002;

Slobodkina et al., 2009). Thus, during the initial growth of hyperthermophilic exoelectrogens half of the inoculated bottles were pressurized with a mixture of H_2:CO_2 gas mixture (80%:20%) after sterilization. In order to support their faster growth and survival inoculated bottles containing both hydrogen and acetate have been prepared. Inoculations were made at 1:10 and 1:100 ratios taking into account the specific instructions published by DSMZ, and the general trend observed was that growth was faster in 1:10 and hydrogen pressurized serum bottles (data not shown). Inside of the anaerobic chamber was sterilized with ethanol before and after each session and to prevent cross-contamination between the hyperthermophilic exoelectrogens, subculturing was done in different sessions for each archaeon. Between the sessions each laboratory supply has been either replaced with a new one (such as serum bottle, syringe etc.) or sterilized, and the anaerobic chamber has been sterilized.

G. acetivorans were reported to reduce the soluble iron (III) in the form of ferric citrate although providing slower growth than the insoluble iron (III) oxides (Slobodkina et al., 2009). Growth was observed with acetate consumption, concentration of reduced iron forms (*i.e.* ferrous iron) and the colour change/precipitate formation due to the iron reduction coupled to acetate oxidation. Procedure for acetate and ferrous iron measurements are described in details in Chapter 3.4.3 and 3.4.4 respectively. During the initial subculturing of the hyperthermophilic archaea, uninoculated ferric citrate medium was also placed at 80 °C to act as control group. No colour change or precipitates were observed in the control medium similar to the findings of previous incubation study (Slobodkina et al., 2009) and in the inoculated bottles solution colour turned from transparent dark brown to olive green colour with black precipitates formed (Figure 3.5).

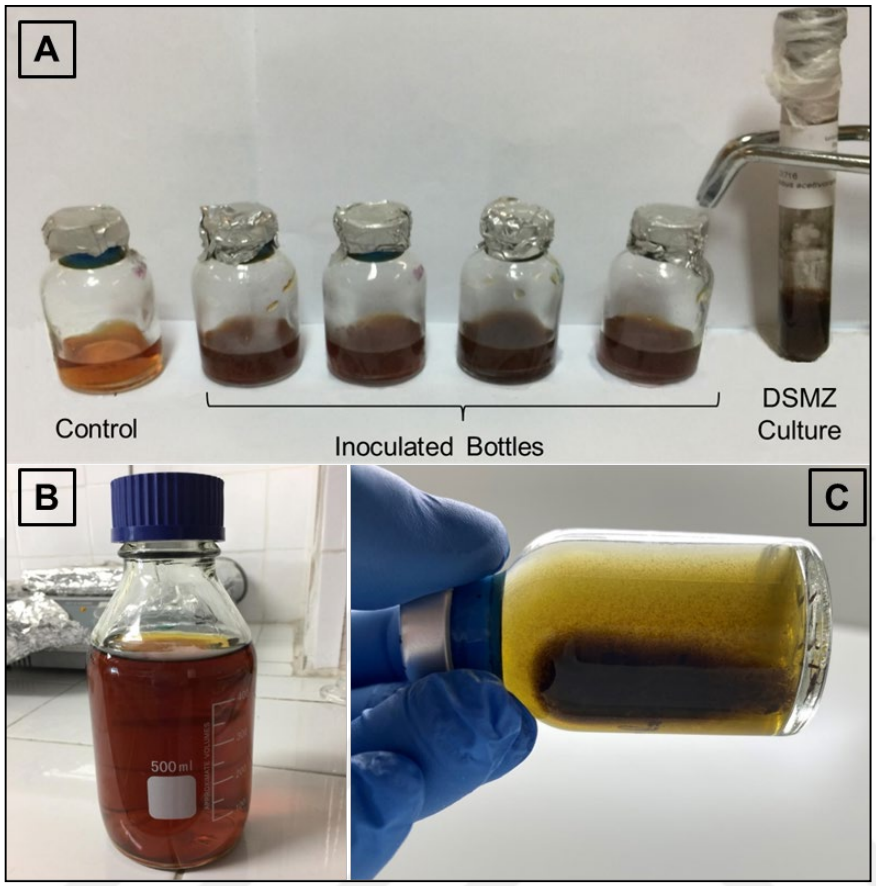

Figure 3.5. Initial growth of *G. acetivorans* culture; **A**: Uninoculated control, inoculated bottles (t = 12 h) and actively grown DSMZ culture, **B**: Ferric citrate medium, **C**: Precipitates formed and colour change due *G. acetivorans* growth

This precipitate formation and colour change were consistent for all subculture samples of *G. acetivorans* and Figure 3.6 presents the colour change in *G. acetivorans* culture tubes. Similarly, visible pink aggregates were observed in the subculturing of *G. sulfurreducens* (Figure 3.7) while no aggregate was observed in the control medium at 35 °C. Visual methods were also previously used for *G. sulfurreducens* where visible formation of pink layer of the cells were to show readiness of the culture prior to reactor inoculation (Liu et al., 2020) .

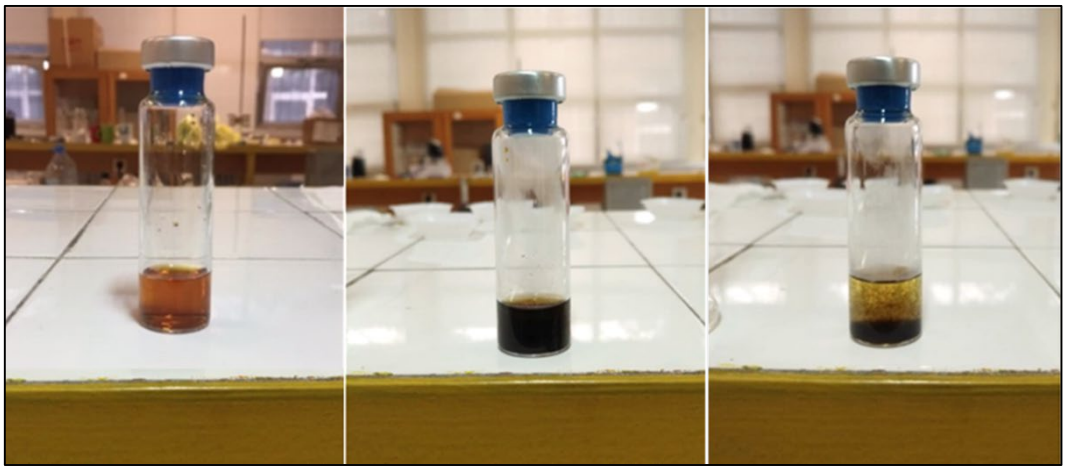

Figure 3.6.*G. acetivorans* subculture bottle at; t=0 (left), at t = 12 h (center) and t = 24 h (right)

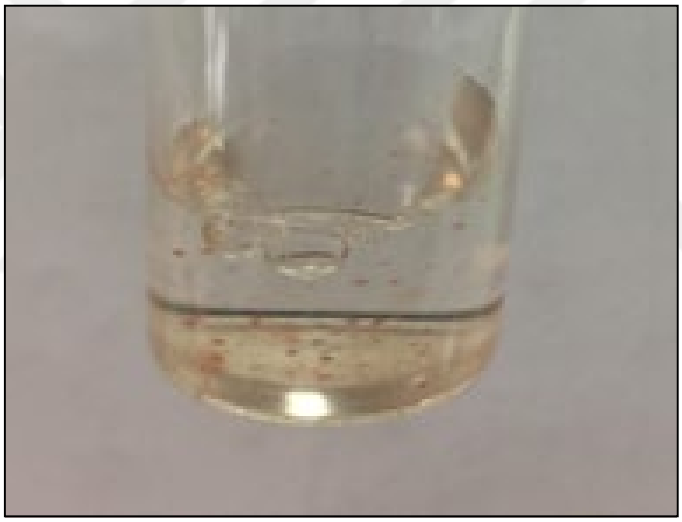

Figure 3.7. Pink aggregates of *G. sulfurreducens* after incubation at t = 24 h

3.3 MEC Construction and Operation

3.3.1 MEC Reactor Materials and Configuration

Single chamber MEC reactors, 5 mL so called Mini-MECs were constructed with materials as described previously (Yilmazel et al., 2018). MEC media contained the

exact components of corresponding growth solutions in the absence of any electron acceptors (*i.e.* ferric citrate and sodium fumarate). For the second set of experiments with *G. acetivorans*, Mid-Size MEC reactors (15 mL) were assembled and the same materials with slightly larger size were prepared through identical processing. Anode material used in the experiments was graphite plate and cathode electrodes were stainless steel mesh (type 304, mesh size 50x50) (Figure 3.8). Electrode surface areas (same for anode and cathode) were 4.5 cm^2 in Mini-MECs and 5.8 cm^2 in Mid-Size MEC reactors. To ensure consistent bioelectrochemical operation, contact resistance of the electrodes was set below 2 Ω. Graphite electrodes were sandpapered using 400, 1200 and 2000 grit size sandpapers and left overnight in 1N HCl. SS Mesh electrodes were sandpapered with the same grit sizes and sonicated with deionized water. After processing all electrodes had contact resistance around 0.7 Ω. Electrodes were connected to conductive wiring and pierced through the butyl rubber stopper. Titanium and stainless steel wiring in 0.7 mm diameter was used for connecting graphite plate and stainless steel mesh electrodes respectively.

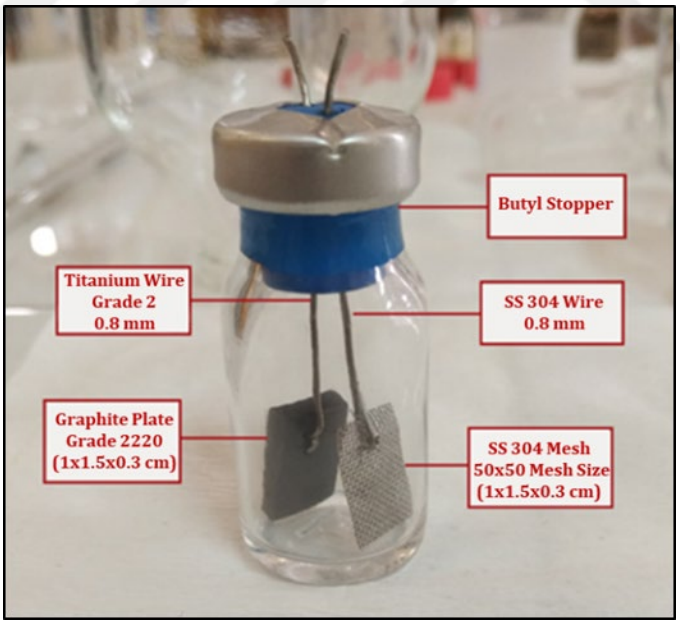

Figure 3.8**.** Mini-MEC reactor configuration used in this study

3.3.2 MEC Operation

Reactors for *G. acetivorans* experimental sets (AT and M-AT) were operated at 80 °C and filled with MEC media for hyperthermophilic archaea (80% of active volume) and *G. acetivorans* culture (20% active volume).

Reactors for *G. sulfurreducens* experimental set (GS) was filled with modified 4 mL DSMZ Medium 826 in the absence of sodium fumarate and inoculated with 1 mL of actively growing *G. sulfurreducens* culture and operated at 35 °C in the dark.

The operation mode of the MECs were fed-batch; reactor content was replaced with new media through piercing the stopper, when the current drops below a certain value. It was initially planned this value being approximately 25% of the peak current value, however, current production by *G. acetivorans* MECs showed a behavior of levelling out to a minimum value after following a sharper decrease and media replacements were based on the time closest to this observed behavior. Media replacements was done around 50% to 70% and 65% to 80% of the peak current density, for Mini-MECs and Mid-Size MECs respectively. For *G. sulfurreducens* MECs this media replacement process was done near the 25% of the peak current value.

A cycle represents the time passed between the feeding of the reactors until its replacement. Initially in the first cycles 80% of the liquid inside the reactor was replaced and later all liquid was replaced with fresh medium between cycles. Media replacements were done inside the anaerobic chamber by piercing the butyl stopper using sterile needle and after media replacement the reactor headspace was purged with N_2:CO_2 gas mixture (80%:20%). All MECs were operated at an applied voltage of 0.7 V.

Electrochemical activity on the bioanode was observed with continuous measurements of DC voltage acquired with the help of a 10 Ω resistor connected in series to the cables connecting to the anode (Figure 3.9). Voltage at the resistor

connected to anode cables was recorded by a data acquisition unit (model no: 34972A, Keysight Technologies, USA) equipped with a 20-channel multiplexer (model no: 34901A, Keysight Technologies, USA) at 10 min intervals.

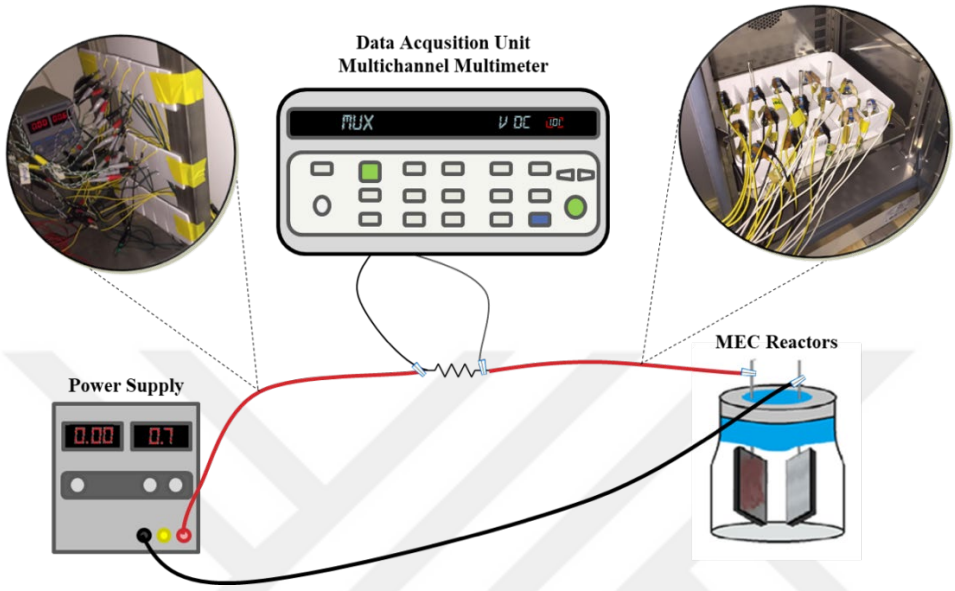

Figure 3.9. Experimental set-up used for the external voltage application and current monitoring during incubation of MECs

3.3.3 Operational Parameters and Stages of MEC Experimental Sets

3.3.3.1 Mini-MEC Reactors

G. acetivorans Mini-MEC set (referred to as AT) were operated as triplicate while *G. sulfurreducens* Mini-MEC set (referred to as GS) operated as quadruplicate. Both AT and GS sets included 4 different experimental groups including: (1) Abiotic control, (2) open-circuit control, (3) acetate control and (4) active reactors (Table 3.2). Aim of the AT set is to test whether *G. acetivorans* culture can be utilized in a BES as a new exoelectrogenic specie. Graphite plate was intended to act as electron acceptor if *G. acetivorans* could oxidize acetate and donate electron donors to the anode. This configuration was selected in order to relate the results to the previous study with closely related species (Yilmazel et al., 2018)

Table 3.2. Summary of AT and GS Experimental Sets

Reactor Group	Abiotic Control	Open Circuit Control	Acetate Control	Active Reactors
Inoculum	-	*G. acetivorans* *or* *G. sulfurreducens*	*G. acetivorans* *or* *G. sulfurreducens*	*G. acetivorans* *or* *G. sulfurreducens*
External Voltage	0.7	-	0.7	0.7
Electron Donor	Acetate	Acetate	-	Acetate
Explanation	Determining the noise caused by media in abiotic controls.	To show that the hydrogen gas, produced in the test reactors is due to EET done by the exoelectrogens.	To show the effect of acetate originating from the inoculum to current and hydrogen production.	Hydrogen gas production, current production and biofilm formation are expected to be observed in MECs reactors fed with simple substrate.

After the completion of AT set operation, 3 different time periods were identified (Figure 3.10) based on the current production data. These periods are named as start-up period, biofilm formation period and test period. The "Start-up" period, lasted for 7 days after the first inoculation and the current density production in the Acetate Control (3) group were notable indicating the acetate originating from the inoculum liquid was still present in the reactors and contributing to the current production. Control group reactors were not expected to generate a significant amount of current or hydrogen gas after the initial inoculation and start-up since the electron donor (acetate) coming from the inoculum was quickly depleted. After current density decreased for acetate control, all reactors were operated for 30 days until high degree of replication (coefficient of variation < 5%) in current densities were achieved in a period identified as "Biofilm Formation". After evidence of biofilm formation on the anode electrodes was observed (day 37), 8 more cycles of operation were completed (day 55) in the "Test" period. Hydrogen and current production were measured throughout the operation; CV and SEM analysis of the biofilm were conducted after the test period was completed.

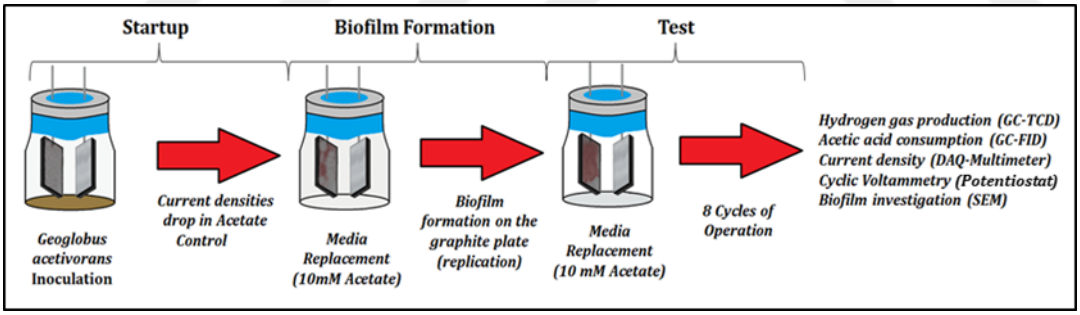

Figure 3.10. Three periods of reactor operation identified for *G. acetivorans* MECs

GS set is operated in a similar way to a previous work in Mini-MECs (Yilmazel et al., 2018). The reason to include *G. sulfurreducens* set is to assess whether the mini MEC configuration and the materials used in this thesis were comparable to the literature; since *G. sulfurreducens* is identified as a model exoelectrogenic

microorganism (Logan et al., 2019). Besides the current and hydrogen production, various supplementary analysis such as cyclic voltammetry (CV), scanning electron microscopy (SEM) imaging and protein measurements were conducted for mini MEC sets.

3.3.3.2 Mid-Size MEC Reactors

Mid-size MEC reactors (15 mL) for *G. acetivorans* (referred as M-AT) were operated with 4 replicates for the active reactors, 2 replicate for hydrogen cycling test and triplicate reactors for acetate controls (see Table 3.2 for reactor details). AT set open circuit control group (for hydrogen) and abiotic control group (hydrogen and current) did not produce any significant results. Therefore, these control groups were not included in this reactor set due to the fact that they use same reactor materials, inoculum, media and inoculum ratio. Main aim of this reactor set was to test the scaling up potential of this single chamber MECs inoculated with *G. acetivorans*. Same periods described in Figure 3.10 were also observed for this reactor set. After high level of replication is achieved, operation was branched out to test (i) the impact of increased acetate dosage, (ii) the potential for utilization of dark fermentation effluent as acetate source and (iii) the potential for internal hydrogen cycling (Figure 3.11). This reactor set was also used for various analysis including cyclic voltammetry (CV), scanning electron microscopy (SEM) and protein analysis.

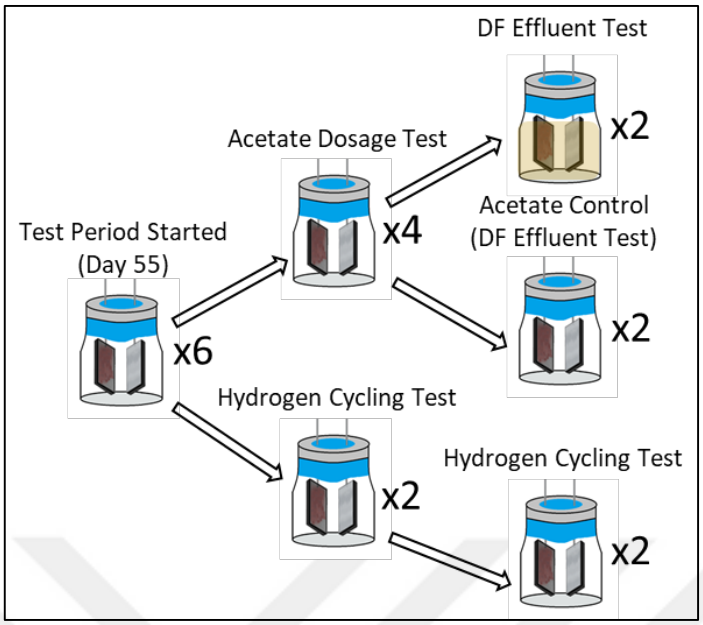

Figure 3.11. Various test conducted during the M-AT reactor set

In the substrate dosage test, immediately after high level of replication occurred dosage of acetate was increased to 20 mM from 10 mM.

During the tests with dark fermentation (DF) effluent, 2 test reactors were fed with DF effluent that was diluted in order to have the required acetate concentration. Other set of duplicates were fed with MEC medium containing pure acetate to act as control groups. DF effluent was sparged with high purity nitrogen gas and sterilized with 0.22 µm pore size PES syringe filters before being added into the MEC media in order to ensure the hydrogen gas production is due to the activity of exoelectrogens. For cycles operated with 10 mM acetate, DF effluent was diluted so that its final acetate concentration was 10 mM. Same applies for 20 mM acetate cycles.

Furthermore, 2 Mid-Size MEC reactors were used to test the phenomenon known as hydrogen cycling where hydrogen produced at the cathode was utilized by the bioanode as electron donor when proton selective membrane is not present in the BESs (Lee & Rittmann, 2010). This way self-produced hydrogen is contributing to current and increasing the Coulombic efficiency.

3.3.3.3 Dark Fermentation Effluent MECs

This reactor set included Mini-MEC reactor sets inoculated with *G. acetivorans* (referred as DF-AT), *F. placidus* (referred as DF-FP) and co-culture of these two cultures (referred as DF-CCT) (1:1 mixture in the inoculum). Reactors were operated at 80 °C and directly fed with DF effluent from the beginning in order to assess whether they can form biofilms with only complex organics as acetate source provided to the MECs. Main difference of this reactor set from the DF fed MECs in the M-AT set is that in the previous set bioanode was formed using pure acetate, while for this reactor set only available acetate would be from the DF fermentation effluent. Various inhibitory products such as phenolic compounds could be produced as a result of the DF process (Feng et al., 2008) *F. placidus* was previously described for its ability to utilize aromatic compounds including phenolic compounds (Anderson et al., 2011) and genes involved in phenol metabolism was lacking in *G. acetivorans* (Mardanov et al., 2015). In the case of inhibitory effect by DF effluent content, it was hypothesized that co-culture of these two exoelectrogenic species could help *G. acetivorans* to show more resilience in MEC operation. Although 80 °C was less than the optimum growth temperature of *F. placidus* 85 °C, growth was confirmed at 80 °C with acetate and ferrous iron measurement before inoculating the MEC reactors.

3.4 Analytical Methods

3.4.1 Cattle Manure and Dark Fermentation Effluent Characterization

Liquid cattle manure was acquired from a biogas plant in Polatlı, Ankara. Cattle manure sample was blended for 15 min and stored at 4 ˚C until characterization was completed. COD, TKN, TS, VS and pH were determined (Table 3.3) by following Standard Methods (Apha, 2005).

Table 3.3. Cattle manure and DF effluent sample characterization

Parameter	APHA Standard Method
COD (mg/L)	5220 D
TKN (mg/L)	4500-Norg B
TS (%)	2540 B
VS (%)	2540 E
pH	4500-H^+ B

DF experiments were conducted with hyperthermophilic *Caldicellulosiruptor bescii* by another member of the Bioprocess Engineering Research Group (BIOERG) at METU Environmental Engineering Department. Prior to use, DF effluents of different organic loads were pooled together, acetate concentration was measured as described in Chapter 3.4.3 then the sample was diluted to adjust the required acetate concentration.

3.4.2 Hydrogen Gas Measurements

Total gas production in MEC reactors were determined with a glass syringe to find the total amount of produced gas. A gas chromatograph (TRACE GC Ultra, Thermo Scientific) equipped with a thermal conductivity detector (TCD) and a packed column (Part number: CP7429, Agilent Technologies) was used to determine the gas composition in the headspace. Temperatures of oven, injector and detector were 35 ˚C, 50 ˚C and 80 ˚C, respectively. Helium was used as carrier gas at a constant pressure of 75 kPa. The injection volume was 200 µL and a glass GC syringe (Part number: 050051-LL, VICI AG, USA) was used for manual injections. By using 5-point triplicate injections between 25 µL and 125 µL (Table 3.4) Calibration equation (Figure 3.12) was derived. Hydrogen production rate (Q_{H2}) was calculated using the hydrogen gas measurement data as described in Chapter 3.5.2.

Table 3.4. Hydrogen gas calibration for GC-TCD

Injected Volume (µl)	Peak Area	Mean	Std. Dev.	Coefficient of Variation (%)	Estimated Volume (µl)	Estimated / Injected (%)
20	6290	6300	43	0,68	19,68	98,40
	6348					
	6264					
40	12262	12398	123	1,00	38,63	96,59
	12502					
	12432					
80	26915	26354	362	1,38	82,01	102,52
	26191					
	26517					
160	51659	51719	181	0,35	160,86	100,54
	52016					
	51780					
200	63862	63928	135	0,21	198,81	99,41
	64084					
	63839					

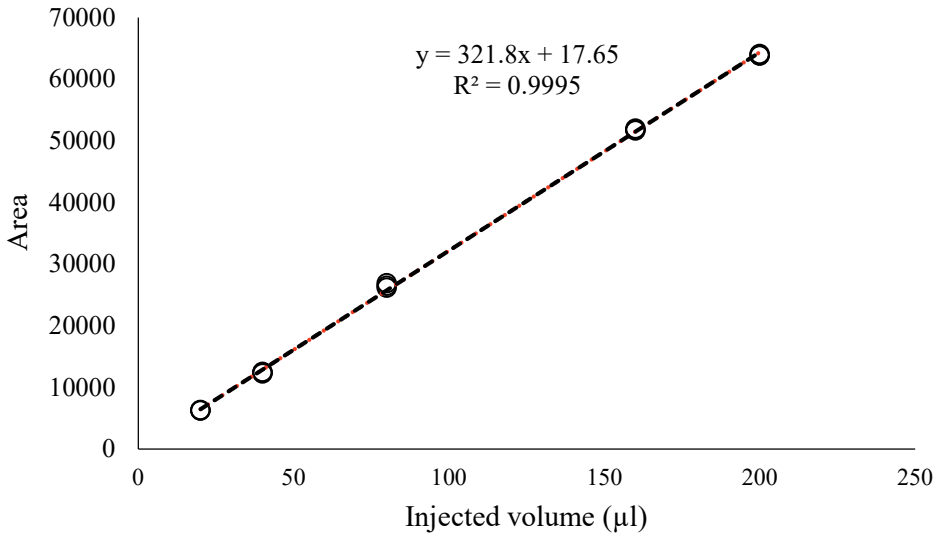

Figure 3.12. Hydrogen gas calibration curve and calibration equation

3.4.3 Acetic Acid Measurements

Determination of acetic acid in the prepared mediums, DF effluents and MEC reactor supernatants were done by using a gas chromatograph (TRACE GC Ultra, Thermo Scientific) equipped with a flame ioniziation detector (FID) equipped with a free carboxylic acids analysis column (part number: Nukol-25326, Supelco). Helium was used as carrier gas with the flow rate of 6 mL/min dry air and hydrogen gas were used for detector gases. Inlet was set to 250 ˚C FID detector was set to 280 ˚C. Oven temperature was increased from 100 ˚C to 200 ˚C with a rate of 8 ˚C per minute.

Samples for acetic acid measurement were filtered through 0.22 uM pore-sized PES syringe filters. pH of the samples was dropped below 2.5 by diluting the samples to 5:6 ratios with 1 N HCl to ensure free forms of the organic acids were present. 2 µL Injections were done manually using a 10 µL liquid GC syringe. Needle was cleaned with acetone before each injection and the GC column was purged with methanol after every 2 injections to ensure accurate results. Two different calibrations were used for acetic acid determination one for lower concentrations between 0.1 mM and 1 mM (Table 3.5) and the other calibration for higher concentrations between the ranges of 1 mM and 10 mM (Table 3.6). Figure 3.13 presents the corresponding calibration curves.

Table 3.5. Acetic acid calibration injections for lower concentrations

Concentation (mM)	Area	Mean	Std. Dev.	Coefficient of Variation (%)
0.1	3631663	4027316	519709	12.90
	3834385			
	4615901			
0.3	6118732	6352605	234513	3.69
	6587754			
	6351331			
0.7	11798522	12451378	636597	5.11
	12485247			
	13070365			
1	16948722	15613343	1509347	9.67
	13975756			
	15915552			

Table 3.6. Acetic acid calibration injections for higher concentrations

Concentation (mM)	Area	Mean	Std. Dev.	Coefficient of Variation (%)
1	16948722	15613343	1509347	9.67
	13975756			
	15915552			
2.5	27314596	30516743	2776266	9.10
	31986107			
	32249527			
5	60382948	66669464	5769067	8.65
	67904339			
	71721105			
10	143244737	139175910	7593938	5.46
	143868412			
	130414581			

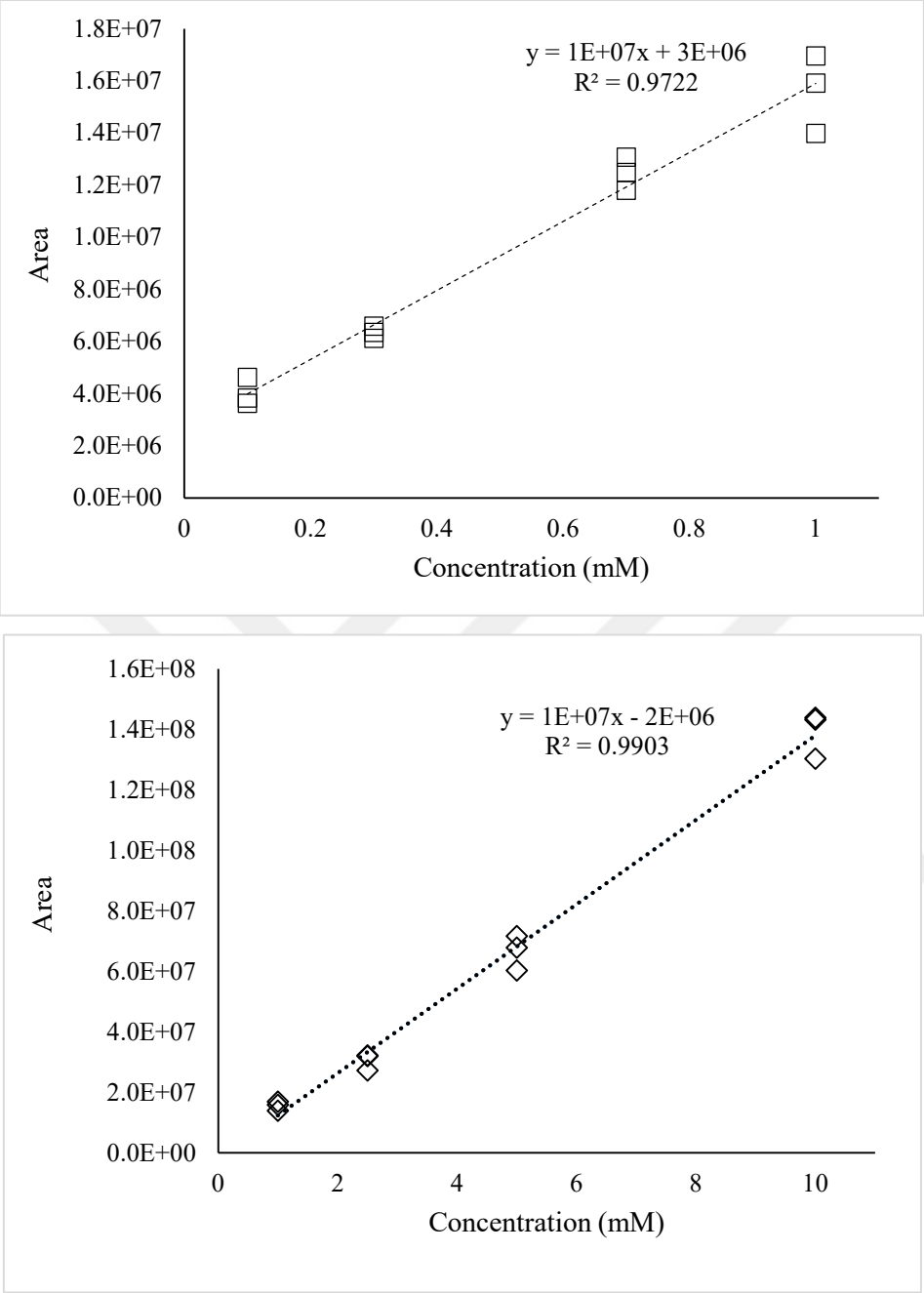

Figure 3.13. Acetic acid calibration curves and calibration equations for lower concentration range (top) and higher concentration range (bottom)

3.4.4 Ferrous Iron Measurements

Ferrous iron concentration in the incubated reactor bottles was determined with phenanthroline method (Hach 8146) with a spectrophotometer (model number: DR 2700, Hach, USA). *G. acetivorans* is dependent on ferric iron reduction to ferrous iron coupled during microbial growth (Slobodkina et al., 2009). Therefore, ferrous iron concentration was used as a tool to assess growth and checked against the initial ferric iron concentration of 56 mM. For ferrous iron measurements, accuracy check with ferrous ammonium sulfate solution (2 mg/L ferrous iron) was done to provide measurements within 95% confidence interval as described in Method 8146.

3.5 Calculations

3.5.1 Current Density

Current density (j) was calculated by using Ohm's Law with the following information (Equation 3-1). Data acquisition unit continuously measured DC voltage (V) across the 10 Ω resistors (R) shown in Figure 3.9. Hence, current was calculated via Ohm's law and for current density it was divided to the total the electrode surface area (A). Current normalized over active volume is shown with jv.

$$j\left(\frac{\mathrm{A}}{\mathrm{m}^2}\right) = \frac{I}{A} = \frac{V}{R.A} \qquad j_v\left(\frac{\mathrm{A}}{\mathrm{m}^3}\right) = \frac{I}{v} \qquad \text{(Equation 3-1)}$$

3.5.2 Hydrogen Production Rate

Hydrogen gas was production was measured with the chromatographic method described in Chapter 3.4.2. The maximum volumetric hydrogen production rate (Q_{H2}) was calculated by Equation 3-2 (Logan et al., 2008) using I_V (A/m^3); current value averaged over 6 hours of peak production and normalized to active volume,

cathodic hydrogen recovery (r_{CAT}); c_g (mol/L) molar density of hydrogen gas at 298.15 K and 1 bar, F is the Faraday' constant (96,485 C/mol.e$^-$). Sample calculation for maximum volumetric hydrogen production is shown in Appendix C.

$$Q_{H_2}\left(\frac{\mathrm{m^3H_2}}{\mathrm{m^3\ active\ volume\ .\ day}}\right) = \frac{43.2\ I_V\ r_{cat}}{F\ c_g(T)} \qquad \text{(Equation 3-2)}$$

3.5.3 Coulombic Efficiency

Coulombic efficiency (C_E) is used to determine the ratio of charge theoretically passed through the electrode to actual transferred amount. It was described as overall electron efficiency of the exoelectrogens (Korth et al., 2020). C_E provides knowledge on the amount of substrate converted to electrons and was calculated from (Equation 3-3). The integration of current over time to find total coulombs (nC_E) and divided by converting the acetate consumption (eight electrons per acetate) to the total Coulombs consumed (n_{th}) and using g COD/g acetate conversion rate of 1.07 (Call et al., 2009; Logan et al., 2008). In Equation 3-3 I is the current (voltage across the 10 Ω external resistance), F is the Faraday' constant (96,485 C/mol.e$^-$).

$$C_E(\%) = \frac{n_{C_E}}{n_{th}} = 100 \times \frac{\int_{t=0}^{t} Idt}{n_{th}} \qquad \text{(Equation 3-3)}$$

3.5.4 Cathodic Hydrogen Recovery

Cathodic hydrogen recovery (r_{CAT}) was calculated (Equation 3-4) to demonstrate the efficiency of electron capture at the cathode, produced from substrate as current at anode (Call & Logan, 2008). r_{CAT} was calculated by dividing the amount of hydrogen gas (n_R) (mole H_2) measured via GC to the amount of hydrogen that could be produced based on current (n_E) (Call et al., 2009). The amount of hydrogen that could

be produced based on current is calculated by integration area under the current density curve and dividing it into the Faraday's constant (96,485 C/mol.e^-).

$$r_{CAT}(\%) = 100 \times \frac{n_R}{n_E} = 100 \times \frac{n_R}{\frac{\int_{t=0}^{t} Idt}{2F}} \quad \text{(Equation 3-4)}$$

3.5.5 Overall Hydrogen Recovery

Overall hydrogen recovery (R_{H_2}) was calculated from the Coulombic efficiency (C_E) and cathodic hydrogen recovery (r_{CAT}) (Cheng & Logan, 2007).

$$R_{H_2}(\%) = \frac{C_E \times r_{cat}}{100} \quad \text{(Equation 3-5)}$$

3.6 Electrochemical Analysis

3.6.1 Cyclic Voltammetry

In order to further investigate and characterize the extracellular electron transfer to anode by *G. acetivorans* biofilm, cyclic voltammetry (CV) was performed by using a potentiostat (model no: 1010B, Gamry Instruments, USA) with an Ag/AgCl reference electrode (part number: MF-2052, BASI, USA) at 80 °C in three electrode system. Initially tests were conducted between the ranges of -0.7 V to 0 V vs. Ag/AgCl and later adjusted to -0.7 V to 0.2 V vs Ag/AgCl using a scan rate of 1 mV/s. Potentials reported for CV analysis with reference electrodes were reported versus Ag/AgCl (+165 mV vs. SHE at 80 °C) (Bates & Bower, 1954) in this chapter, Chapter 4.3.3 and Chapter 4.4.4 .

Analyses were performed for bioanodes under turnover (acetate present) and non-turnover (without acetate) conditions. Abiotic electrodes (sterile reactors) were used for spent medium (reactor content) and sterile medium (growth medium) CV

analyses. For turnover CV analyses, reactors were operated until the peak current of their respective cycle was reached before a reference electrode is placed inside of the reactor in the anaerobic chamber. This is to prevent leakage of reference electrode content into the reactor due to high incubation temperature. Non-turnover CV analyses was conducted by filling MECs with MEC media that is lacking acetate (no substrate). Spent medium analysis was conducted by feeding the reactor content (after the cycle completion) into a sterile reactor with bare electrodes. The aim of conducting spent medium CV was to check for redox peaks in the voltammograms that could indicate electron mediators or planktonic cells were involved in the extracellular electron transfer.

3.6.2 Scan Rate Analysis

Scan rate analysis were performed to establish whether direct electron transfer (DET) is occurring between electron transfer elements of exoelectrogens and anode electrodes, under both turnover and non-turnover conditions with the scan rates between 1 mV/s and 100 mV/s. Peak anodic currents densities (j_{max}) were checked against the scan rate (ν) and deviation from linear relationship (Equation 3-5) is described as diffusion limited system, whereas a linear relationship shows a direct interaction by the biofilm on the electrode surface (Rousseau et al., 2014). The "α" exponent value described in the Equation 3-5 was calculated with the dimensionless plot of of peak current density and the scan rate ($\log j_{max}$ and $\log \nu$).

$$j_{max} \text{ vs. } \nu^{\alpha} \qquad \text{(Equation 3-5)}$$

This diffusion dependent process can be seen in the Randles-Sevcik equation (Equation 3-6), which describes the electron transfer processes of redox species. In this equation, it describes how the scan rate of peak current j_{max} (A) increases linearly with the square root of scan rate (Vs^{-1}); where n is the number of electrons transferred in the redox event, A (cm^2) is the electrode surface area, D_o ($cm^2\ s^{-1}$) is

the diffusion coefficient of the oxidized analyte, and C_0 (mol cm^{-3}) is the concentration of the analyte.

$$j_{max} = 0.446\, nFAC^0 \left(\frac{nF\nu\, D_o}{RT}\right)^{\frac{1}{2}} \quad \text{(Equation 3-6)}$$

To summarize, when scan rate vs. peak current shows a linear trend corresponding to unity level of "α" exponent; this is accepted as direct evidence of the presence of biofilm on the electrode and the electron transfer is confined to the electrode surface.

3.7 Scanning Electron Microscopy

After the completion of the reactor operations for *G. acetivorans* anodes of MEC reactors were sacrificed for SEM analysis of biofilms. For immobilization of the biofilm on the electrodes paraformaldehyde (PFA) solution was used. 8% PFA solution was prepared by slightly modifying the method previously described (Sanchez et al., 2015) 8 g of paraformaldehyde was added to 70 mL of de-ionized water, heating the solution to 70 °C, adding sodium hydroxide pellets until the solution cleared, then completing the solution to 100 mL and refrigerating it overnight. 8% PFA solution was later diluted to 4% PFA solution with phosphate buffer. Phosphate buffer was prepared by mixing 22.4 mL 1 M KH_2PO_4 and 79.6 mL 1 M K_2HPO_4 solutions in a total volume of 1 L deionized water. Electrodes were removed from the reactors, placed inside the glass screw cap vials and completely covered with 4% PFA in 0.1 M Phosphate Buffer at pH 7.4 and refrigerated at 4 °C for 8 hours. After refrigeration, 4% PFA solution was discarded with a sterile Pasteur pipette and the bioelectrodes were washed with buffer 3 times with 5 minutes intervals. Series of dehydration was done with 25%, 50%, 75%, 95% and 100% ethanol each for 3 times for a duration of 5 minutes. Fixed anode samples were kept in a 100% fresh ethanol solution until air drying. Air drying was performed in the sterile fume hood at room temperature for about half a day. Fixed anodes were stored at room temperature in dark.

After fixation, samples were sent for SEM analysis to METU-Central Laboratory. Before imaging at METU-Central Laboratory, samples were coated with Au/Pd and a thin strip of carbon tape was attached to increase conductivity.

Figure 3.14 - Bioelectrode after fixation is completed

3.8 Protein Measurement

Total protein measurements were used previously for the analysis of biofilm formation in MECs and the analysis was conducted for attached biofilm on the electrodes and the planktonic cells that may be present in the reactor content (*i.e.* spent medium) (Yilmazel et al., 2018).

3.8.1 Sample Preparation

Total protein is extracted from the electrode surface and the MEC spent medium as previously described (Holmes et al., 2004). Briefly, 4.5 mL of spent medium was taken from the reactor before disassembly and placed into a falcon tube and was centrifuged at 4500 rpm for 15 minutes. Bioelectrodes were flushed with 3 mL 0.2 N NaOH solution 8 times over 30-minute period. After 2-3 cycles visible biofilm on the electrode started to disappear. Protein extracted liquids were kept in the -20 °C overnight, next day they were thawed at room temperature and immediately after thawing samples were incubated at 100 °C oven for 10 mins.

3.8.2 Calibration and Measurement

Protein concentrations for both the extracted biofilm and spent mediums were measured by Bradford Assay kit (part number: 5000202, Bio-Rad, USA). A calibration curve (Figure 3.15) was produced before each batch of measurements using bovine serum albumin (BSA) standards. 980 µl Bradford Reagent was added to 20 µl protein extracted samples using micropipettes. Blanks were prepared using 20 µl deionized water instead of protein extracted samples. Same dilution rate was also applied to the BSA Standards. Cuvettes were incubated at room temperature for 5 minutes (Figure 3.16) then measured with a spectrophotometer (model number: DR 3900, Hach, USA) at 595 nm.

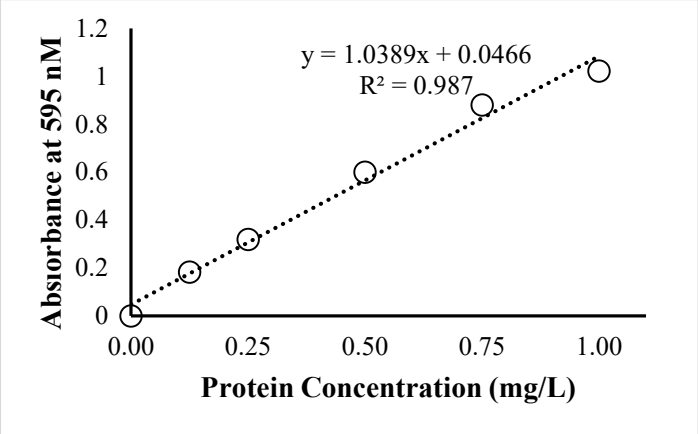

Figure 3.15. Total protein calibration curves and calibration equations with BSA

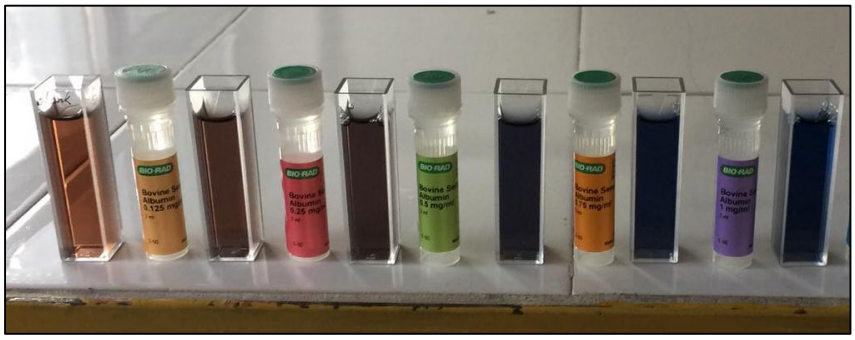

Figure 3.16. BSA standards between 0.125 – 1.0 mg/L after incubation

CHAPTER 4

RESULTS AND DISCUSSION

4.1 Acetate Oxidation Coupled to Fe(III) Reduction During Growth

Growth medium of *G. acetivorans* included acetate as electron donor and ferric citrate as electron acceptor (Table 3.1). *G. acetivorans* is known for its ability to oxidize acetate into carbon dioxide with ferric forms of iron (Fe^{+3}) as electron acceptor and soluble ferric iron was reported to enable less culture growth (Slobodkina et al., 2009). Stoichiometric reaction for this iron reduction process is provided in the Equation 4.1.

$$CH_3COO^- + 8Fe(III) + 4H_2O \rightarrow 2HCO^- + 9H^+ + 8Fe\ (II \qquad \text{(Equation 4.1)}$$

In the growth tubes, the growth was visible through the colour change due to iron reduction and precipitate formation after incubation. To quantify this iron reduction and the coupled acetate oxidation process, a growth study was conducted (Figure 4.1) as described in Chapter 3.2.2. When the colour of the medium changed from transparent light brown to olive green with precipitates, the culture was accepted as ready to be used as inoculum for either subculturing or MEC reactor startup within a day.

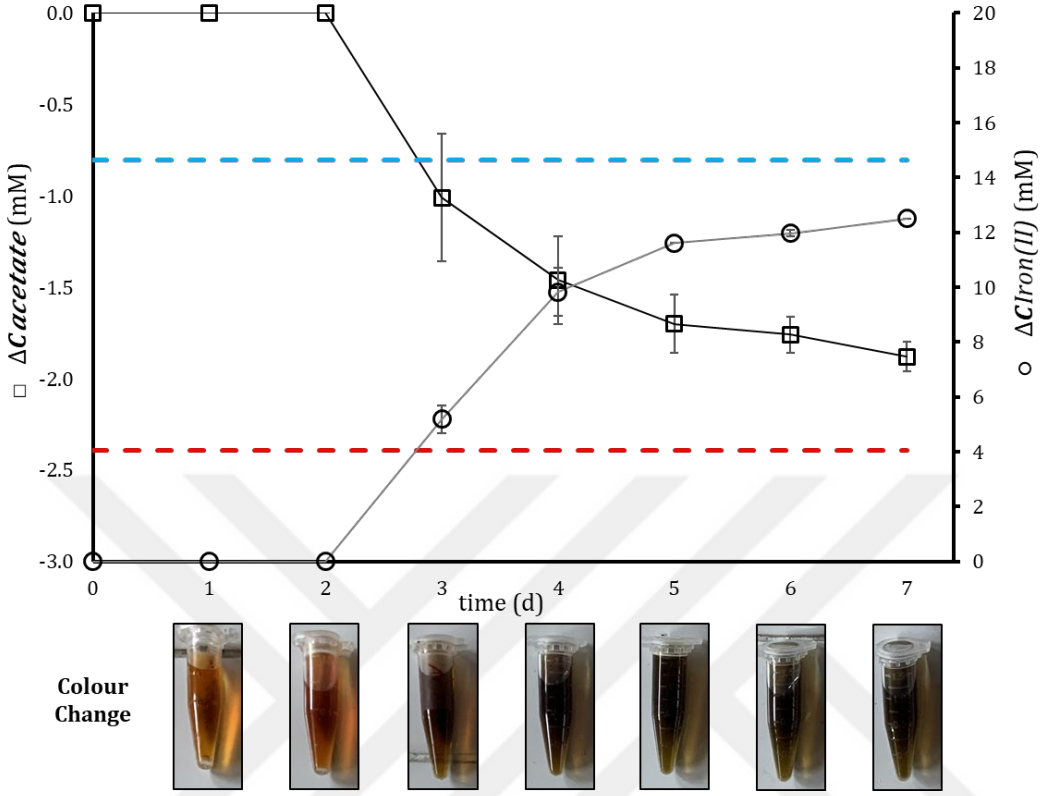

Figure 4.1. Growth study of *G. acetivorans* with acetate and ferric citrate (red dashed line: acetate consumption for 35-day incubation; blue dashed line: iron(II) formation for 35-day incubation)

Acetate consumption and iron (II) formation was shown to overlap with the change in colour of the medium shown in the bottom part of the Figure 4.1 after an initial lag phase of 2 days. This lag phase is a shortened version of what it was observed in previous incubations (data not shown) possibly due to series of frequent subculturing before this growth study. After 7 days of incubation, 1.88 ± 0.08 mM acetate was consumed from the initial concentration of 11.2 mM. Iron (II) concentration was initially 1.07 mM possibly due to the presence of ferrous iron in the inoculum, later increased to 13.58 mM after 7 days. After a longer incubation test which was conducted for 35 days, the acetate consumption was found as 2.39 ± 0.13 mM and

iron (II) formation 15.73 ± 0.05 mM indicating a much slower reaction rate after a short period of high microbial activity in the initial days of incubation. Around 17% of the total acetate was consumed and 24% of the initial iron (III) dose (56 mM) was reduced to iron (II) in 35 days. Incomplete oxidation is consistent with the previous findings for hyperthermophilic iron reducer archaea including *G. acetivorans* (Kashefi et al., 2002; Slobodkina et al., 2009). Previously, iron (II) formation by *G. acetivorans* reached to a maximum level of 5-6 mM when ferric iron was provided in soluble form of ferric citrate and the ratio for iron (II) production to acetate consumption was reported as 7.5 (Slobodkina et al., 2009). In our study the reported maximum of ferric iron reduction was higher than the previous report and the ratio was found 6.86 ± 0.08; indicating a slightly increased deviation from the stoichiometry of this reaction with a ratio of 8 (Equation 4.1).

It was expected that providing ferric iron the soluble form might result in less and slower growth for *G. acetivorans* since slower utilization of acetate was described for the other member of *Geoglobus* genus with an extended lag phase for soluble iron as electron acceptor (Kashefi et al., 2002). However, other alternatives such as using ferric iron sludge for growth were not used due to possible effects of insoluble iron on the electrodes (used intentionally to enhance performance) reported previously (Kim et al., 2005; Zhang et al., 2013).

4.2 Characterization of Complex Organic Wastes

Liquid cattle manure sample prior to utilization in dark fermentation study and the effluent of this process were characterized using methods described in Chapter 3.4. Acetate concentration was the most important factor since it affected the media preparation for the MEC reactors. All further calculations were based on the adjusting the dilution ratio to achieve 10 mM acetate (originating from DF effluent) in MEC mediums. Summary of the results are provided in Table 4.1.

Table 4.1. Characterization results of Cattle Manure and DF Effluent

Parameter	Liquid Cattle Manure	Dark Fermentation Effluent
COD (mg/L)	123610 ± 2679	22343 ± 335
TS (%)	11.19± 0.14	1.87 ± 0.02
VS (%)	8.89 ± 0.12	0.78 ± 0.01
VS/TS	0.79 ± 0.01	0.42 ± 0.02
pH	6.98 ± 0.38	6.46 ± 0.12
Acetic Acid (mM)	N.D.	57.21 ± 0.19

N.D. : Not determined

4.3 Mini-MEC Reactors (Set AT and Set GS)

4.3.1 Reactor Performance of AT and GS Sets

4.3.1.1 Current Production

First reactor set operated with the *G. acetivorans* inoculated Mini-MECs (AT reactor set) produced high peak current densities (j_{max}) after the initial period of biofilm formation was completed. After this period noticeable biofilms were formed (Figure 4.2) on the anode electrodes (discussed in Chapter 4.3.4). As mentioned earlier in Chapter 3, three periods were identified for this set; the start-up, the biofilm formation period and the test period. Reactors were operated for a total of 55 days where the start-up period lasted about 7 days and the biofilm formation 30 days (Figure 4.3). In the test period, current density values started to replicate to higher extent (CoV < 5%) at the 37th day of operation (Figure 4.4). However, after 6th cycle was completed, biofilm detachment was observed (Figure 4.2D) and current

production decreased. Before the biofilm detachment, peak current densities were averaged for triplicate reactors 1.53 ± 0.27 A/m^2 over 6 cycles of operation at 80 ˚C. Abiotic controls did not produce any current throughout the operation *G. sulfurreducens* is accepted as a model exoelectrogen in the literature (Logan et al., 2019). Therefore, *G. sulfurreducens* reactor set (GS reactor set) was operated as a control in order to assess the performance of the self-assembled reactor configuration and the locally purchased electrode materials. Quadruplicate reactors operated at 35 ˚C for GS reactor set produced 2.1 ± 0.1 A/m^2 peak current densities excluding the first 2 cycles assuming this period for the biofilm formation on the anode (Figure 4.2). Previous operations for *G. sulfurreducens* produced similar peak current densities of 1.9 A/m^2 and 2.2 A/m^2 (Rotaru et al., 2015; Yilmazel et al., 2018).

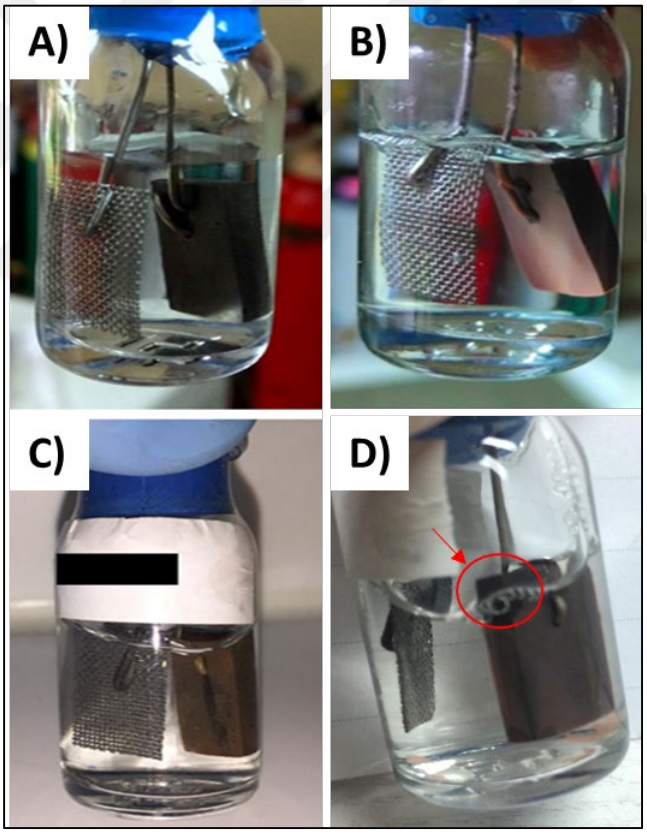

Figure 4.2. Abiotic electrode (A), GS anode biofilm (B), AT anode biofilm (C) AT anode biofilm detachment (D)

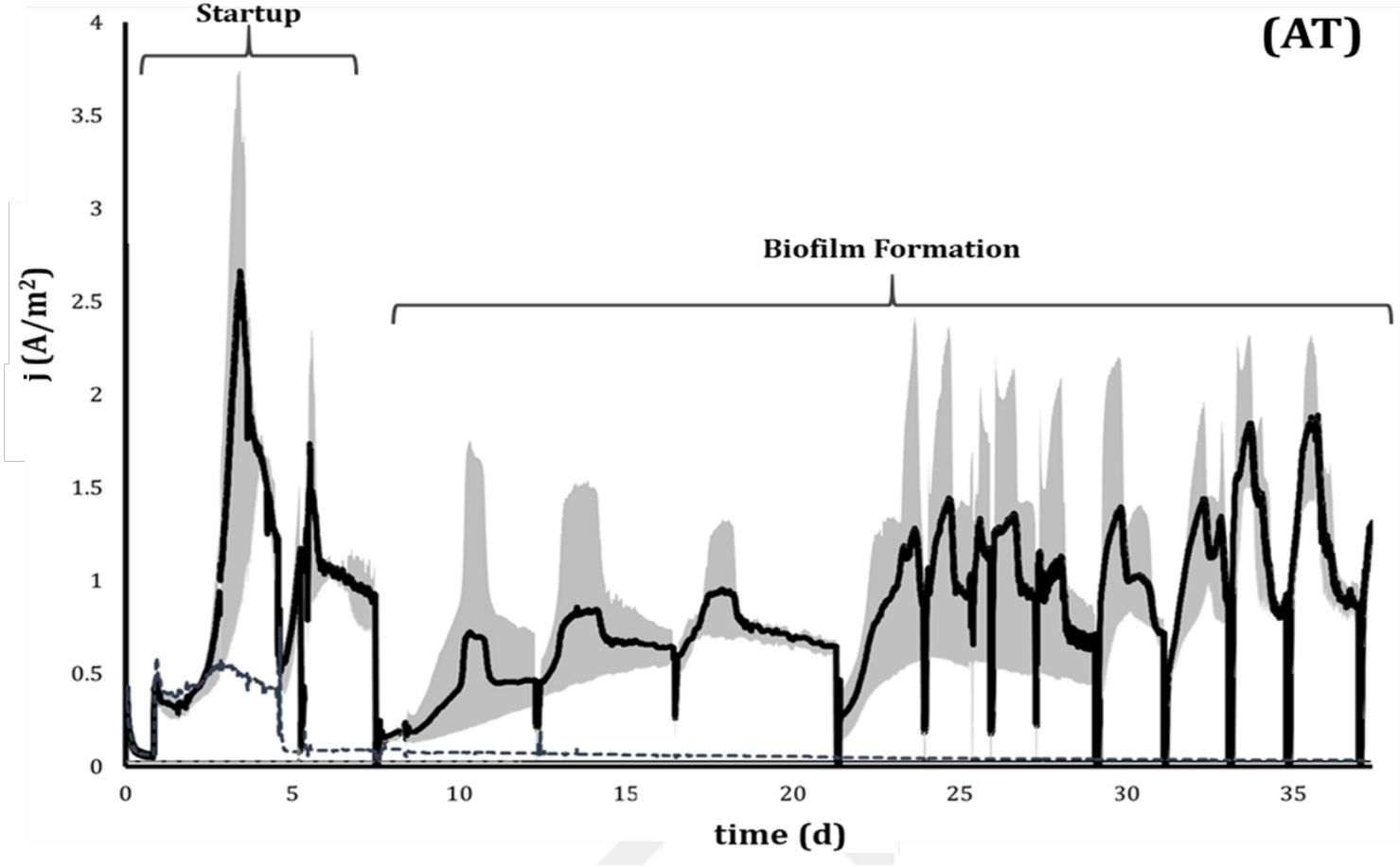

Figure 4.3. Normalized current production for AT reactor set prior to test period (black line: test average; blue dashed line: acetate control; grey dashed line: abiotic control; grey gray area: variation)

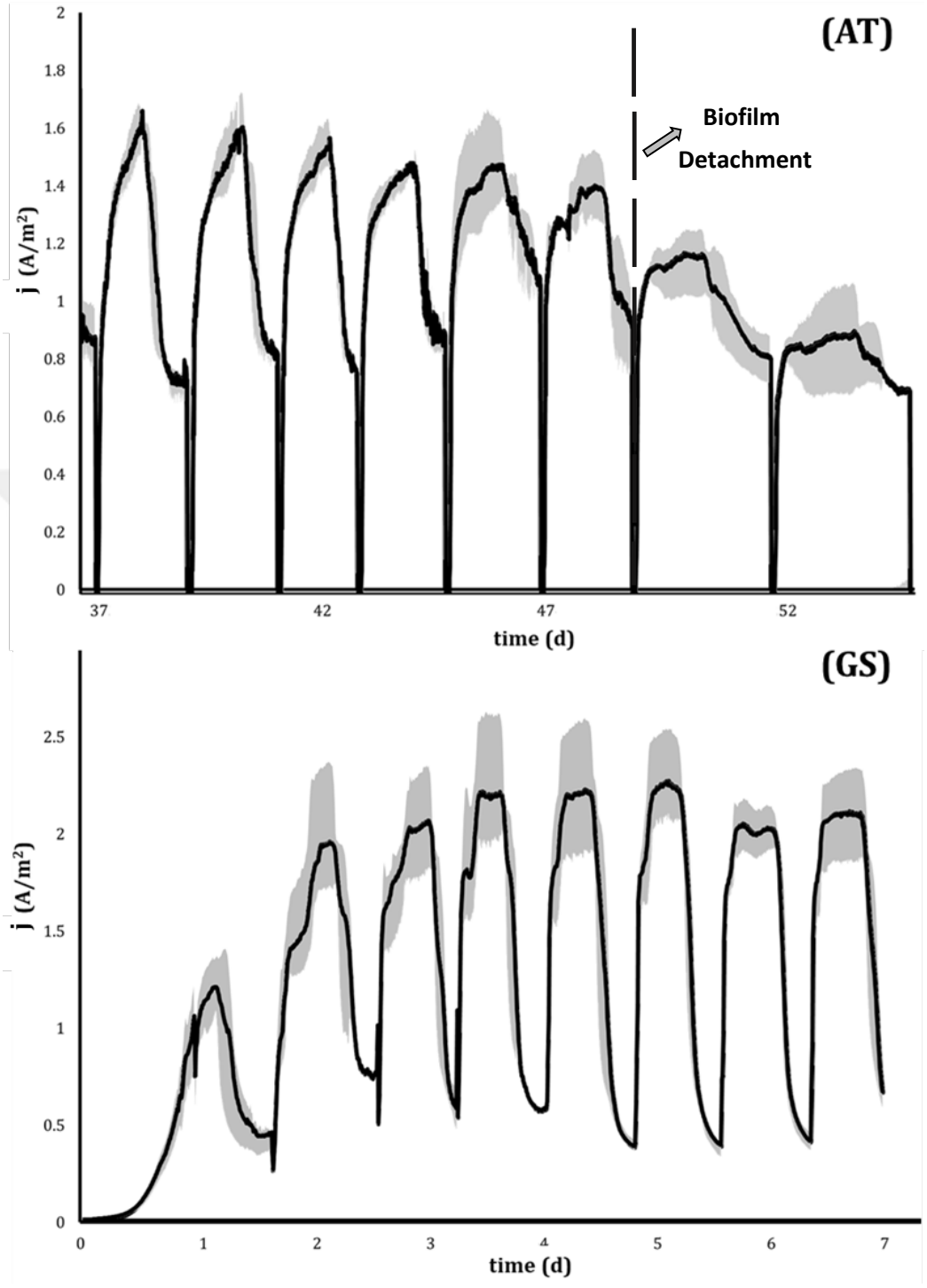

Figure 4.4. Current density of *G. acetivorans* MECs during test period (AT set, top graph, and *G. sulfurreducens* MECs (GS set, bottom graph) (black line: average; gray area: variation)

For comparison, the peak current production of different microorganisms are presented in Figure 4.5. *G. ahangari* and *F. placidus* are close relatives of *G. acetivorans* that shows significant similarities in their genomic structure (Manzella et al., 2015; Mardanov et al., 2015), produced peak current densities of 0.57 ± 0.10 A/m^2 and 0.68 ± 0.11 A/m^2 using the same reactor configuration (Yilmazel et al., 2018). Among the 4 hyperthermophilic exoelectrogens known to date, *G. acetivorans* produced the highest peak current density with 1.53 ± 0.27 A/m^2 (j_V: 137.7 ± 24.3 A/m^3).

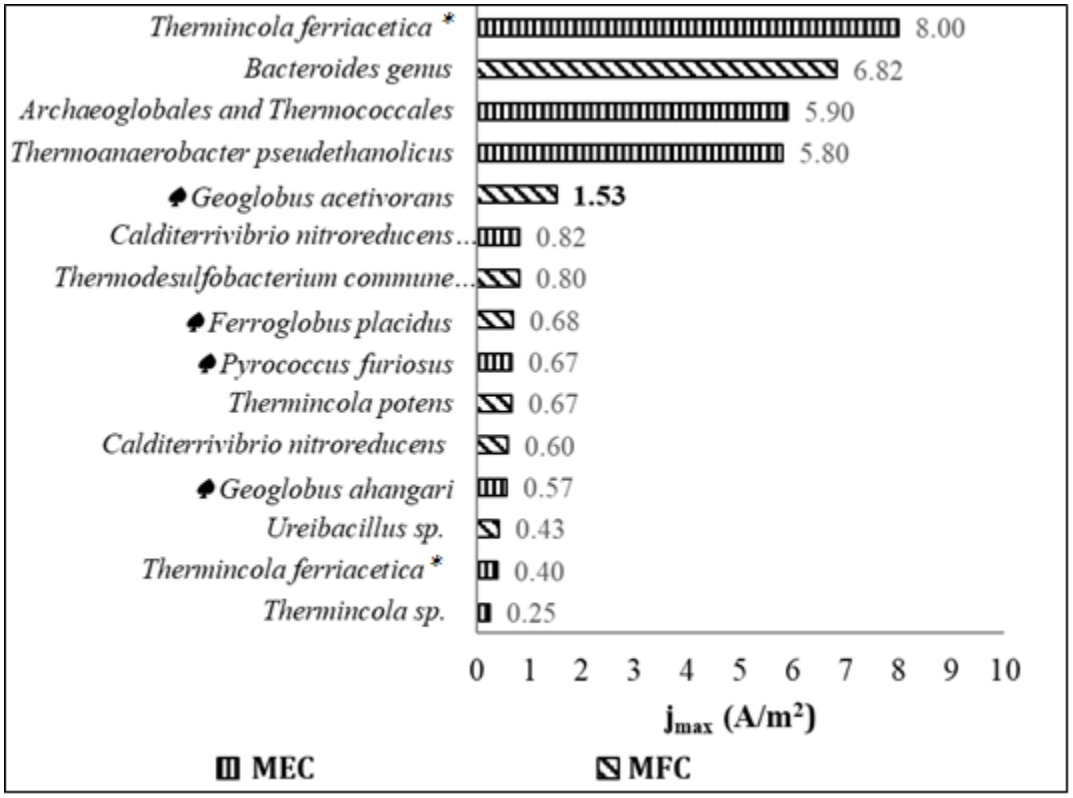

Figure 4.5. Peak current production (j_{max}) for thermophilic and hyperthermophilic BESs (*References provided in Appendix B, ♠: hyperthermophilic BESs)

Due to the complexity of the interactions between the electrode and exoelectrogens; reactor configuration and operating conditions requires serious optimization studies as it was evident for *T. ferriacetica.* For example, for *T. ferriacetica*, a thermophilic exoelectrogen, the initially reported peak current density was 0.4 A/m^2 (Marshall &

May, 2009) yet this value was increased to the highest value in thermophilic applications of 8.0 A/m^2 later when two-chamber MECs were used (Parameswaran et al., 2013).

For the Mini-MEC reactor sets, reactor materials were rather simple (*i.e.* no coating applied) compared to the literature. Although the conditions were not optimized for *G. acetivorans* as well as *G. sulfurreducens,* peak current density values produced comparable results to the literature (Figure 4.6). An important point to consider while evaluating these current production results will be that biofilm formation period was completed in 2-3 days for GS set (first 2 cycles in Figure 4.3). Whereas biofilm formation for *G. acetivorans* was much longer and AT set cycle count represents the number of cycles during the test period. Prior to the test period AT set was operated for 13 cycles (~ 37 days).

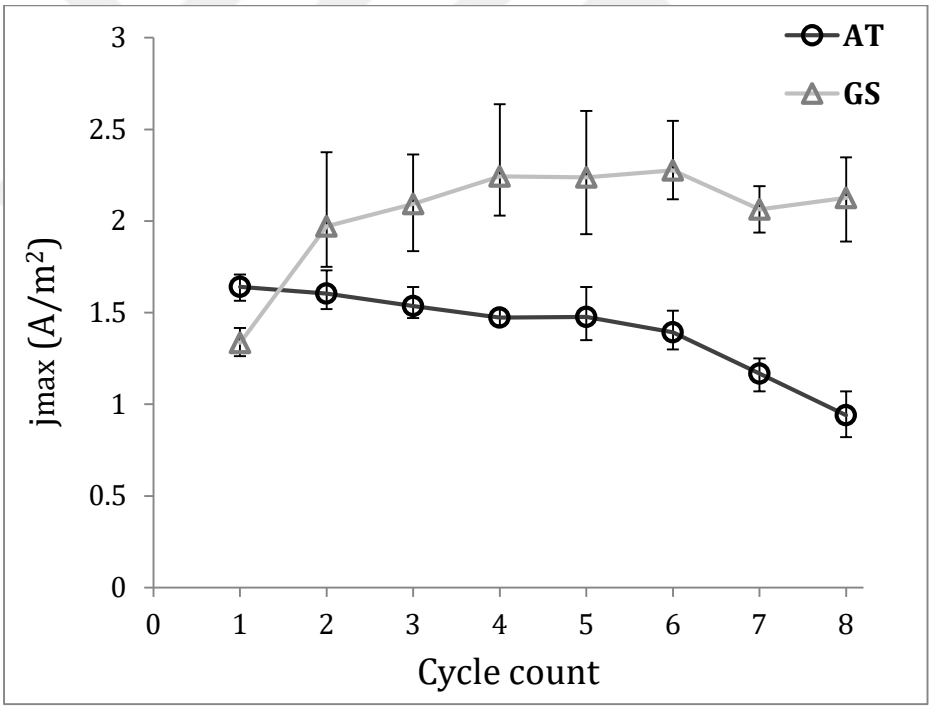

Figure 4.6. Peak current density of *G. acetivorans* (AT) in the test period and *G. sulfurreducens* (GS) Mini-MECs

4.3.1.2 Hydrogen Production

Stable hydrogen generation throughout the test period of *G. acetivorans* inoculated MEC reactors was observed. Similar to the current generation, reactor performance based on hydrogen gas production rate (Q_{H_2}) were adversely affected by the biofilm detachment after the Cycle 6 (Figure 4.7). Hydrogen gas percent in the headspace was maximum in the 2nd cycle with 31.5 ± 1.5 % and lowest in the 8th cycle with 17.6 ± 0.2 %.

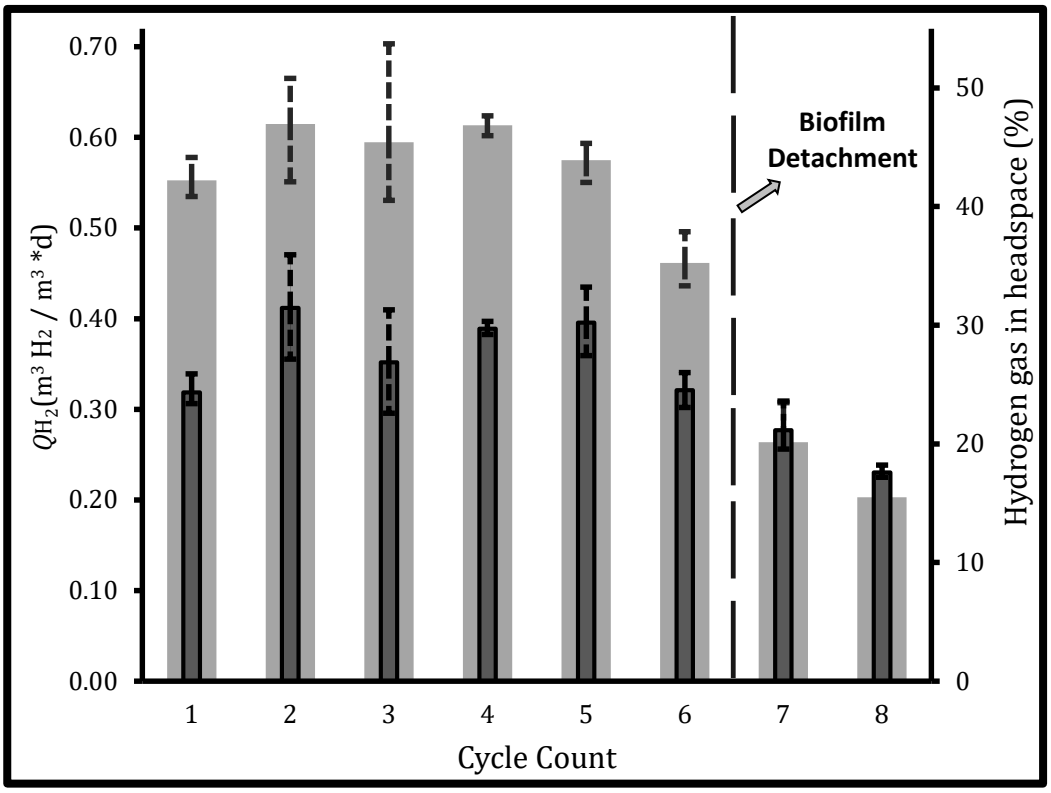

Figure 4.7. Hydrogen production rate (Q_{H_2}) and hydrogen gas in headspace of *G. acetivorans* (AT) Mini-MECs during test period (light gray bars: Q_{H_2}; dark grey bars: gas percentage)

Although not visible at the time, biofilm detachment could have started earlier since hydrogen production rates dropped significantly between cycle 5 and 6. Figure 4.2D shows the visual of the biofilm detachment observed after cycle 6. Hydrogen

production was quantified at the end of each cycle for each MEC and normalized to the reactor active volume. Using the cycle durations, average hydrogen production rate (Q_{H2}) was calculated as 0.57 ± 0.06 m^3H_2 / m^3d and 0.94 ± 0.06 m^3H_2 / m^3d for *G. acetivorans* (6 cycles before biofilm detachment) and *G. sulfurreducens* (excluding first two cycles for biofilm formation) respectively (Figure 4.8).

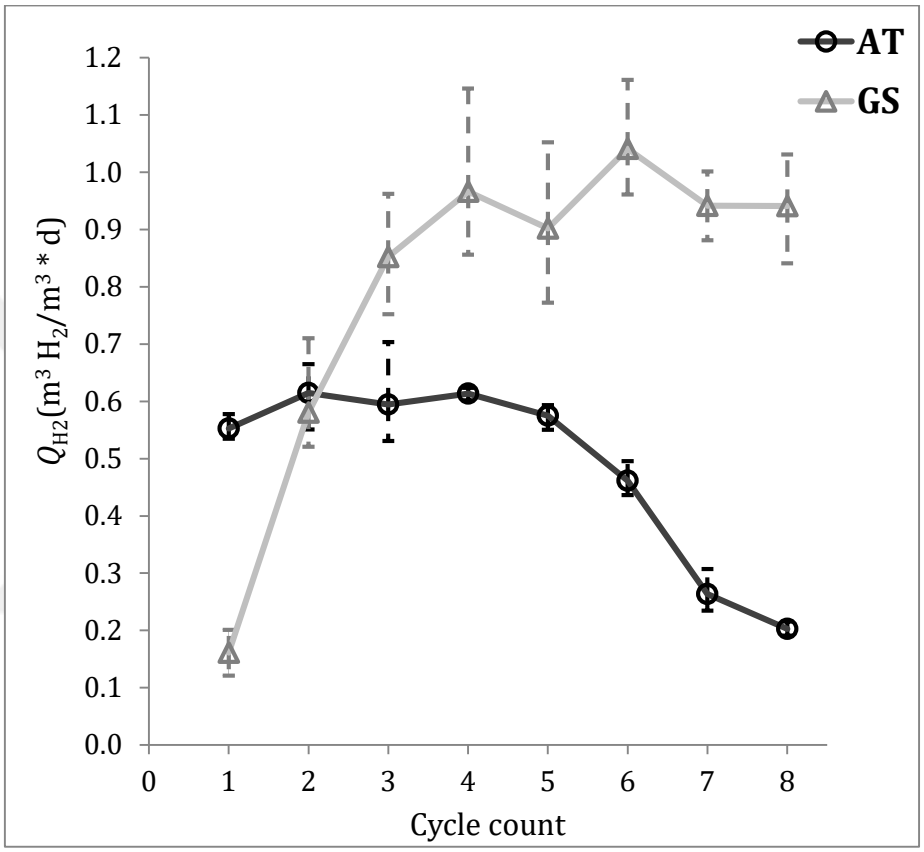

Figure 4.8. Hydrogen production rates (Q_{H2}) of *G. acetivorans* (AT) and *G. sulfurreducens* (GS) Mini-MECs (AT set operated for 13 cycles ≈ 37 days prior)

Peak current densities in the GS set were 1.4 times higher than AT set, maximum hydrogen production rates similarly was 1.6 times higher in GS set than in AT set. The small difference in the current production and hydrogen production ratios of the two sets could stem from different contributions of internal hydrogen recycling to the current production. Internal hydrogen cycling refers to the use of hydrogen gas

as electron donor by exoelectrogens inside the single chamber MECs (Lee & Rittmann, 2010).

In our study, hydrogen production rates recorded for *G. sulfurreducens* (~ 0.9 m^3H_2 / m^3d) were also lower than previously reported values of 1.9 m^3 H_2 / m^3d (Call et al., 2009) and 3.1 m^3 H_2 / m^3d (Call & Logan, 2008). This could be explained by Pt coated cathodes used in these studies that could improve catalytic activity for the production of hydrogen gas.

4.3.2 Efficiency Calculations for AT Set

Efficiency of the *G. acetivorans* Mini-MEC reactors were assessed as described in Chapter 3.5.3 and Chapter 3.5.4 with parameters Coulombic efficiency (%C_E) and cathodic hydrogen recovery (%r_{Cat}). To quantify the substrate utilized during the operational cycles and calculate Coulombic efficiency, concentration of acetate was determined at the end of each cycle. Almost all of acetate was consumed in the MECs; acetate consumption (%n_{AC}) were found as 95.0 ± 2.6 % for 6 cycles of the test period. Coulombic efficiencies (C_E) for 10 mM acetate fed *G. acetivorans* Mini-MECs were averaged at 245.1 ± 26.9 % for 6 cycles of the test period (Figure 4.9). C_E value was above %100 for all cycles and indicating that charge passed through the cycle duration was not exclusively due to acetate consumption during that period. In other words, *G. acetivorans* was using another electron donor during the operation of Mini-MECs. Hyperthermophilic iron reducing archaea species of *G. acetivorans*, *G. ahangari* and *F. placidus* were all reported to use hydrogen gas as electron donor in with various electron acceptors (Hafenbradl et al., 1996; Kashefi et al., 2002; Slobodkina et al., 2009). However, for *F. placidus* and *G. ahangari* use of hydrogen gas in a MECs were not reported to be significant and the C_E values were found as 76.4 ± 42.5% and 70.9 ± 21.3%, respectively (Yilmazel et al., 2018).

Cathodic recovery (r_{Cat}) values were averaged at 32.1 ± 3.6 %, showing that only indicating that only one third of the hydrogen was recovered than expected based on

the current. The average overall H_2 recovery (R_{H_2}) is calculated as 78.6 ± 10.4 %. Other experiments were conducted to assess the contribution of internal hydrogen recycling and discussed in Chapter 4.4.3. Even after the biofilm detachment started around 6th cycle, acetate was almost completely consumed (99.1 ± 0.8 %) by the exoelectrogenic biofilm. This might be due to an attempt to replenish the biofilm on the anode surface by *G. acetivorans* however, shortly after this period biofilm was almost completely detached during media replacement and CV analysis. Summary of performance and efficiency of AT set is presented in Table 4.2.

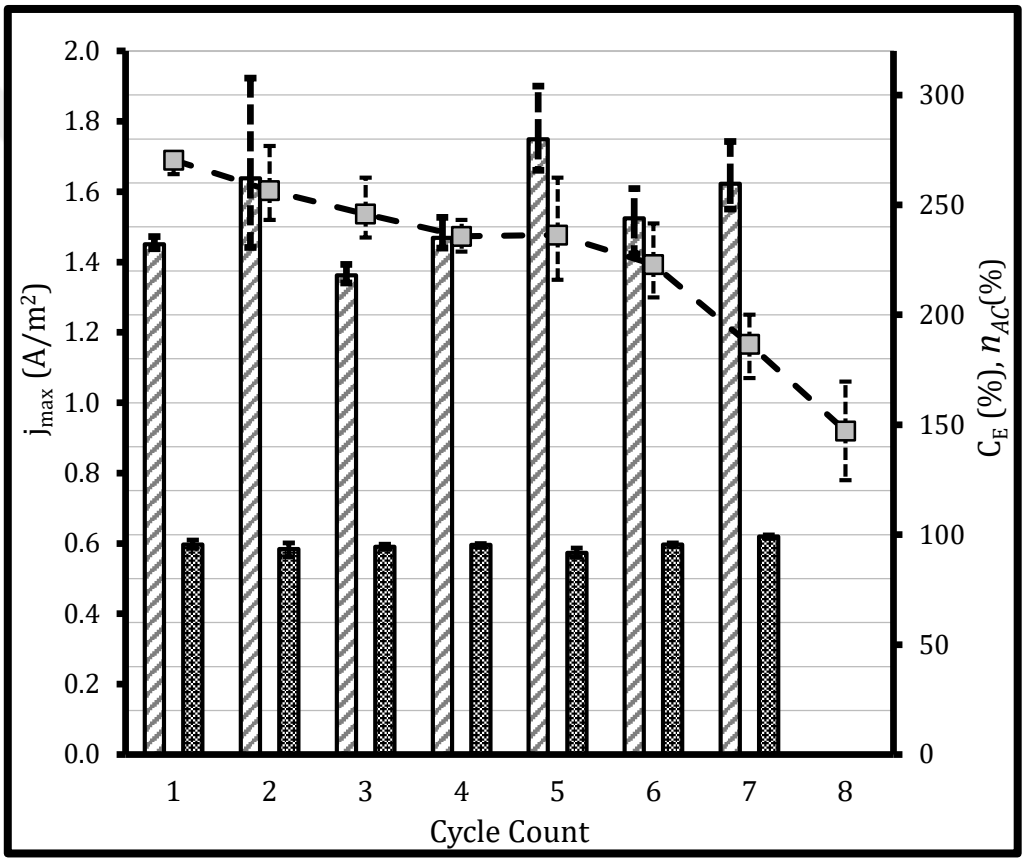

Figure 4.9. Acetate removal (%, black diamond bar), Coulombic efficiency (%, grey diagonal bar), and j_{max} (A/m^2, square markers) for AT set

Table 4.2. Summary of AT *G. acetivorans* Mini-MEC (AT) Set

Cycle Count	j_{max} (A/m^2)	t (d)	Q_{H2} (m^3H_2/m^3)	n_{AC} (%)	C_E (%)	r_{Cat} (%)	R_{H2} (%)
1	1.69 ± 0.03	1.9	0.55 ± 0.02	95.5 ± 1.9	232.1 ± 3.6	29.7 ± 0.6	68.9 ± 2.3
2	1.60 ± 0.11	2.0	0.61 ± 0.06	93.5 ± 3.2	262.0 ± 45.6	32.1 ± 5.1	84.1 ± 11.5
3	1.54 ± 0.09	1.7	0.59 ± 0.09	94.5 ± 1.2	217.9 ± 5.1	33.5 ± 3.2	72.9 ± 6.4
4	1.47 ± 0.05	1.9	0.61 ± 0.01	95.3 ± 1.0	235.0 ± 9.3	36.0 ± 1.1	84.5 ± 0.6
5	1.48 ± 0.15	2	0.57 ± 0.02	91.7 ± 2.1	279.9 ± 24.1	33.3 ± 3.1	93.1 ± 4.9
6	1.39 ±0.11	1.9	0. 46 ± 0.03	95.5 ± 0.8	243.9 ± 13.5	28.4 ± 2.7	69.3 ± 3.1
7	1.17 ± 0.09	2.9	0.26 ± 0.04	99.1 ± 0.8	259.6 ± 19.2	19.4 ± 1.7	50.2 ± 1.8
8	0.92 ± 0.15	2.9	0.20 ± 0.01	-	-	19.5 ± 2.8	-

4.3.3 Electrochemical Analysis of AT Biofilm

After biofilm detachment was observed for AT set, operation of reactors stopped and the reactors were stored at room temperature until preparations for CV analyses were finalized. Initially for AT reactor set, CV analyses were performed in the range of -0.7 V and 0 V vs Ag/AgCl reference electrode. An S-shaped sigmoid wave was observed for the test reactor in the turnover conditions indirectly showing that the *G. acetivorans* culture performs direct electron transfer (DET) in the MEC reactor by interacting with the graphite anode. In another CV cycle, range of applied potentials was readjusted to -0.7 V to 0.2 V. At this point test reactors in AT set were producing a small portion of the peak current densities of the earlier cycles possibly due to biofilm detachment and stresses related to oxygen leakages. CV analyses conducted at this period showed small anodic peak currents but still a sigmoid (S-shaped) voltammograms were observed (Figure 4.10). If biofilm is involved in the extracellular electron transfer and carry out direct electron transfer (DET) CV analysis under turnover conditions produces a sigmoid (S-shaped) catalytic wave (Fourmond et al., 2019) and no significant redox peaks are observed in the abiotic and spent medium analyses (Marshall & May, 2009).

Redox peak points were determined by looking at the 1st derivative of these curves (Figure 4.11), and a clear redox peak with the midpoint potential around -400 mV was observed for *G. acetivorans* MECs. In the previous study with *F.placidus* and *G.ahangari* a redox peak at this applied anode potential (-400 mV) was also observed (Yilmazel et al., 2018). Redox peak points were compared to those known of electron mediators and no redox peaks were observed in spent medium analysis; supporting the DET capability of *G. acetivorans*.

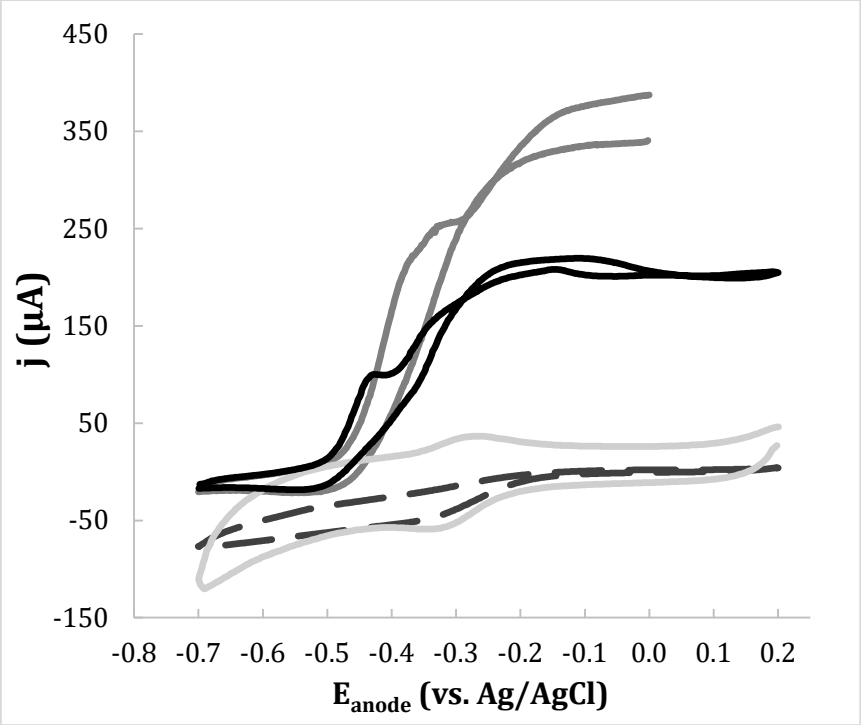

Figure 4.10. Cyclic voltammograms of *G. acetivorans* MEC set (AT) (gray and black line: turnover; light gray line: non-turnover; dashed gray line: abiotic)

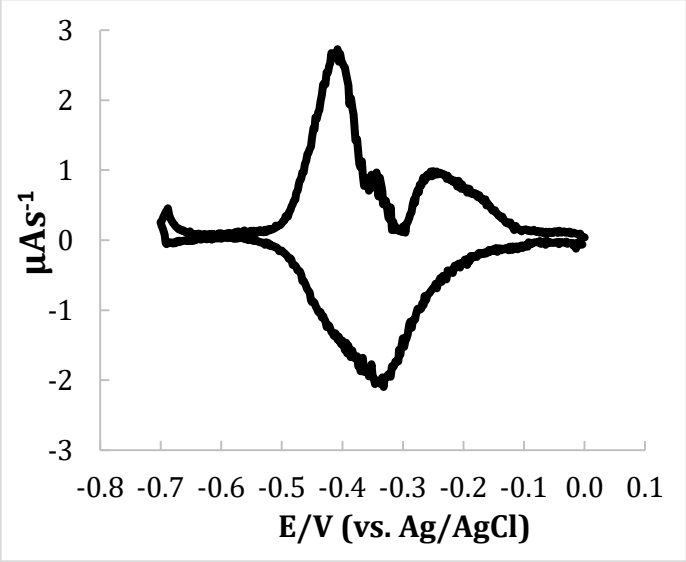

Figure 4.11. First derivative of turnover CV of AT set

4.3.4 Scanning Electron Microscopy (SEM) of Mini-MECs Anodes

SEM imaging is a destructive analysis and yet biofilm visibility is dependent on the viability of the biofilm. Immediately after the operation was finalized for *G. acetivorans* (AT set) on the anode of the 2 reactors SEM analysis were performed. Although there was a visible biofilm formation on AT set anodes at day 37 (Figure 4.2), biofilm detachment was significant at the point where SEM analysis was conducted. A control sample was also prepared with a bare abiotic graphite plate (Figure 4.12) electrode went through the same sample preparation process as the bioanodes for the SEM analysis.

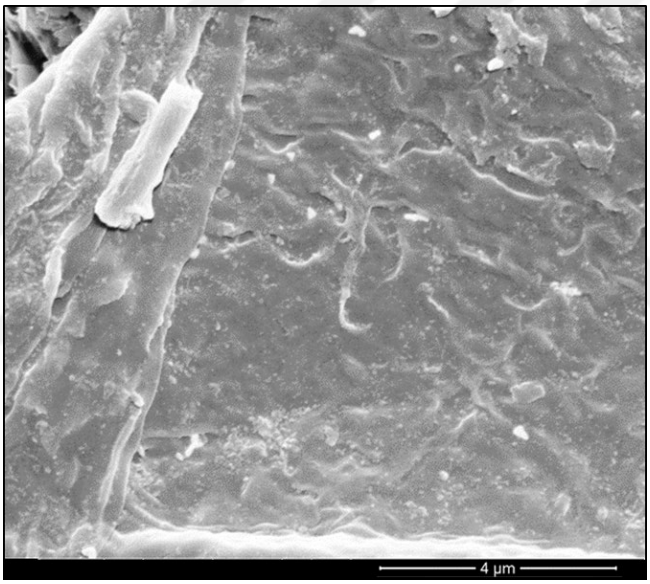

Figure 4.12. SEM image of bare electrode at x24000 magnification

SEM imagery on *G. acetivorans* bioanode were not conclusively showing individual cells or extracelullar attachments that was previously shown for connecting to Fe(III) minerals (Mardanov et al., 2015). However, electrode surface showed complex structures formed and circular shapes repeatedly encountered (Figure 4.13) that are consistent with the size (0.3 – 0.5 µM diameter) and irregular cocci shape of a single cell of *G. acetivorans* archaea.

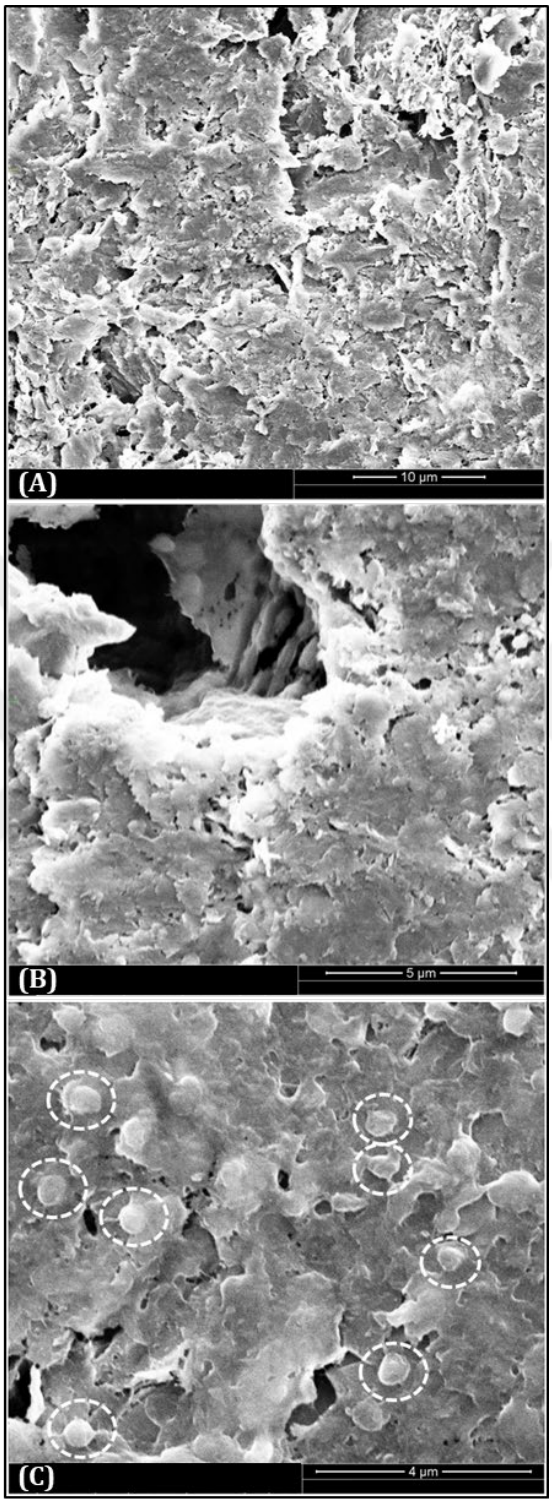

Figure 4.13. SEM images of *G. acetivorans* inoculated MEC (AT) anodes (t ≈ 60 d) at x6000 (A), x18000 (B), and x25000 (C) magnification

4.4 Mid-Size MEC Scale-Up Study (Set M-AT)

4.4.1 Reactor Performance of M-AT Set

4.4.1.1 Current Production

Bioelectrochemical behavior of *G. acetivorans* in Mini-MECs was previously described as showing 3 distinct time periods of "Start-up", "Biofilm Formation" and "Test" period. Exoelectrogenic behavior of *G. acetivorans* in Mid-Size MECs had shown similar pattern to this previous set with an important difference of significantly extended cycle durations (Figure 4.14). The start-up period operation duration increased from 7 days to 14 days and the biofilm formation period lasted for 55 days in comparison to 37 days. Cycle 7 was cut short because cables connecting the power supply and reactors needed to be replaced due to deterioration. High extent of replication was achieved around 1.02 ± 0.01 A/m^2 (j_v: 40.6 ± 0.4 A/m^3) on cycle 8. The reason for observing lower current density than AT reactor set (1.53 ± 0.27 A/m^2) could be explained by lower ratio of electrode surface area to the MEC volume (Hu et al., 2008). This ratio was 2.6 in Mini MECs and 1.1 in Mid-Size MECs. Due to the dimensions of the neck of serum bottles used in the fabrication of the Mid-Size MECs it was not possible to maintain the same electrode area to volume ratio as in Mini-MECs.

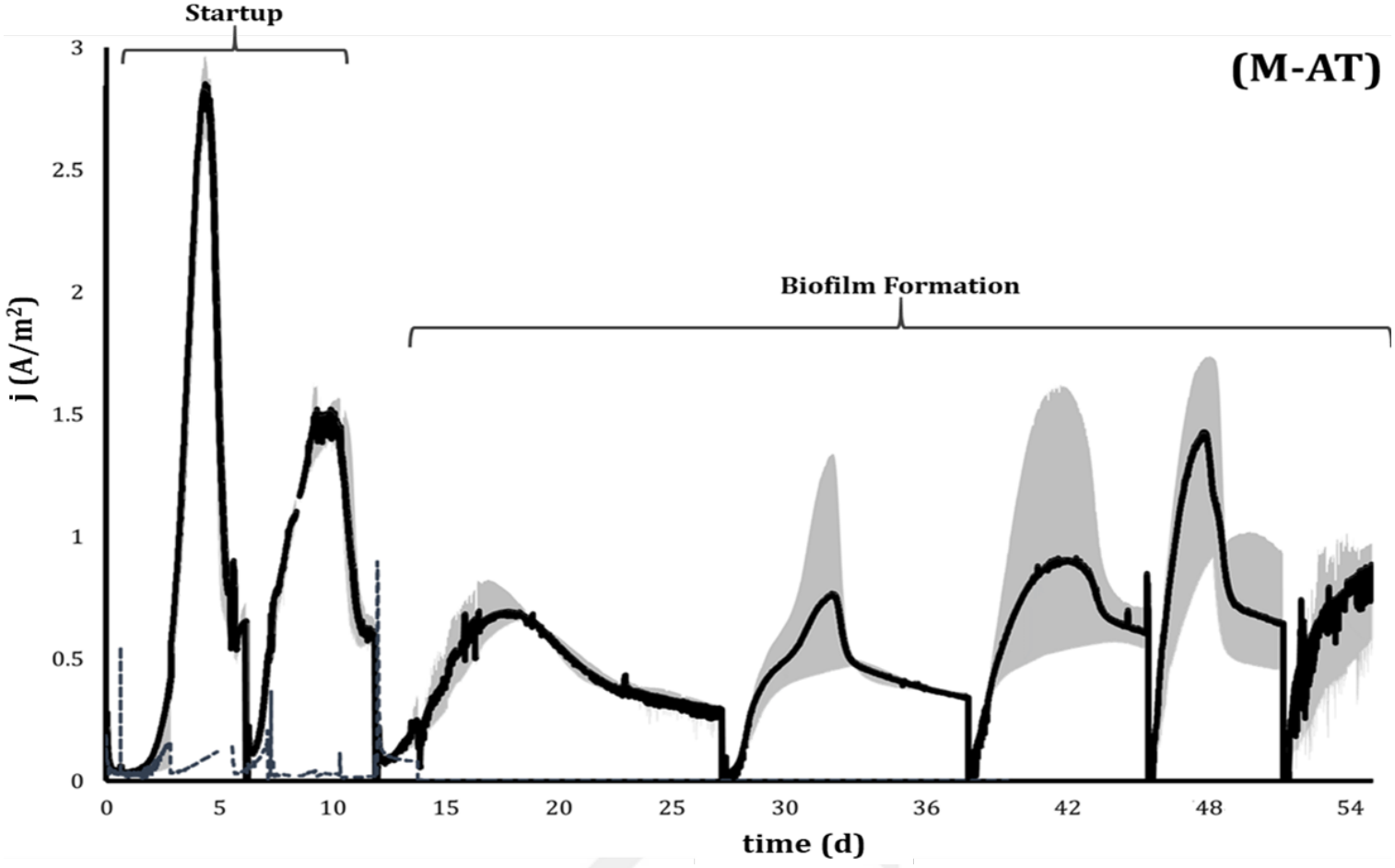

Figure 4.14. M-AT Startup & Biofilm Formation current production (black line: test average; blue dashed line: acetate control; gray area: variation)

Acetate consumption in the AT set was greater than 90% in all cycles when the reactors were fed with 10 mM acetate. In order to test the impact of substrate availability, acetate concentration was doubled to 20 mM when repeatable current density curves were obtained with quadruplicate reactor operation (Figure 4.15). Using higher concentration of acetate is aligned with the objective of feeding complex wastes or process effluents to these MECs, since there will be no need for dilution. After doubling the acetate concentration, peak current densities decreased from 1.02 ± 0.01 A/m^2 to 0.83 ± 0.03 A/m^2 and 0.66 ± 0.02 A/m^2 in the subsequent two cycles of operation and cycle duration was extended by approximately 40% and 70% (Figure 4.15). It was not clear that this decrease is caused by the higher dosage of acetate or biofilm detachment as at this time the reactors had been operated over 60 days. No visible biofilm detachment was observed in the anodes of Mid-Size MECs.

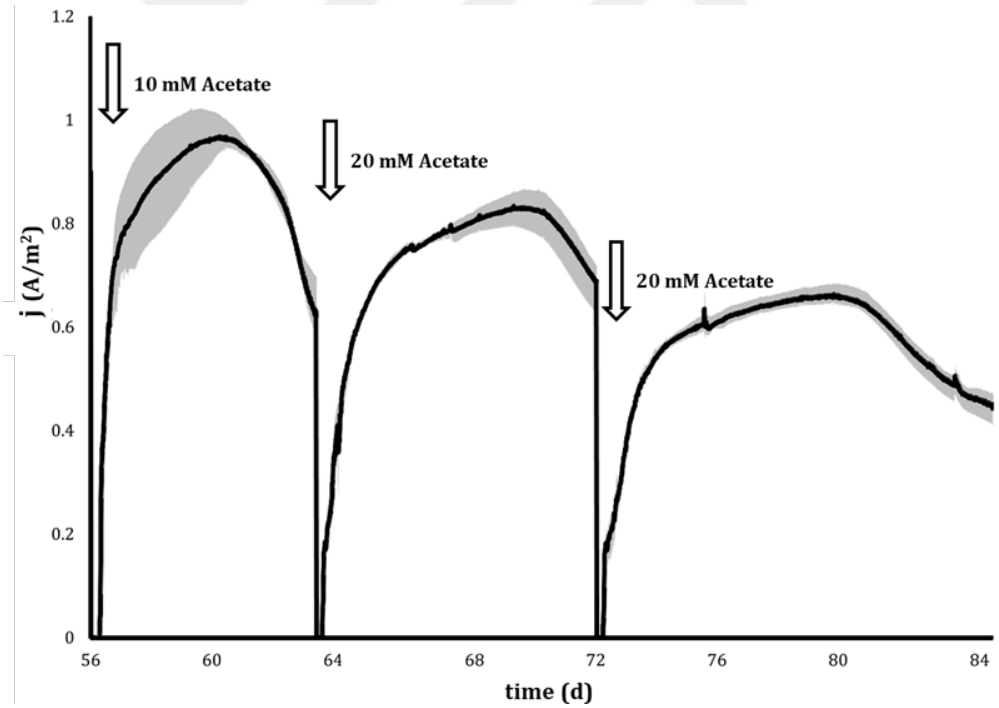

Figure 4.15. M-AT substrate dosage test (black line: average; gray area: variation)

The control set produced about 0.5 A/m^2 of peak current density (Figure 4.16) which is significantly lower than the initial peak current density recorded at the start of test period (Day 55) of 1 A/m^2. This could be due to extended reactor operation period (> 85 days). Current densities acquired with DF effluent fed reactors were almost half of the current produced with the pure acetate fed controls. Doubling the substrate dosage both in acetate controls and DF effluent did not increase the current production.

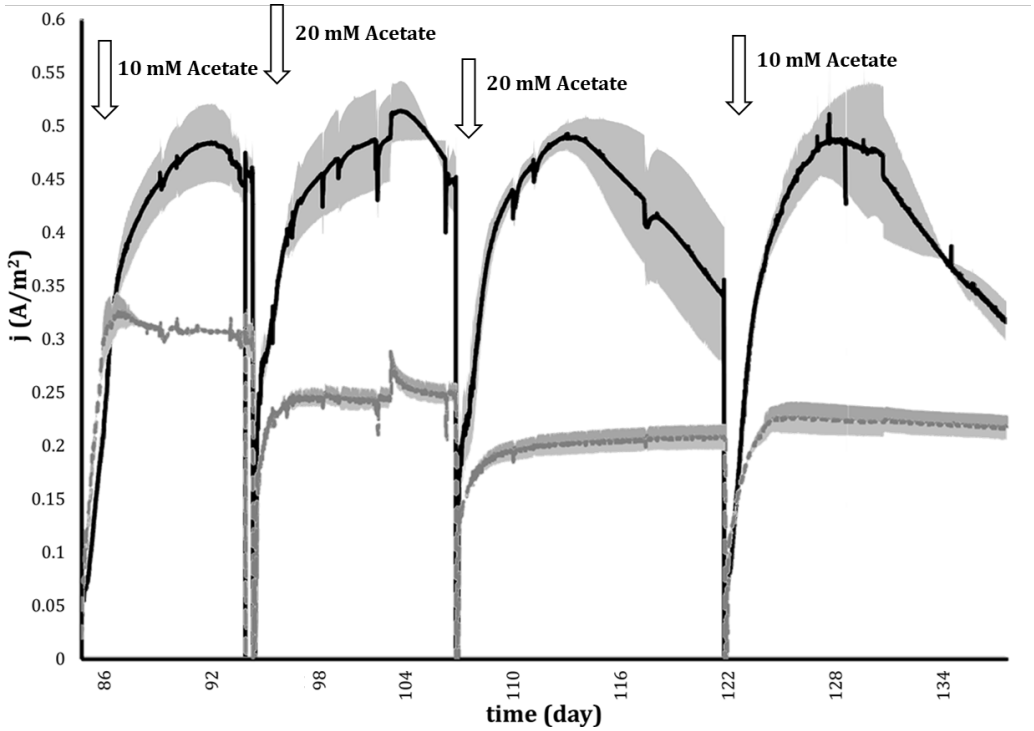

Figure 4.16. Current production in DF effluent fed MECs vs pure acetate fed MECs in M-AT Set (black line: pure acetate control average; dashed gray line: DF effluent average; gray area: variation)

For 10 mM dosage cycles, peak current density was found as 0.32 ± 0.02 A/m^2 for DF effluent fed reactors and 0.48 ± 0.06 A/m^2 for acetate controls. The peak current density in MECs fed with DF effluent reached to more than 65% of peak current density recorded by pure substrate. Doubling the dosage decreased the average of peak current density to 0.23 ± 0.03 A/m^2 for the DF effluent fed reactors in 2

subsequent cycles. This behavior indicated existence of stress inducing compounds in the DF effluent and increasing the dosage resulted in a decrease in the extracellular electron transfer rate of *G. acetivorans* bioanodes.

Previously, it was shown that DF effluent could be used for acetate source in MECs (Khongkliang et al., 2017, 2019; Lalaurette et al., 2009) at thermophilic applications. *G. acetivorans* bioanodes formed with pure acetate feed until 84th day were able to utilize a complex organic acetate source (DF effluent) at hyperthermophilic temperatures. The reactors were operated with DF effluent for over a period of 50 days. This result was shown for the first time in a hyperthermophilic BES.

4.4.1.2 Hydrogen Production

During the M-AT set, on cycle 8, current production of the reactors was replicating each other and during this cycle period of 7.1 days, Q_{H_2} was found as 0.14 ± 0.01 m^3H_2/m^3d, which is around 25% of the average hydrogen production rate in the previous AT set (Figure 4.17). Higher MEC volume to electrode ratio was expected to affect the hydrogen gas production rate (Hu et al., 2008) similar to the lower peak current densities. Another result acquired through this study is also hydrogen gas percent in the headspace was increased to highest observed (44.9 ± 4.2 %) with the doubling of acetate dosage to 20 mM (2nd cycle of increased dosage). This could indicate the affinity for the acetate as electron donor could be enhanced with increasing the acetate dosage. During the initial isolation of *G. acetivorans,* acetate was used for initial enrichment from environmental sample and later hydrogen gas was used as the final purification/enrichment process (Slobodkina et al., 2009). Distinctive behavior of utilizing these two electron donors that would be available to the biofilm in a membraneless MEC reactor makes operation with *G. acetivorans* more complicated. Current production (Figure 4.16) was affected by the addition of DF effluent detrimentally but, difference between hydrogen production rates (Figure 4.18) were not statistically different (*t*-test P<0.001) from acetate control reactors.

This result might indicate that the hydrogenase enzymes used by *G. acetivorans* during the phenomenon described as hydrogen cycling (discussed in Chapter 4.4.3) or other enzymes involved in EET could be suppressed by the content of the DF effluent.

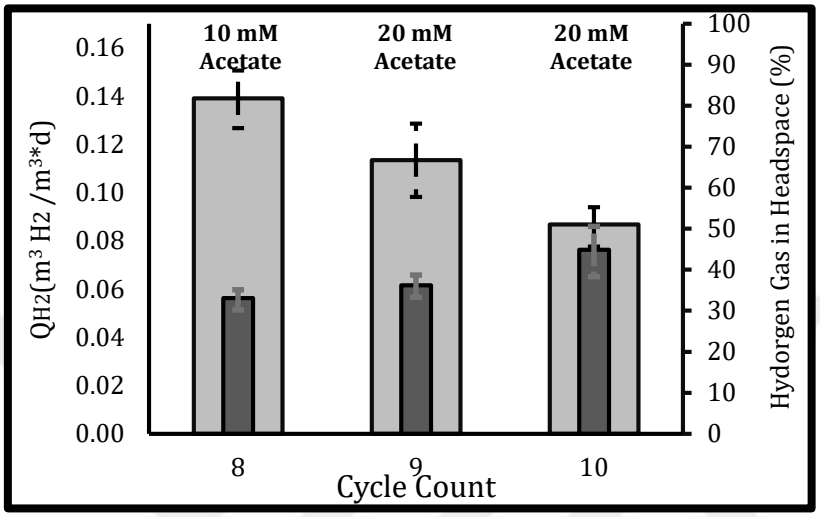

Figure 4.17. Hydrogen production rates and headspace hydrogen content for M-AT Set substrate dosage test (light gray bars: Q_{H_2}; dark grey bars: gas percentage)

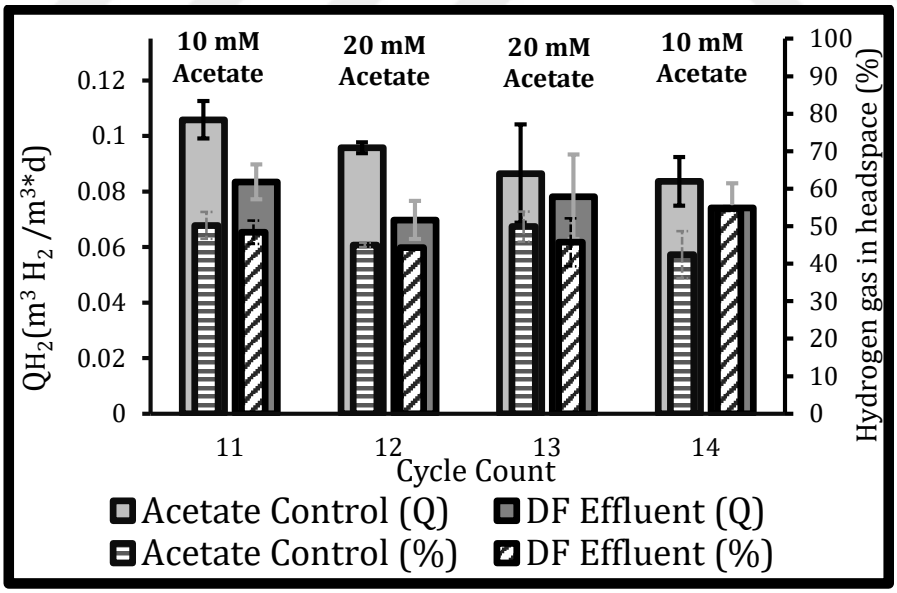

Figure 4.18. Hydrogen production rates and headspace hydrogen content for DF effluent fed MECs vs. pure acetate fed controls

4.4.2 Efficiency Calculations for M-AT Set

Acetate consumption exceeded 10 mM that was initially used for M-AT set after doubling the dosage. In the final cycle for substrate dosage test, acetate consumption of quadruplicate reactors was averaged around 71.3 ± 3.9% (14.3 ± 0.8 mM consumed). Increasing the dosage could provide advantages in terms of fed-batch MEC operation since reactors are only exposed to stresses (oxygen leakage, washout effect, lower temperatures) during analysis and media replacement after the cycle has been completed. Cathodic recovery rate was unaffected by the increase in the acetate concentration while coulombic efficiency decreased from 287.5 ± 14.6 % to an average of 229.9 ± 14.7 % (Table 4.3) possibly due to the increase in charge passed as a result of providing unlimited substrate conditions. Overall hydrogen recovery also decreased from an average of 81.8 ± 8.7 % to 68.1 ± 7.7 % and 56.7 ± 3.2 % in the subsequent cycles with increased acetate dosage.

Table 4.3. Summary of M-AT Set substrate dosage test with acetate

Cycle Count	j_{max} (A/m^2)	t (d)	Q_{H_2} (m^3H_2/m^3)	n_{AC} (%)	C_E (%)	r_{Cat} (%)	R_{H_2} (%)
8 ***(10 mM)***	1.02 ± 0.01	7.1	0.14 ± 0.01	89.6 ± 3.0	287.5 ± 14.6	28.5 ± 3.4	81.8 ± 8.7
9 ***(20 mM)***	0.83 ± 0.03	9.0	0.11 ± 0.02	55.4 ± 1.6	247.1 ± 5.2	27.5 ± 2.7	68.1 ± 7.7
10 ***(20 mM)***	0.66 ± 0.02	12.2	0.09 ± 0.01	71.3 ± 3.9	212.7 ± 13.8	26.7 ± 2.6	56.7 ± 3.2

Before the start of DF effluent utilization test, quadruplicate reactors used in this study was producing results with low variation for all performance parameters considered. In the duplicate reactors fed with DF effluent, acetate consumption and Coulombic efficiencies was less compared to the pure acetate controls and while overall hydrogen recoveries were similar (Figure 4.19). Summary of results for this study is provided in Table 4.4

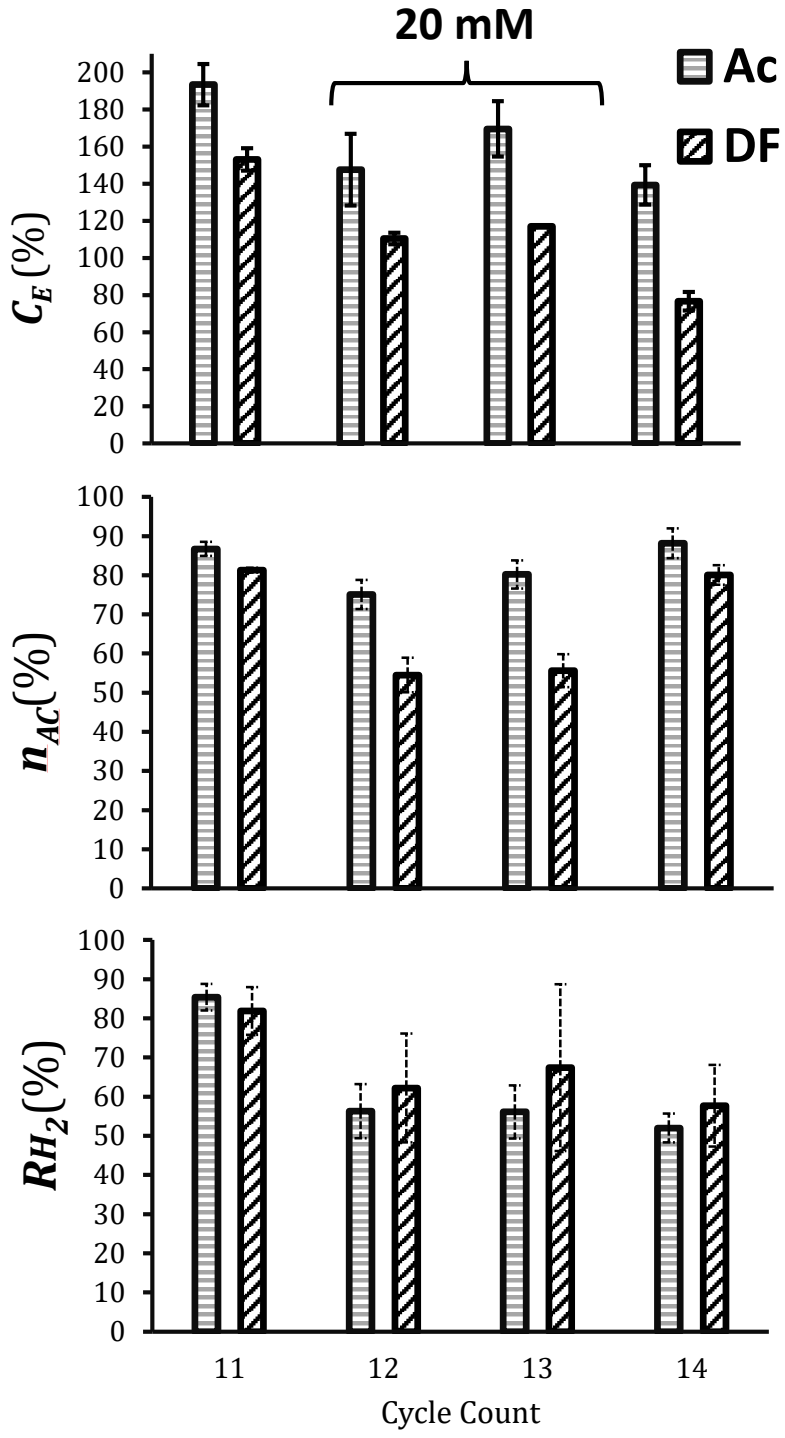

Figure 4.19. Coulombic efficiency (C_E), acetate consumption (n_{AC}) and overall hydrogen production (RH_2) efficiencies for DF effluent test in M-AT set

Table 4.4. Summary of M-AT Set DF effluent test

Cycle Count	j_{max} (A/m^2)	t (d)	Q_{H2} (m^3H_2/m^3)	n_{AC} (%)	C_E (%)	r_{Cat} (%)	R_{H2} (%)
11 (DF)	0.32 ± 0.02	9.1	0.08 ± 0.01	81.3 ± 0.6	153.1 ± 6.0	53.7 ± 6.1	81.9 ± 6.1
11 (AC)	0.48 ± 0.04	9.1	0.11 ± 0.01	86.7 ± 1.8	193.4 ± 11.1	44.1 ± 0.8	85.4 ± 3.4
12 (DF)*	0.25 ± 0.03	11.4	0.08 ± 0.01	54.5 ± 4.4	110.4 ± 3.1	56.2 ± 11.0	62.2 ± 13.9
12 (AC)*	0.51 ± 0.03	11.4	0.10 ± 0.00	75.1 ± 3.7	147.6 ± 19.3	38.1 ± 0.3	56.3 ± 6.9
13 (DF)*	0.20 ± 0.01	15.2	0.08 ± 0.02	55.6 ± 4.2	117.0 ± 0.0	56.3 ± 17.0	67.4 ± 21.3
13 (AC)*	0.49 ± 0.02	15.2	0.09 ± 0.02	80.2 ± 3.6	169.5 ± 14.9	37.9 ± 0.8	56.1 ± 6.8
14 (DF)	0.22 ± 0.02	15.8	0.08 ± 0.01	80.1 ± 2.5	76.7 ± 5.0	75.9 ± 18.2	57.7 ± 10.4
14 (AC)	0.48 ± 0.05	15.8	0.07 ± 0.01	88.2 ± 3.8	139.3 ± 10.6	43.8 ± 4.6	52.0 ± 3.7

*During Cycle 12 and Cycle 13 20 mM acetate was fed into reactors

4.4.3 Internal Hydrogen Cycling Test

Reactors fed with 10 mM acetate in the AT reactor set, consumed acetate to high extent after the biofilm formation period was completed (95.0 ± 2.6 % on average), but the fact that the C_E values were above 100% indicated a phenomenon known hydrogen cycling as it was seen in previous studies (Call et al., 2009; Lee & Rittmann, 2010). *G. acetivorans* was previously reported for its ability to grow with H_2 as sole electron donor and CO_2 as carbon source while Fe(III) iron is present as electron acceptor (Slobodkina et al., 2009). There is a potential that similar metabolic activities occur in the membraneless MEC where the solid-state electrode is used as the electron acceptor by *G. acetivorans*. After the initial consumption of acetate that is coupled to electron transfer to the anode, both H_2 and CO_2 gases are produced in the MEC. The accumulated hydrogen in the headspace of the reactors may then be reused as electron donor to produce further current; increasing the C_E over 100 %.

Reactors used in hydrogen cycling study was previously operated for 87 days and the current densities dropped significantly from around 1 A/m^2 to 0.45 A/m^2. However, it was clearly shown that *G. acetivorans* utilized hydrogen gas as the sole electron donor in a membraneless single chamber MEC reactor, producing current in a steady rate rather than a bell-shaped curve that was observed when reactors were fed with 10 mM acetate (Figure 4.20). These duplicate reactors were tested for hydrogen cycling by having 3 subsequent cycles of current production with only acetate, only hydrogen gas and no electron donor in the reactor. When fed with acetate *G. acetivorans* MECs produced clear peaks. When media was replaced without acetate and the reactor was pressurized with hydrogen gas reactors showed a steady current production behavior to the extent of 40% to 60% of the current produced in the acetate-fed cycles (Figure 4.20). When media was replaced and no electron donors were present in the form of acetate or hydrogen gas, reactors did not produce any significant current. These tests were conducted at a later stage of biofilm formation thus the full extent of hydrogen cycling to the current production is

unknown. Specifically, the contribution of hydrogen to the current at the start-up period and early stages of the test period of MECs is not clear. Two-chamber reactor configuration (H-Cell MECs) should be used to further understand the contribution of hydrogen cycling to the current production (Lee & Rittmann, 2010). The proton selective membrane present between the anode and cathode chambers will prevent hydrogen leakage to the anodic chamber (Lee & Rittmann, 2010)

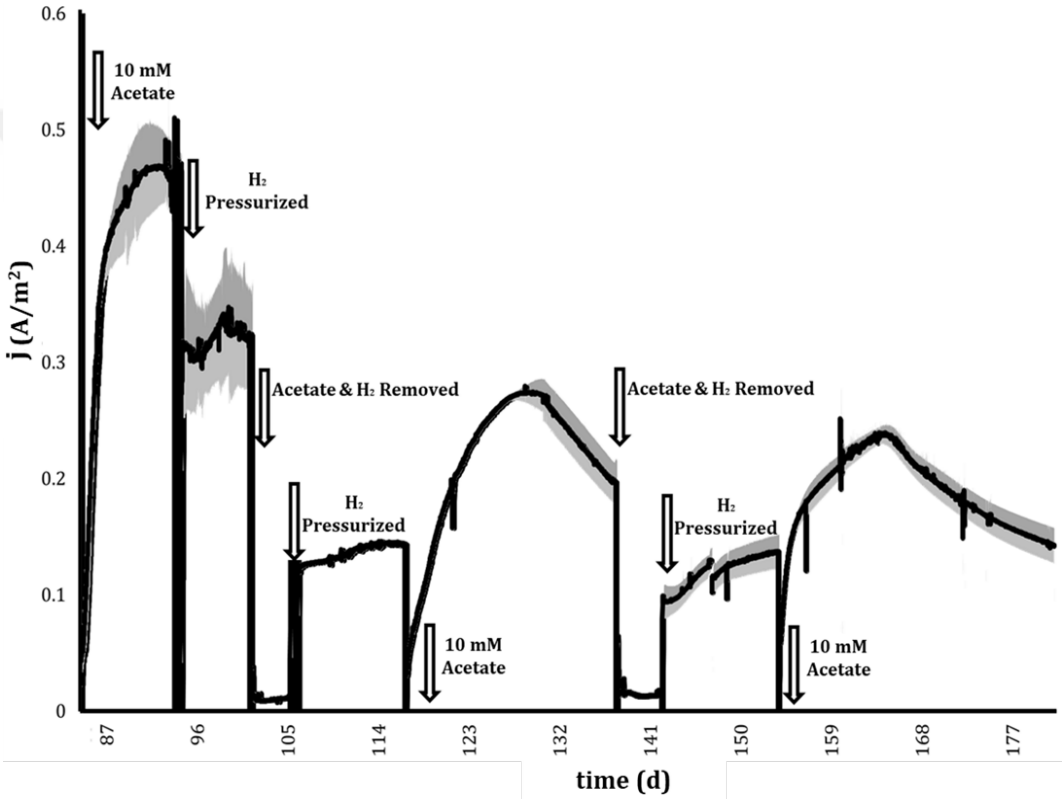

Figure 4.20. Current density graphs of hydrogen cycling test (black line: average; gray area: variation)

4.4.4 Electrochemical Analysis of M-AT Biofilm

After finalizing substrate dosage test (84th day of operation) M-AT set reactors were investigated with CV. Resulting voltammograms produced smaller peak currents (Figure 4.21) but similar to the previous set, S-shaped (sigmoid) curves under turnover conditions was recorded. Also, smaller peaks observed for non-turnover and start of cycle (turnover) at similar redox potentials as turnover S-shaped curves indicate redox enzymes were utilized at this potential with slightly different anode potentials around -350 mV midpoint potential compared to -400 mV of the previous analysis.

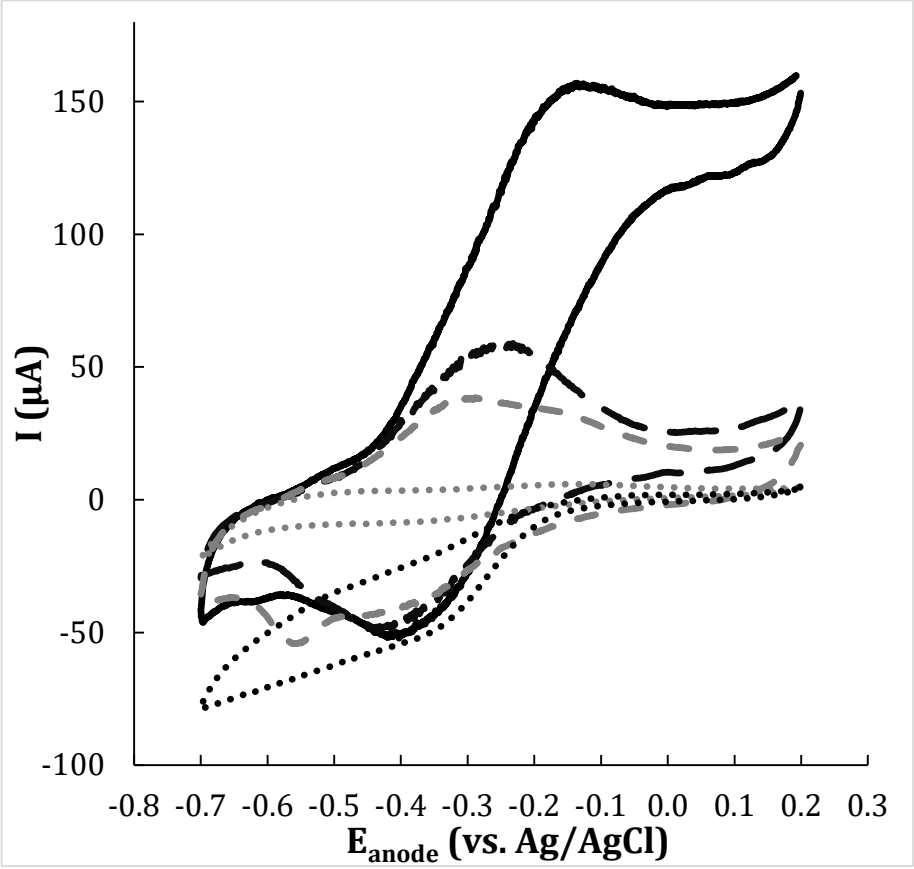

Figure 4.21. Cyclic voltammogram of *G. acetivorans* M-AT Set; turnover (solid black line), turnover start-of-cycle (dashed black line), non-turnover (dashed grey line), spent medium (dotted grey line), abiotic control (dotted black line)

It is expected that the peak anodic current and the peak cathodic current will increase proportionally for the species adsorbed on the electrode surface with the change of the scan rate in CV analysis (Richter et al., 2009) . In other words, if the electron transfer is due to the biofilm grown on the electrodes, the value of "α" exponent given in Equation 3-5 is equal to 1. If the peak anodic current increases linearly with respect to the square root of the scan rate (α = 0.5), with the change of scan rate in CV analysis, the electron transfer mechanism is considered to be diffusion-limited since electrons in the biofilm vicinity could not reach the electrodes at faster potential changes (Marsili et al., 2010). This relation is based on Randles-Sevick equation desribed for electron transfer processes of redox species (Kang et al., 2012) given in Equation 3-6.

In other words, when a linear relationship is observed between the peak current values and the square root of scan rate under non-turnover conditions, it is shown that the electron transfer occurs in the biofilm at the electrode interface with immobile redox cofactors (Gregoire et al., 2014; Katuri et al., 2012). By rearranging the Equation 3-5, calculation of "α" exponent is possible through deriving the linear equation for dimensionless current density versus dimensionless scan rate shown in the Equation 4-1.

$$\log(j_{max}) = \alpha \log(\nu) \qquad \text{(Equation 4-1)}$$

This analysis is frequently used in bioelectrochemical systems because it provides information about the electron transfer mechanism of the electro-active microorganism. However, results such as rapid recovery current production after media replacement and a thick biofilm formation are also accepted as supporting evidence of DET capability (Marshall & May, 2009; Parameswaran et al., 2013). The linear relationship is shown in Figure 4.22 for voltammograms produced with *G. acetivorans* from the peak separation analysis conducted between the scan rate ranges of 1 mV/s to 100 mV/S (Figure 4.23) .

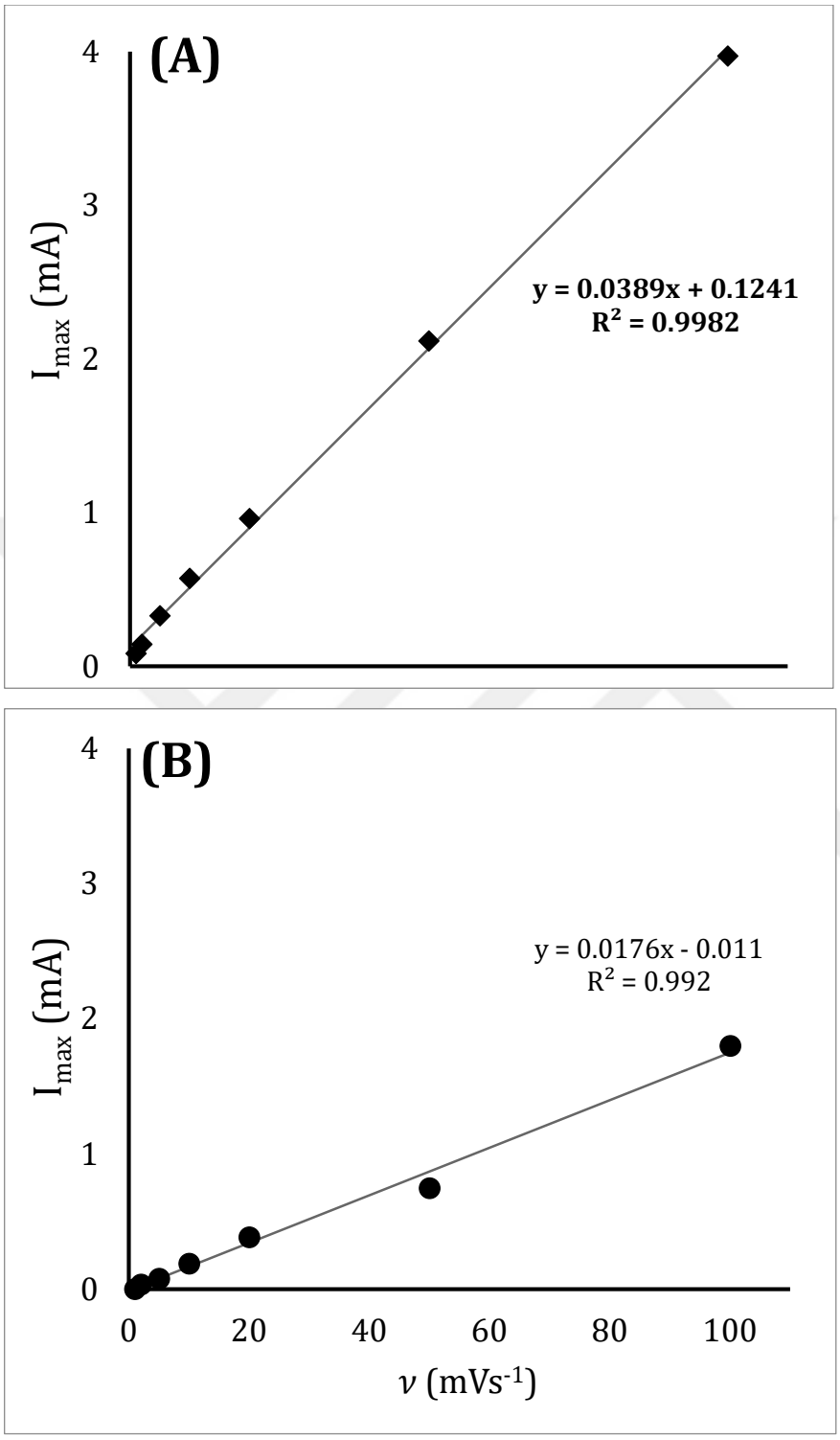

Figure 4.22. Scan rate analysis under turnover **(A)** and non-turnover **(B)** for *G. acetivorans*

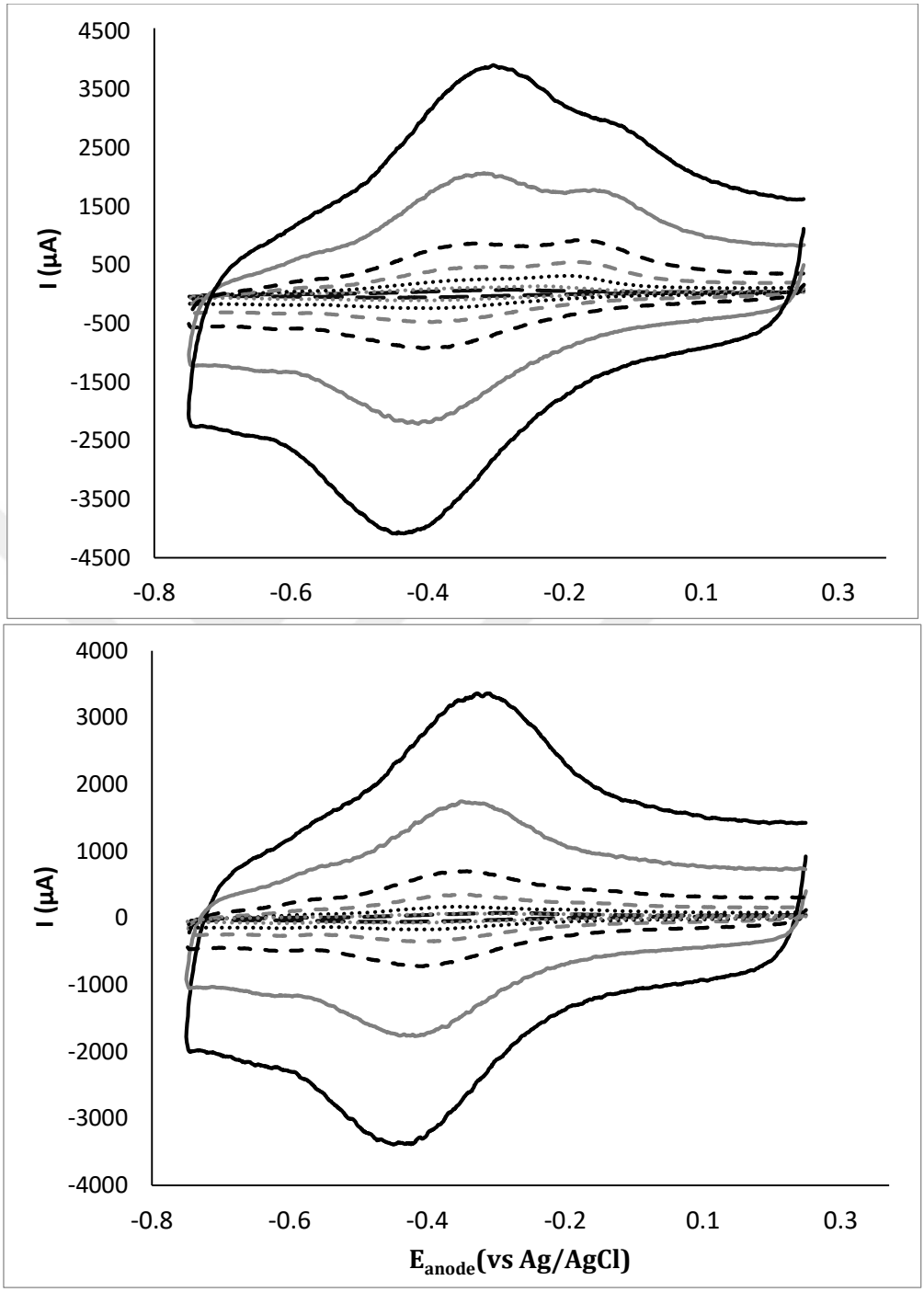

Figure 4.23. Peak separation analysis for M-AT reactor set turnover (top) and non-turnover (bottom) conditions (black line: 100 mV/s; gray line: 50 mV/s; black dashed line: 20 mV/s; gray dashed line: 10 mV/s; black dotted line: 5 mV/s; gray dotted line: 2 mV/s; black long-dashed line: 1 mV/s)

Under non-turnover conditions, α=1 was previously described for the case which electron transfer is confined in the biofilm and under turnover conditions α value around 1 electron transfer is faster than metabolic reaction (i.e. acetate oxidation) (Rousseau et al., 2014). *G. acetivorans* through this peak separation analysis were shown to produce a biofilm in which the electron transfer system is confined in and also metabolic reaction is the rate limiting step with α values of 0.989 and 0.836 (Figure 4.24) for non-turnover and turnover conditions respectively. This is another supporting and clear evidence of the presence of DET in the *G. acetivorans* MECs.

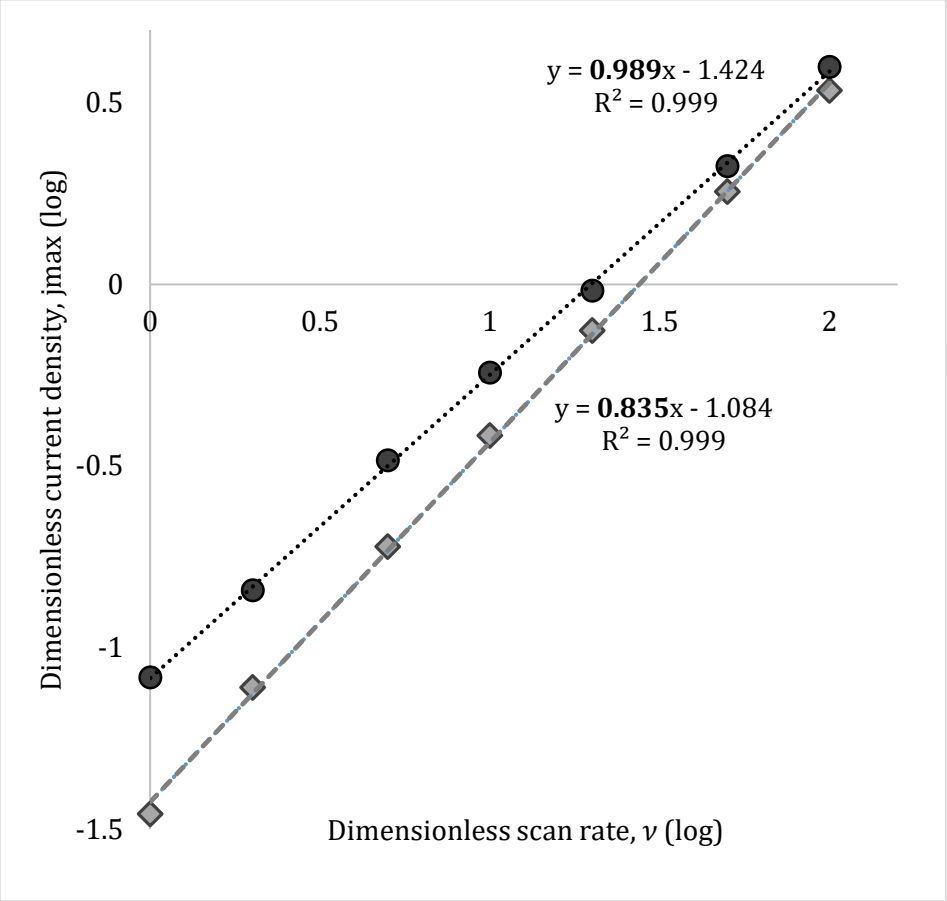

Figure 4.24. Calculation of alpha exponent from current density and scan rate plot (black circle markers: non-turnover, gray diamond markers: turnover)

4.4.5 Scanning Electron Microscopy (SEM) of Mid-Size MECs Anodes

An extra reactor of Mid-Size MECs was set up and operated for 1 feeding cycle of M-AT set, with acetate then sacrificed for SEM. Resulting SEM imagery (Figure 4.25) showed a stacked formation of circular shapes that was similar to the size (0.3-0.5 μm in diameter) and the irregular cocci morphology of *G. acetivorans*. At this stage (t=7 days) *G. acetivorans* attachment to the anode surface were limited to certain areas.

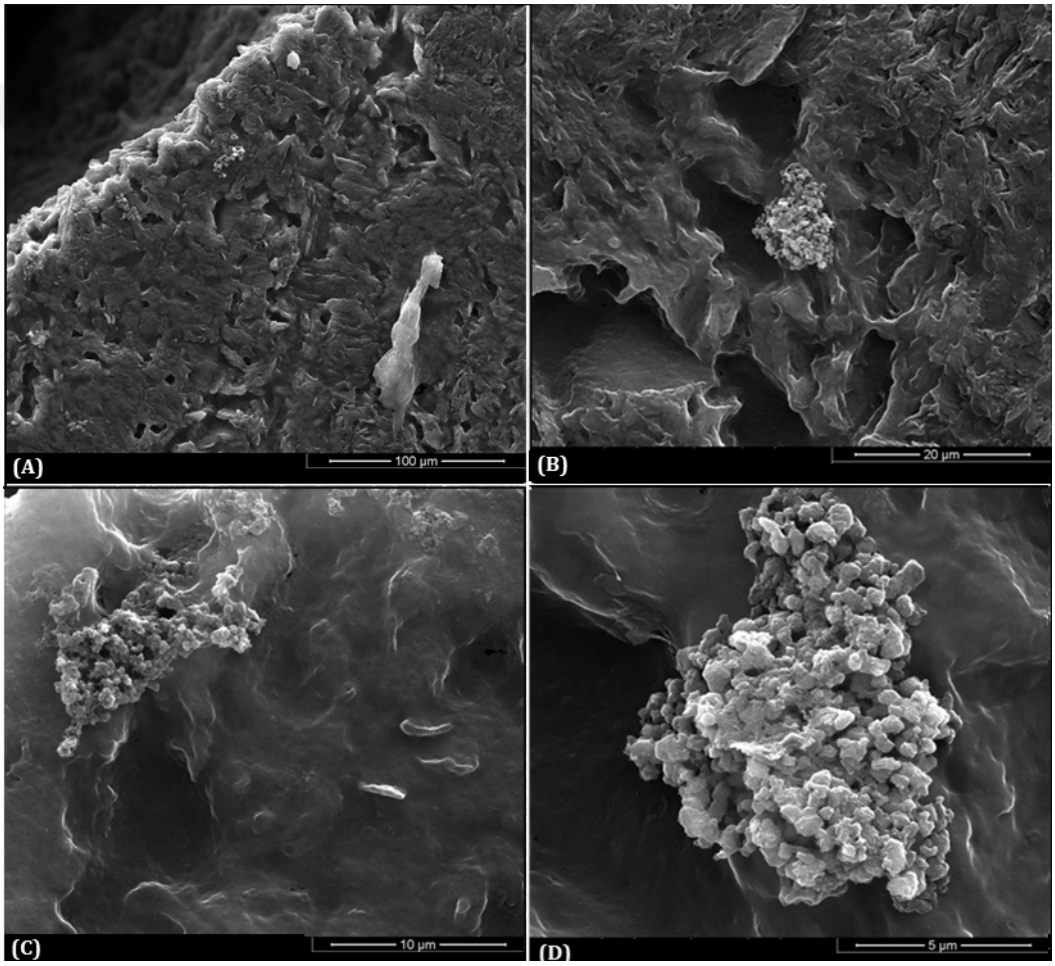

Figure 4.25. M-AT Bioanode investigation with SEM after 1st cycle (t=7 days) at x1000 (A), x5000 (B), x10000 (C) and x20000 magnification

Compared to the bioanode after the first cycle (Figure 4.26), sample prepared after M-AT set operation was finalized show SEM imagery with complex structures similar to the previous results of AT reactor set anodes. Marked area on Figure 4.25 shows the stacked circular cells on the graphite surface forming complex connections.

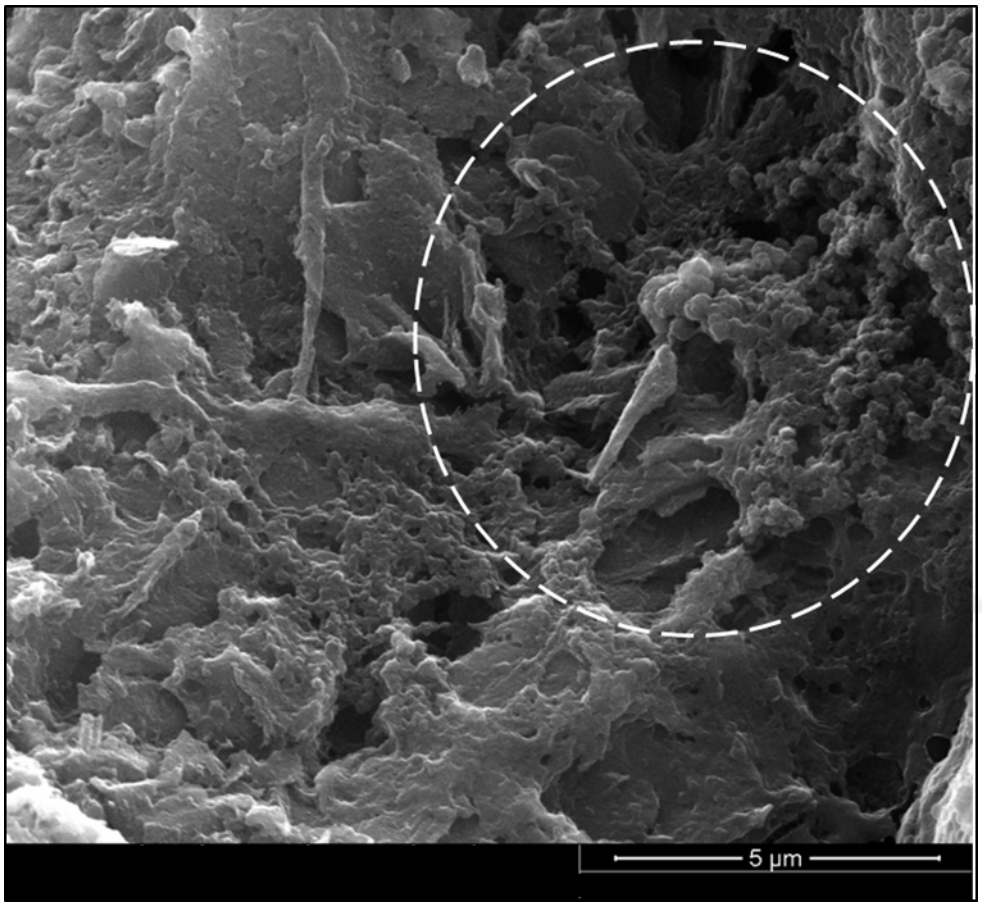

Figure 4.26. M-AT Bioanode investigation with SEM after operation was finalized (t=177 days) at x20000 magnification

4.4.6 Protein Measurement

Protein measurement for graphite anode electrode and the reactor supernatant was done to assess the formation of cells on electrode surface. Additionally, among the

different pathways for extracellular electron transfer, cell surface proteins are known to play a major role in DET (Costa et al., 2018). This role is attributed to the *c*-type cytochromes for model exoelectrogenic species of *G. sulfurreducens* and *S. onisendiensis* MR-1 (Shi et al., 2007). *G. acetivorans* were reported to have second highest number of genes for putative *c*-type cytochrome used for dissimilatory iron reduction after *F. placidus* (Smith et al., 2015). Since these proteins involved in the DET directly interacting at the electrode surface, proteins from anode surface was extracted and quantified with Bradford Assay. *G. acetivorans* reactors from M-AT set produced 0.038 mg/cm^2. Total protein concentration was 1.65 times higher than the reactor supernatant for *G. acetivorans* MECs; indicating the attachment of biofilm to the anode. This value is much lower than what was recorded for the closely related hyperthermophilic iron-reducing species of *F. placidus* (0.135 mg/cm^2) and *G. ahangari* (0.139 mg/cm^2) in single chamber MECs (Yilmazel et al., 2018); where 3-3.2 times more protein was present in comparison to the reactor content. One important factor to consider here is that *G. acetivorans* MECs were operated for 180 days when protein measurement was conducted since it is a destructive analysis. Also due to extended period of MEC operation, there was a possibility of biofilm detachment from the electrode surface and increasing the total protein concentration in the reactor supernatant.

4.5 Utilization of Dark Fermentation Effluent by Hyperthermophilic Exoelectrogenic Archaea (Set DF-MEC)

4.5.1.1 Current Production

Use of fermentative process effluent as acetate source in MECs was shown and discussed for the *G. acetivorans* previously in Chapter 4.4.1.1 and 4.4.1.2 This application was conducted under the conditions of a biofilm formed with pure acetate feed. This test DF-MEC set aimed to check whether the biofilm could be formed

with the DF effluent as acetate source in the MEC medium. Although the current production (Figure 4.27 and Figure 4.28) and hydrogen production (Figure 4.29) was observed throughout the operation for 54 days these reactor sets inoculated with *G. acetivorans, F. placidus* and co-culture of these two species were unable to achieve a high extent of replication in the results. Reactors that were unable to produce current comparable to the previous Mini-MEC sets results or replicates producing lower current densities in their respective group were reinoculated with the freshly grown culture bottles. Even after supplementing the reactors with freshly grown cultures biofilm formation period (previously described for AT and M-AT set) was not completed with this DF effluent fed reactors within the same allocated time period of 54 days.

For the reactors that were inoculated with *G. acetivorans*, AT reactor set operated for this thesis study was used as a reference point, since it was started with the same culture and reactor set-up except with pure acetate. On the other hand, for *F. placidus* MECs, a previous study (Yilmazel et al., 2018) conducted with pure acetate feed where the same reactor set-up formed the baseline for comparison.

Cycle duration were 5-6 times higher than the pure acetate fed Mini-MECs for *G. acetivorans* reactors, indicating a slow rate of utilization for acetate in DF effluent. Current production behavior of the co-culture MECs (DF-CCT), were similar to the reactor set with *F. placidus* inoculated reactors (DF-FP) (Figure 4.27) although the *G. acetivorans* reactors was able to produce higher currents when used as mono culture (Figure 4.26). This result was unexpected since reactor operation temperature (80 °C) was lower than the optimum growth conditions and the previously used operation temperature of 85 °C (Yilmazel et al., 2018). The basis for testing a co-culture of *G. acetivorans* and *F. placidus* was that *F. placidus* showed more variability in terms of substrate utilization (Anderson et al., 2011; Hafenbradl et al., 1996; Smith et al., 2015) and potentially could utilize compounds that could otherwise have a suppressing impact on *G. acetivorans* enzymes involved in EET.

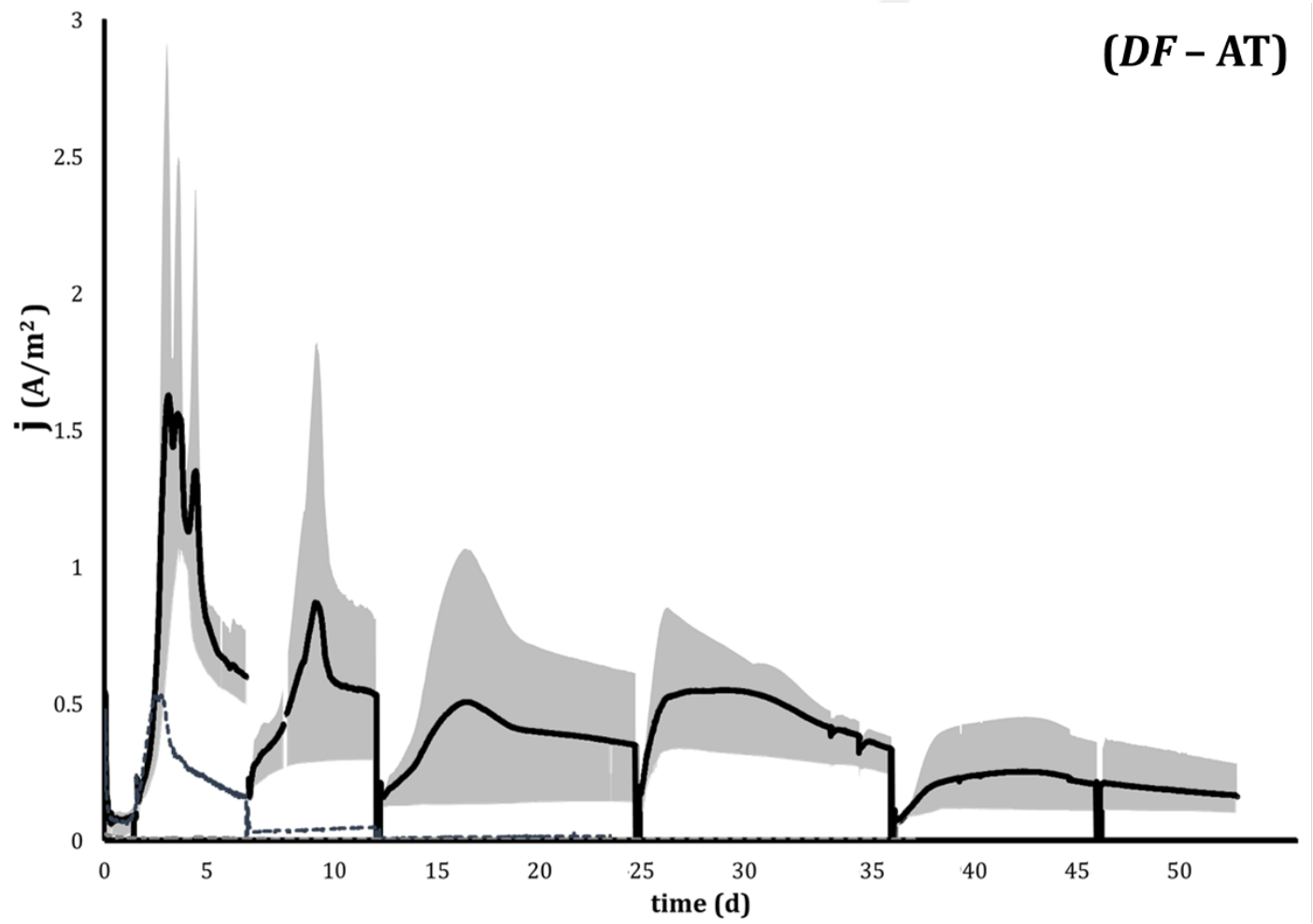

Figure 4.27. Current production of DF effluent fed Mini-MECs of *G. acetivorans* (DF-AT Set) (black line: average; gray area: variation)

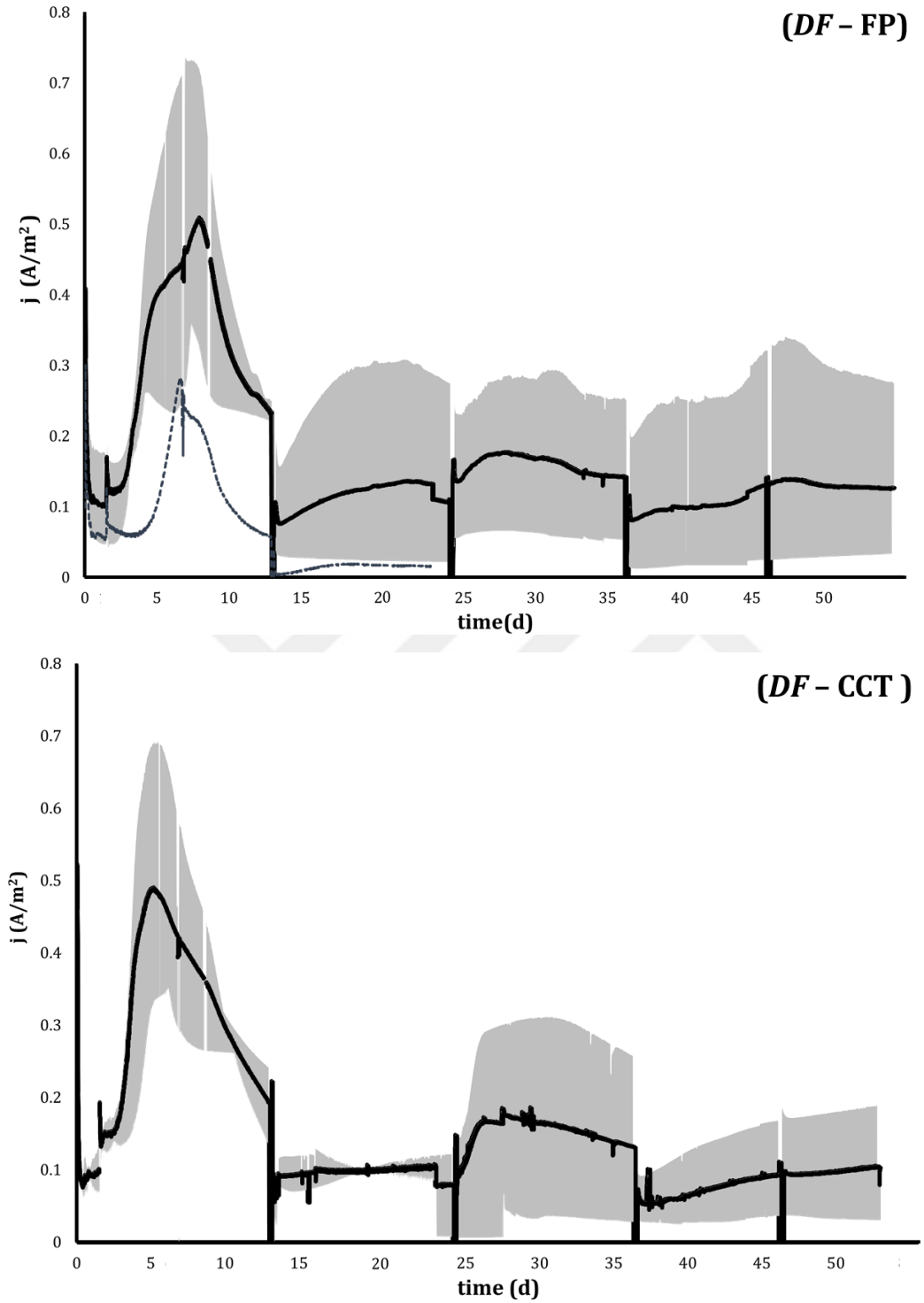

Figure 4.28. Current production of DF effluent fed Mini-MECs of *F. placidus* (DF-FP Set) and co-culture test of *G. acetivorans and F. placidus* (DF-CCT) (black line: average; gray area variation)

4.5.1.2 Hydrogen Production

Q_{H_2} on average was found as 0.33 ± 0.03, 0.13 ± 0.06 and 0.08 ± 0.03 m^3H_2/m^3d for the 3 cycles of DF-AT set respectively. Hydrogen production rates at the 3rd cycle were slightly lower the than the DF effluent fed reactors in the M-AT reactor set (Figure 4.18) although the variation is too high. This could be explained with the fact that biofilm formation was not completed for these cycles shown on Figure 4.29.

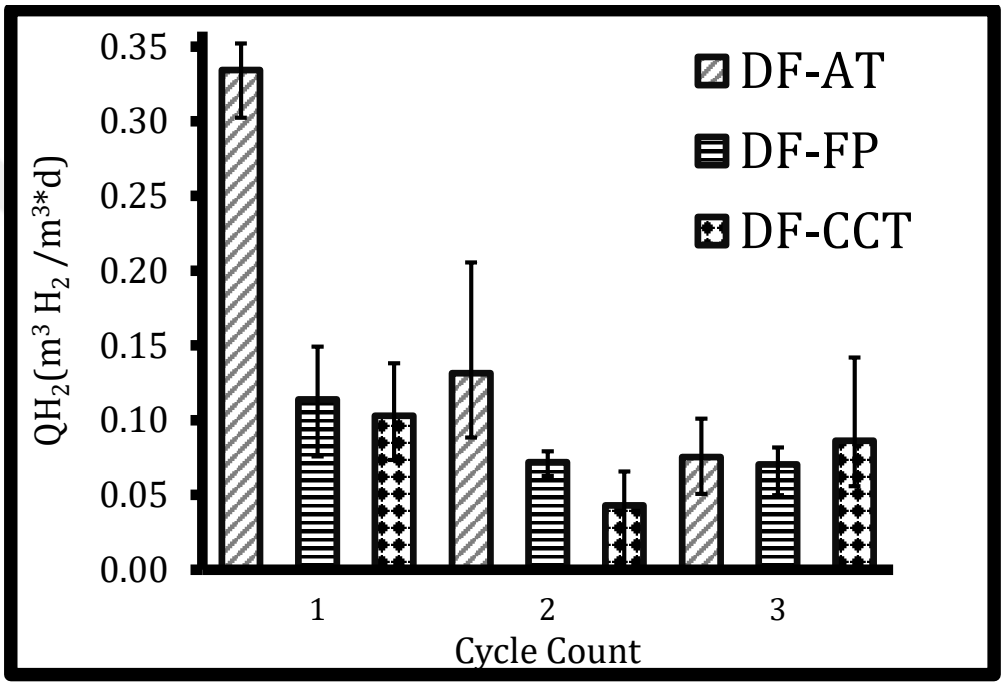

Figure 4.29. Hydrogen production rates for DF effluent fed Mini-MECs of *G. acetivorans, F. placidus* and co-culture test

Q_{H_2} for DF-FP set resulted in less variation after each cycle and between the replicates. On average Q_{H_2} was found as 0.11 ± 0.04, 0.07 ± 0.01 and 0.07 ± 0.02 m^3H_2/m^3d for the 3 cycles. Hydrogen production rate of DF-CCT was almost close to zero on one replicate in second cycle and improved to an average of 0.09 ± 0.04 m^3H_2/m^3d after reionoculation of the replicate with fresh inoculum. However, for all 3 reactor sets variation of hydrogen production rates between the reactors was too

high after the initial cycle. It was not clear whether the hydrogen cycling previously shown for *G. acetivorans* inoculated MECs in Chapter 4.4.3 were occurring inside of these DF effluent fed reactors. According to these results, it was possible to use DF effluent as acetate source in hyperthermophilic MECs inoculated with both *G. acetivorans* and *F. placidus* as it is evident with the current production and hydrogen gas production, however, this application requires further investigation of possible stress inducing compounds in the complex organic substrates such as DF effluent.

CHAPTER 5

CONCLUSIONS

This thesis work was focused on hydrogen production potential of a novel hyperthermophilic BES; where an iron reducing hyperthermophilic archaeon *G. acetivorans* was used as inoculum for the first time in the literature. In this experimental work, important results have been obtained regarding high temperature applications, which are very limited in number in the BES literature. In summary the following conclusions can be drawn: The ability of hyperthermophilic archaea,

- *G. acetivorans*, to transfer electrons out of the cell by using the anode electrode in a microbial electrochemical reactor has been proved for the first time in the literature.
- *G. acetivorans* is the fourth hyperthermophilic exoelectrogenic microorganism identified to date.
- When acetate was fed to the *G. acetivorans* MECs produced a current density of 1.53 A/m^2, and this is the highest current density recorded among other hyperthermophilic pure culture exoelectrogens.
- Electron transfer mechanisms of *G. acetivorans* using CV and scan rate test (peak separation) via calculation of the "α" exponent value. Multiple evidences such as an "α" exponent value being equal to unity, during MEC operation current density reaching the peak in a short time after media replacement, visible biofilm formation on the anode electrode surface as shown by the presence of complex connections and layered structures in SEM images prove that *G. acetivorans* is performing DET instead of using mediators for the electron transfer.

- *G. acetivorans* biofilm grown with pure acetate (bioanode) could also utilize dark fermentation effluent to produce hydrogen. This was the first time application showing the utilization of fermentation effluent in MECs at hyperthermophilic temperatures.
- It was not possible to start an MEC that was directly fed with DF effluent with the following three inoculums (i) *G. acetivorans only,* (ii) *F. placidus* only, (iii) *G. acetivorans and F. placidus* co-culture.

CHAPTER 6

RECOMMENDATIONS

The interaction between the electrode and exoelectrogens in bioelectrochemical systems occurs through a series of complex events and reactions. For this reason, it is essential to carry out a serious optimization study in these systems.

- Optimization of applied voltage and testing of different electrode materials for higher performance is required.
- Compared to the model exoelectrogen *G. sulfurreducens* MECs, *G. acetivorans* inoculated MECs required much longer start-up and biofilm formation periods. To reduce the start-up period, different growth medium including soluble or insoluble iron compounds could be tested.
- In order to understand the full extent of internal hydrogen cycling phenomenon with *G. acetivorans,* 2-chamber MECs with proton selective membrane could be utilized so that hydrogen produced at the surface of cathode transferring to anode side is minimized.

REFERENCES

Anderson, I., Risso, C., Holmes, D., Lucas, S., Copeland, A., Lapidus, A., Cheng, J. F., Bruce, D., Goodwin, L., Pitluck, S., Saunders, E., Brettin, T., Detter, J. C., Han, C., Tapia, R., Larimer, F., Land, M., Hauser, L., Woyke, T., … Ivanova, N. (2011). Complete genome sequence of *Ferroglobus placidus* AEDII12DO. *Standards in Genomic Sciences*. https://doi.org/10.4056/sigs.2225018

Apha, W. E. F. (1998). AWWA, 1995. Standard Methods for the Examination of Water and Wastewater. *Amer. Pub. Health Association. Washington DC*.

Bard, A. J., & Faulkner, L. R. (2008). Electrochemical Methods: Fundamentals and Applications, 2nd Edition | Wiley. In *Electrochemical Methods: Fundamentals and Applications, 2nd Edition*.

Bates, R. G., & Bower, V. E. (1954). Standard potential of the silver-silver-chloride electrode from 0 degrees to 95 degrees C and the thermodynamic properties of dilute hydrochloric acid solutions. *Journal of Research of the National Bureau of Standards*. https://doi.org/10.6028/jres.053.037

Bond, D. R., & Lovley, D. R. (2003). Electricity production by *Geobacter sulfurreducens* attached to electrodes. *Applied and Environmental Microbiology*. https://doi.org/10.1128/AEM.69.3.1548-1555.2003

Borole, A. P., Reguera, G., Ringeisen, B., Wang, Z. W., Feng, Y., & Kim, B. H. (2011). Electro-active biofilms: Current status and future research needs. *Energy and Environmental Science*, *4*(12), 4813–4834. https://doi.org/10.1039/c1ee02511b

Byrne-Bailey, K. G., Wrighton, K. C., Melnyk, R. A., Agbo, P., Hazen, T. C., & Coates, J. D. (2010). Complete genome sequence of the electricity-producing "*Thermincola potens*" strain JR. *Journal of Bacteriology*, *192*(15), 4078–

4079. https://doi.org/10.1128/JB.00044-10

Byung Hong Kim, Doo Hyun Park, P. K. S. and S., & Kim, H. J. (1999). Mediator-less biofuel cell. In *U.S. patent 5976719*.

Caccavo, F., Lonergan, D. J., Lovley, D. R., Davis, M., Stolz, J. F., & McInerney, M. J. (1994). *Geobacter sulfurreducens sp.* nov., a hydrogen- and acetate-oxidizing dissimilatory metal-reducing microorganism. *Applied and Environmental Microbiology*, *60*(10), 3752–3759. https://doi.org/10.1128/aem.60.10.3752-3759.1994

Call, D. F., & Logan, B. E. (2011). Lactate oxidation coupled to iron or electrode reduction by *Geobacter sulfurreducens* PCA. *Applied and Environmental Microbiology*, *77*(24), 8791–8794. https://doi.org/10.1128/AEM.06434-11

Call, D. F., Wagner, R. C., & Logan, B. E. (2009). Hydrogen production by *Geobacter* species and a mixed consortium in a microbial electrolysis cell. *Applied and Environmental Microbiology*, *75*(24), 7579–7587. https://doi.org/10.1128/AEM.01760-09

Call, D.F., & Logan, B. E. (2008). Hydrogen production in a single chamber microbial electrolysis cell lacking a membrane. *Environmental Science and Technology*, *42*(9), 3401–3406. https://doi.org/10.1021/es8001822

Cappai, G., Gioannis, G. De, Muntoni, A., Polettini, A., & Spiga, D. (2015). Effect of Inoculum to Substrate Ratio (ISR) on Hydrogen Production Through Dark Fermentation of Food Waste. *Proceedings of the Atti Del "Sardinia 2015 15th International Waste Management and Landfill Symposium, Cagliari, Italy*.

Chae, K. J., Choi, M. J., Kim, K. Y., Ajayi, F. F., Chang, I. S., & Kim, I. S. (2009). A solar-powered microbial electrolysis cell with a platinum catalyst-free cathode to produce hydrogen. *Environmental Science and Technology*. https://doi.org/10.1021/es9022317

Chae, K. J., Choi, M. J., Lee, J., Ajayi, F. F., & Kim, I. S. (2008). Biohydrogen

production via biocatalyzed electrolysis in acetate-fed bioelectrochemical cells and microbial community analysis. *International Journal of Hydrogen Energy*. https://doi.org/10.1016/j.ijhydene.2008.05.013

Chandrasekhar, K., Lee, Y. J., & Lee, D. W. (2015). Biohydrogen production: Strategies to improve process efficiency through microbial routes. *International Journal of Molecular Sciences*, *16*(4), 8266–8293. https://doi.org/10.3390/ijms16048266

Chen, S., Fang, Y., Jing, X., Luo, H., Chen, J., & Zhou, S. (2018). Enhanced electrosynthesis performance of *Moorella thermoautotrophica* by improving cell permeability. *Bioelectrochemistry*, *121*, 151–159. https://doi.org/10.1016/j.bioelechem.2018.02.003

Cheng, S., & Logan, B. E. (2007). Sustainable and efficient biohydrogen production via electrohydrogenesis. *Proceedings of the National Academy of Sciences of the United States of America*. https://doi.org/10.1073/pnas.0706379104

Cheng, S., Xing, D., Call, D. F., & Logan, B. E. (2009). Direct biological conversion of electrical current into methane by electromethanogenesis. *Environmental Science and Technology*, *43*(10), 3953–3958. https://doi.org/10.1021/es803531g

Choi, M. J., Yang, E., Yu, H. W., Kim, I. S., Oh, S. E., & Chae, K. J. (2019). Transition metal/carbon nanoparticle composite catalysts as platinum substitutes for bioelectrochemical hydrogen production using microbial electrolysis cells. *International Journal of Hydrogen Energy*. https://doi.org/10.1016/j.ijhydene.2018.07.020

Choi, Y., Jung, E., Park, H., Paik, S. R., Jung, S., & Kim, S. (2004). Construction of microbial fuel cells using thermophilic microorganisms, *Bacillus licheniformis* and *Bacillus thermoglucosidasius*. *Bulletin of the Korean*

Chemical Society, *25*(6), 813–818. https://doi.org/10.5012/bkcs.2004.25.6.813

Chong, M. L., Sabaratnam, V., Shirai, Y., & Hassan, M. A. (2009). Biohydrogen production from biomass and industrial wastes by dark fermentation. *International Journal of Hydrogen Energy*, *34*(8), 3277–3287. https://doi.org/10.1016/j.ijhydene.2009.02.010

Chu, H. P., & Li, X. Y. (2005). Membrane fouling in a membrane bioreactor (MBR): Sludge cake formation and fouling characteristics. *Biotechnology and Bioengineering*. https://doi.org/10.1002/bit.20409

Costa, N. L., Clarke, T. A., Philipp, L. A., Gescher, J., Louro, R. O., & Paquete, C. M. (2018). Electron transfer process in microbial electrochemical technologies: The role of cell-surface exposed conductive proteins. In *Bioresource Technology*. https://doi.org/10.1016/j.biortech.2018.01.133

Cusick, R. D., Bryan, B., Parker, D. S., Merrill, M. D., Mehanna, M., Kiely, P. D., Liu, G., & Logan, B. E. (2011). Performance of a pilot-scale continuous flow microbial electrolysis cell fed winery wastewater. *Applied Microbiology and Biotechnology*. https://doi.org/10.1007/s00253-011-3130-9

Dessì, P., Lakaniemi, A. M., Lens, P. N. L., Porca, E., Waters, N. R., & Collins, G. (2018). Thermophilic versus mesophilic dark fermentation in xylose-fed fluidised bed reactors: Biohydrogen production and active microbial community. *International Journal of Hydrogen Energy*.

Dessì, Paolo, Chatterjee, P., Mills, S., Kokko, M., Lakaniemi, A. M., Collins, G., & Lens, P. N. L. (2019). Power production and microbial community composition in thermophilic acetate-fed up-flow and flow-through microbial fuel cells. *Bioresource Technology*, *294*(July), 122115. https://doi.org/10.1016/j.biortech.2019.122115

Ding, C., Yang, K. L., & He, J. (2016). Biological and fermentative production of hydrogen. In *Handbook of Biofuels Production: Processes and Technologies:*

Second Edition. https://doi.org/10.1016/B978-0-08-100455-5.00011-4

Ditzig, J., Liu, H., & Logan, B. E. (2007). Production of hydrogen from domestic wastewater using a bioelectrochemically assisted microbial reactor (BEAMR). *International Journal of Hydrogen Energy*. https://doi.org/10.1016/j.ijhydene.2007.02.035

DSMZ. (2002). Cultivation of Anaerobes. *Leibniz-Institut DSMZ-Deutsche Sammlung von Mikroorganismen Und Zellkulturen GmbH*.

Egorova, K., & Antranikian, G. (2005). Industrial relevance of thermophilic Archaea. *Current Opinion in Microbiology*, *8*(6), 649–655. https://doi.org/10.1016/j.mib.2005.10.015

Ehrlich, H. L. (2008). Are gram-positive bacteria capable of electron transfer across their cell wall without an externally available electron shuttle? *Geobiology*, *6*(3), 220–224. https://doi.org/10.1111/j.1472-4669.2007.00135.x

Feng, Y., Wang, X., Logan, B. E., & Lee, H. (2008). Brewery wastewater treatment using air-cathode microbial fuel cells. *Applied Microbiology and Biotechnology*, *78*(5), 873–880. https://doi.org/10.1007/s00253-008-1360-2

Fiala, G., & Stetter, K. O. (1986). *Pyrococcus furiosus sp.* nov. represents a novel genus of marine heterotrophic archaebacteria growing optimally at 100°C. *Archives of Microbiology*. https://doi.org/10.1007/BF00413027

Fourmond, V., Wiedner, E. S., Shaw, W. J., & Léger, C. (2019). Understanding and Design of Bidirectional and Reversible Catalysts of Multielectron, Multistep Reactions. *Journal of the American Chemical Society*. https://doi.org/10.1021/jacs.9b04854

Franks, A. E., Nevin, K. P., Jia, H., Izallalen, M., Woodard, T. L., & Lovley, D. R. (2009). Novel strategy for three-dimensional real-time imaging of microbial fuel cell communities: Monitoring the inhibitory effects of proton accumulation within the anode biofilm. *Energy and Environmental Science*.

https://doi.org/10.1039/b816445b

Fu, Q., Fukushima, N., Maeda, H., Sato, K., & Kobayashi, H. (2015). Bioelectrochemical analysis of a hyperthermophilic microbial fuel cell generating electricity at temperatures above 80 °C. *Bioscience, Biotechnology and Biochemistry*, *79*(7), 1200–1206. https://doi.org/10.1080/09168451.2015.1015952

Fu, Q., Kobayashi, H., Kawaguchi, H., Wakayama, T., Maeda, H., & Sato, K. (2013). A thermophilic gram-negative nitrate-reducing bacterium, *Calditerrivibrio nitroreducens*, exhibiting electricity generation capability. *Environmental Science and Technology*, *47*(21), 12583–12590. https://doi.org/10.1021/es402749f

Fu, Q., Kuramochi, Y., Fukushima, N., Maeda, H., Sato, K., & Kobayashi, H. (2015). Bioelectrochemical analyses of the development of a thermophilic biocathode catalyzing electromethanogenesis. *Environmental Science and Technology*, *49*(2), 1225–1232. https://doi.org/10.1021/es5052233

Gavrilov, S. N., Zavarzina, D. G., Elizarov, I. M., Tikhonova, T. V., Dergousova, N. I., Popov, V. O., Lloyd, J. R., Knight, D., El-Naggar, M. Y., Pirbadian, S., Leung, K. M., Robb, F. T., Zakhartsev, M. V., Bretschger, O., & Bonch-Osmolovskaya, E. A. (2021). Novel Extracellular Electron Transfer Channels in a Gram-Positive Thermophilic Bacterium. *Frontiers in Microbiology*. https://doi.org/10.3389/fmicb.2020.597818

Ge, Z., Zhang, F., Grimaud, J., Hurst, J., & He, Z. (2013). Long-term investigation of microbial fuel cells treating primary sludge or digested sludge. *Bioresource Technology*, *136*, 509–514. https://doi.org/10.1016/j.biortech.2013.03.016

Geelhoed, J. S., Hamelers, H. V., & Stams, A. J. (2010). Electricity-mediated biological hydrogen production. In *Current Opinion in Microbiology*. https://doi.org/10.1016/j.mib.2010.02.002

Gorby, Y. A., Yanina, S., McLean, J. S., Rosso, K. M., Moyles, D., Dohnalkova, A., Beveridge, T. J., Chang, I. S., Kim, B. H., Kim, K. S., Culley, D. E., Reed, S. B., Romine, M. F., Saffarini, D. A., Hill, E. A., Shi, L., Elias, D. A., Kennedy, D. W., Pinchuk, G., … Fredrickson, J. K. (2006). Electrically conductive bacterial nanowires produced by *Shewanella oneidensis* strain MR-1 and other microorganisms. *Proceedings of the National Academy of Sciences of the United States of America*, *103*(30), 11358–11363. https://doi.org/10.1073/pnas.0604517103

Gregoire, K. P., Glaven, S. M., Hervey, J., Lin, B., & Tender, L. M. (2014). Enrichment of a High-Current Density Denitrifying Microbial Biocathode. *Journal of The Electrochemical Society*. https://doi.org/10.1149/2.0101413jes

Hafenbradl, D., Keller, M., Dirmeier, R., Rachel, R., Roßnagel, P., Burggraf, S., Huber, H., & Stetter, K. O. (1996). *Ferroglobus placidus* gen. nov., *sp.* nov., a novel hyperthermophilic archaeum that oxidizes Fe2+ at neutral pH under anoxic conditions. *Archives of Microbiology*, *166*(5), 308–314. https://doi.org/10.1007/s002030050388

Hara, M., Onaka, Y., Kobayashi, H., Fu, Q., Kawaguchi, H., Vilcaez, J., & Sato, K. (2013). Mechanism of electromethanogenic reduction of CO2 by a thermophilic methanogen. *Energy Procedia*, *37*, 7021–7028. https://doi.org/10.1016/j.egypro.2013.06.637

Hatchikian, E. C., Ollivier, B., & Garcia, J.-L. (2015). *Thermodesulfobacteria* class. nov. In *Bergey's Manual of Systematics of Archaea and Bacteria*. https://doi.org/10.1002/9781118960608.cbm00049

Holmes, D. E., Bond, D. R., & Lovley, D. R. (2004). Electron Transfer by *Desulfobulbus propionicus* to Fe(III) and Graphite Electrodes. *Applied and Environmental Microbiology*. https://doi.org/10.1128/AEM.70.2.1234-1237.2004

Hu, H., Fan, Y., & Liu, H. (2008). Hydrogen production using single-chamber membrane-free microbial electrolysis cells. *Water Research*. https://doi.org/10.1016/j.watres.2008.06.015

Iino, T., Nakagawa, T., Mori, K., Harayama, S., & Suzuki, K. ichiro. (2008). *Calditerrivibrio nitroreducens* gen. nov., *sp.* nov., a thermophilic, nitrate-reducing bacterium isolated from a terrestrial hot spring in Japan. *International Journal of Systematic and Evolutionary Microbiology*, *58*(7), 1675–1679. https://doi.org/10.1099/ijs.0.65714-0

Jackson, B. E., & McInerney, M. J. (2002). Anaerobic microbial metabolism can proceed close to thermodynamic limits. *Nature*. https://doi.org/10.1038/415454a

Kang, J., Kim, T., Tak, Y., Lee, J. H., & Yoon, J. (2012). Cyclic voltammetry for monitoring bacterial attachment and biofilm formation. *Journal of Industrial and Engineering Chemistry*. https://doi.org/10.1016/j.jiec.2011.10.002

Kashefi, K., Tor, J. M., Holmes, D. E., Gaw Van Praagh, C. V., Reysenbach, A. L., & Lovley, D. R. (2002). *Geoglobus ahangari* gen. nov., *sp.* nov., a novel hyperthermophilic archaeon capable of oxidizing organic acids and growing autotrophically on hydrogen with Fe(III) serving as the sole electron acceptor. *International Journal of Systematic and Evolutionary Microbiology*, *52*(3), 719–728. https://doi.org/10.1099/ijs.0.01953-0

Kastury, F., Juhasz, A., Beckmann, S., & Manefield, M. (2015). Ecotoxicity of neutral red (dye) and its environmental applications. *Ecotoxicology and Environmental Safety*. https://doi.org/10.1016/j.ecoenv.2015.07.028

Katuri, K. P., Rengaraj, S., Kavanagh, P., O'Flaherty, V., & Leech, D. (2012). Charge transport through *Geobacter sulfurreducens* biofilms grown on graphite rods. *Langmuir*. https://doi.org/10.1021/la2047036

Khongkliang, P., Jehlee, A., Kongjan, P., Reungsang, A., & O-Thong, S. (2019).

High efficient biohydrogen production from palm oil mill effluent by two-stage dark fermentation and microbial electrolysis under thermophilic condition. *International Journal of Hydrogen Energy*. https://doi.org/10.1016/j.ijhydene.2019.10.022

Khongkliang, P., Kongjan, P., Utarapichat, B., Reungsang, A., & O-Thong, S. (2017). Continuous hydrogen production from cassava starch processing wastewater by two-stage thermophilic dark fermentation and microbial electrolysis. *International Journal of Hydrogen Energy*, *42*(45), 27584–27592. https://doi.org/10.1016/j.ijhydene.2017.06.145

Kim, B. H., Ikeda, T., Park, H. S., Kim, H. J., Hyun, M. S., Kano, K., Takagi, K., & Tatsumi, H. (1999). Electrochemical activity of an Fe(III)-reducing bacterium, *Shewanella putrefaciens* IR-1, in the presence of alternative electron acceptors. *Biotechnology Techniques*, *13*(7), 475–478. https://doi.org/10.1023/A:1008993029309

Kim, H. J., Park, H. S., Hyun, M. S., Chang, I. S., Kim, M., & Kim, B. H. (2002). A mediator-less microbial fuel cell using a metal reducing bacterium, *Shewanella putrefaciens*. *Enzyme and Microbial Technology*, *30*(2), 145–152. https://doi.org/10.1016/S0141-0229(01)00478-1

Kim, J. R., Min, B., & Logan, B. E. (2005). Evaluation of procedures to acclimate a microbial fuel cell for electricity production. *Applied Microbiology and Biotechnology*. https://doi.org/10.1007/s00253-004-1845-6

Kobayashi, H., Nagashima, A., Kouyama, M., Fu, Q., Ikarashi, M., Maeda, H., & Sato, K. (2017). High-pressure thermophilic electromethanogenic system producing methane at 5 MPa, 55°C. *Journal of Bioscience and Bioengineering*, *124*(3), 327–332. https://doi.org/10.1016/j.jbiosc.2017.04.001

Korth, B., Kretzschmar, J., Bartz, M., Kuchenbuch, A., & Harnisch, F. (2020). Determining incremental coulombic efficiency and physiological parameters

of early stage *Geobacter spp*. enrichment biofilms. *PLoS ONE*. https://doi.org/10.1371/journal.pone.0234077

Lalaurette, E., Thammannagowda, S., Mohagheghi, A., Maness, P. C., & Logan, B. E. (2009). Hydrogen production from cellulose in a two-stage process combining fermentation and electrohydrogenesis. *International Journal of Hydrogen Energy*, *34*(15), 6201–6210. https://doi.org/10.1016/j.ijhydene.2009.05.112

Lee, H. S., & Rittmann, B. E. (2010). Significance of biological hydrogen oxidation in a continuous single-chamber microbial electrolysis cell. *Environmental Science and Technology*. https://doi.org/10.1021/es9025358

Lee, H. S., Torres, C. I., Parameswaran, P., & Rittmann, B. E. (2009). Fate of H2 in an upflow single-chamber microbial electrolysis cell using a metal-catalyst-free cathode. *Environmental Science and Technology*. https://doi.org/10.1021/es900204j

Lee, H. S., Torres, Ć. I., & Rittmann, B. E. (2009). Effects of substrate diffusion and anode potential on kinetic parameters for anode-respiring bacteria. *Environmental Science and Technology*. https://doi.org/10.1021/es9015519

Levin, D. B., & Chahine, R. (2010). Challenges for renewable hydrogen production from biomass. *International Journal of Hydrogen Energy*. https://doi.org/10.1016/j.ijhydene.2009.08.067

Li, X., Zhao, L., Yu, J., Liu, X., Zhang, X., Liu, H., & Zhou, W. (2020). Water Splitting: From Electrode to Green Energy System. In *Nano-Micro Letters*. https://doi.org/10.1007/s40820-020-00469-3

Lin, H., Wu, X., Hu, B., & Zhu, J. (2016). Microbial Electrochemical Systems for Agro-industrial Wastewater Remediation and Renewable Products Generation: A Review. *Elyns Journal of Microbes*, *01*(01), 1–20. https://doi.org/10.19104/amb.2014.101

Liu, H., Grot, S., & Logan, B. E. (2005). Electrochemically assisted microbial production of hydrogen from acetate. *Environmental Science and Technology*. https://doi.org/10.1021/es050244p

Liu, P., Mohamed, A., Liang, P., & Beyenal, H. (2020). Effect of electrode spacing on electron transfer and conductivity of *Geobacter sulfurreducens* biofilms. *Bioelectrochemistry*. https://doi.org/10.1016/j.bioelechem.2019.107395

Liu, Z., Liu, J., Zhang, S., Xing, X. H., & Su, Z. (2011). Microbial fuel cell based biosensor for in situ monitoring of anaerobic digestion process. *Bioresource Technology*, *102*(22), 10221–10229. https://doi.org/10.1016/j.biortech.2011.08.053

Logan, B. E. (2009). Exoelectrogenic bacteria that power microbial fuel cells. *Nature Reviews Microbiology*. https://doi.org/10.1038/nrmicro2113

Logan, B. E., Call, D., Cheng, S., Hamelers, H. V. M., Sleutels, T. H. J. A., Jeremiasse, A. W., & Rozendal, R. A. (2008). Microbial electrolysis cells for high yield hydrogen gas production from organic matter. *Environmental Science and Technology*, *42*(23), 8630–8640. https://doi.org/10.1021/es801553z

Logan, B. E., Hamelers, B., Rozendal, R., Schröder, U., Keller, J., Freguia, S., Aelterman, P., Verstraete, W., & Rabaey, K. (2006). Microbial fuel cells: Methodology and technology. *Environmental Science and Technology*, *40*(17), 5181–5192. https://doi.org/10.1021/es0605016

Logan, B. E., & Rabaey, K. (2012). Conversion of wastes into bioelectricity and chemicals by using microbial electrochemical technologies. *Science*, *337*(6095), 686–690. https://doi.org/10.1126/science.1217412

Logan, B. E., Rossi, R., Ragab, A., & Saikaly, P. E. (2019). Electro-active microorganisms in bioelectrochemical systems. In *Nature Reviews Microbiology*. https://doi.org/10.1038/s41579-019-0173-x

Lovley, D. R., & Phillips, E. J. P. (1988). Novel mode of microbial energy metabolism: organic carbon oxidation coupled to dissimilatory reduction of iron or manganese. *Applied & Environmental Microbiology*. https://doi.org/10.1128/aem.54.6.1472-1480.1988

Lovley, Derek R. (2008). The microbe electric: conversion of organic matter to electricity. *Current Opinion in Biotechnology*, *19*(6), 564–571. https://doi.org/10.1016/j.copbio.2008.10.005

Lu, L., Xing, D., Liu, B., & Ren, N. (2012). Enhanced hydrogen production from waste activated sludge by cascade utilization of organic matter in microbial electrolysis cells. *Water Research*, *46*(4), 1015–1026. https://doi.org/10.1016/j.watres.2011.11.073

Luque, R., Lin, C. S. K., Wilson, K., & Clark, J. (2016). Handbook of Biofuels Production: Processes and Technologies: Second Edition. In *Handbook of Biofuels Production: Processes and Technologies: Second Edition*.

Lusk, B. G., Badalamenti, J. P., Parameswaran, P., Bond, D. R., & Torres, C. I. (2015). Draft genome sequence of the Gram-positive thermophilic iron reducer *Thermincola ferriacetica* strain Z-0001T. *Genome Announcements*, *3*(5). https://doi.org/10.1128/genomeA.01072-15

Lusk, B. G., Khan, Q. F., Parameswaran, P., Hameed, A., Ali, N., Rittmann, B. E., & Torres, C. I. (2015). Characterization of Electrical Current-Generation Capabilities from Thermophilic Bacterium *Thermoanaerobacter pseudethanolicus* Using Xylose, Glucose, Cellobiose, or Acetate with Fixed Anode Potentials. *Environmental Science and Technology*, *49*(24), 14725–14731. https://doi.org/10.1021/acs.est.5b04036

Lusk, B. G., Parameswaran, P., Popat, S. C., Rittmann, B. E., & Torres, C. I. (2016). The effect of pH and buffer concentration on anode biofilms of *Thermincola ferriacetica*. *Bioelectrochemistry*, *112*, 47–52.

https://doi.org/10.1016/j.bioelechem.2016.07.007

Lusk, B. G., Peraza, I., Albal, G., Marcus, A. K., Popat, S. C., & Torres, C. I. (2018). PH Dependency in Anode Biofilms of *Thermincola ferriacetica* Suggests a Proton-Dependent Electrochemical Response. *Journal of the American Chemical Society*, *140*(16), 5527–5534. https://doi.org/10.1021/jacs.8b01734

Manzella, M. P., Holmes, D. E., Rocheleau, J. M., Chung, A., Reguera, G., & Kashefi, K. (2015). The complete genome sequence and emendation of the hyperthermophilic, obligate iron-reducing archaeon "*Geoglobus ahangari*" strain 234T. *Standards in Genomic Sciences*, *10*(1), 1–19. https://doi.org/10.1186/s40793-015-0035-8

Mardanov, A. V., Slododkina, G. B., Slobodkin, A. I., Beletsky, A. V., Gavrilov, S. N., Kublanov, I. V., Bonch-Osmolovskaya, E. A., Skryabin, K. G., & Ravin, N. V. (2015). The *Geoglobus acetivorans* genome: Fe(III) reduction, acetate utilization, autotrophic growth, and degradation of aromatic compounds in a hyperthermophilic archaeon. *Applied and Environmental Microbiology*. https://doi.org/10.1128/AEM.02705-14

Marshall, C. W., & May, H. D. (2009). Electrochemical evidence of direct electrode reduction by a thermophilic Gram-positive bacterium, *Thermincola ferriacetica*. *Energy and Environmental Science*, *2*(6), 699–705. https://doi.org/10.1039/b823237g

Marsili, E., Sun, J., & Bond, D. R. (2010). Voltammetry and growth physiology of *Geobacter sulfurreducens* biofilms as a function of growth stage and imposed electrode potential. *Electroanalysis*. https://doi.org/10.1002/elan.200800007

Mathis, B. J., Marshall, C. W., Milliken, C. E., Makkar, R. S., Creager, S. E., & May, H. D. (2008). Electricity generation by thermophilic microorganisms from marine sediment. *Applied Microbiology and Biotechnology*, *78*(1), 147–

155. https://doi.org/10.1007/s00253-007-1266-4

Matsunaga, T., & Nakajima, T. (1985). Electrochemical classification of gram-negative and gram-positive bacteria. *Applied and Environmental Microbiology*, *50*(2), 238–242. https://doi.org/10.1128/aem.50.2.238-242.1985

Modestra, J. A., & Mohan, S. V. (2014). Bio-electrocatalyzed electron efflux in Gram positive and Gram negative bacteria: An insight into disparity in electron transfer kinetics. *RSC Advances*. https://doi.org/10.1039/c4ra03489a

Muradov, N. Z., & Veziroğlu, T. N. (2005). From hydrocarbon to hydrogen-carbon to hydrogen economy. *International Journal of Hydrogen Energy*. https://doi.org/10.1016/j.ijhydene.2004.03.033

Myers, C. R., & Myers, J. M. (1992). Localization of cytochromes to the outer membrane of anaerobically grown *Shewanella putrefaciens* MR-1. *Journal of Bacteriology*, *174*(11), 3429–3438. https://doi.org/10.1128/jb.174.11.3429-3438.1992

Nath, K., & Das, D. (2011). Modeling and optimization of fermentative hydrogen production. *Bioresource Technology*. https://doi.org/10.1016/j.biortech.2011.03.108

Nevin, K. P., Woodard, T. L., Franks, A. E., Summers, Z. M., & Lovley, D. R. (2010). Microbial electrosynthesis: Feeding microbes electricity to convert carbon dioxide and water to multicarbon extracellular organic compounds. *MBio*. https://doi.org/10.1128/mBio.00103-10

O-Thong, S., Prasertsan, P., Karakashev, D., & Angelidaki, I. (2008). Thermophilic fermentative hydrogen production by the newly isolated *Thermoanaerobacterium thermosaccharolyticum* PSU-2. *International Journal of Hydrogen Energy*, *33*(4), 1204–1214. https://doi.org/10.1016/j.ijhydene.2007.12.015

Osman, A. I., Deka, T. J., Baruah, D. C., & Rooney, D. W. (2020). Critical challenges in biohydrogen production processes from the organic feedstocks. In *Biomass Conversion and Biorefinery*. https://doi.org/10.1007/s13399-020-00965-x

Parameswaran, P., Bry, T., Popat, S. C., Lusk, B. G., Rittmann, B. E., & Torres, C. I. (2013). Kinetic, electrochemical, and microscopic characterization of the thermophilic, anode-respiring bacterium *Thermincola ferriacetica*. *Environmental Science and Technology*, *47*(9), 4934–4940. https://doi.org/10.1021/es400321c

Patil, S. A., Surakasi, V. P., Koul, S., Ijmulwar, S., Vivek, A., Shouche, Y. S., & Kapadnis, B. P. (2009). Electricity generation using chocolate industry wastewater and its treatment in activated sludge based microbial fuel cell and analysis of developed microbial community in the anode chamber. *Bioresource Technology*, *100*(21), 5132–5139. https://doi.org/10.1016/j.biortech.2009.05.041

Peng, L., You, S. J., & Wang, J. Y. (2010). Carbon nanotubes as electrode modifier promoting direct electron transfer from *Shewanella oneidensis*. *Biosensors and Bioelectronics*. https://doi.org/10.1016/j.bios.2009.10.002

Pham, T. H., Rabaey, K., Aelterman, P., Clauwaert, P., De Schamphelaire, L., Boon, N., & Verstraete, W. (2006). Microbial fuel cells in relation to conventional anaerobic digestion technology. In *Engineering in Life Sciences*. https://doi.org/10.1002/elsc.200620121

Pham, The Hai, Boon, N., Aelterman, P., Clauwaert, P., De Schamphelaire, L., Vanhaecke, L., De Maeyer, K., Höfte, M., Verstraete, W., & Rabaey, K. (2008). Metabolites produced by *Pseudomonas sp.* enable a Gram-positive bacterium to achieve extracellular electron transfer. *Applied Microbiology and Biotechnology*, *77*(5), 1119–1129. https://doi.org/10.1007/s00253-007-1248-6

Pillot, G., Frouin, E., Pasero, E., Godfroy, A., Combet-Blanc, Y., Davidson, S., & Liebgott, P. P. (2018). Specific enrichment of hyperthermophilic electro-active Archaea from deep-sea hydrothermal vent on electrically conductive support. *Bioresource Technology*, *259*, 304–311. https://doi.org/10.1016/j.biortech.2018.03.053

Rabaey, K., Rodríguez, J., Blackall, L. L., Keller, J., Gross, P., Batstone, D., Verstraete, W., & Nealson, K. H. (2007). Microbial ecology meets electrochemistry: Electricity-driven and driving communities. *ISME Journal*, *1*(1), 9–18. https://doi.org/10.1038/ismej.2007.4

Rabaey, K., & Rozendal, R. A. (2010). Microbial electrosynthesis - Revisiting the electrical route for microbial production. *Nature Reviews Microbiology*, *8*(10), 706–716. https://doi.org/10.1038/nrmicro2422

Rabaey, K., & Verstraete, W. (2005). Microbial fuel cells: Novel biotechnology for energy generation. *Trends in Biotechnology*, *23*(6), 291–298. https://doi.org/10.1016/j.tibtech.2005.04.008

Rainey, F. A. (2015). *Clostridiales* . In *Bergey's Manual of Systematics of Archaea and Bacteria*. https://doi.org/10.1002/9781118960608.obm00059

Richter, H., Lanthier, M., Nevin, K. P., & Lovley, D. R. (2007). Lack of electricity production by *Pelobacter carbinolicus* indicates that the capacity for Fe(III) oxide reduction does not necessarily confer electron transfer ability to fuel cell anodes. *Applied and Environmental Microbiology*. https://doi.org/10.1128/AEM.00804-07

Richter, H., Nevin, K. P., Jia, H., Lowy, D. A., Lovley, D. R., & Tender, L. M. (2009). Cyclic voltammetry of biofilms of wild type and mutant *Geobacter sulfurreducens* on fuel cell anodes indicates possible roles of *OmcB*, *OmcZ*, type IV pili, and protons in extracellular electron transfer. *Energy and Environmental Science*. https://doi.org/10.1039/b816647a

Rittmann, B. E. (2008). Opportunities for renewable bioenergy using microorganisms. In *Biotechnology and Bioengineering*. https://doi.org/10.1002/bit.21875

Rittmann, S., & Herwig, C. (2012). A comprehensive and quantitative review of dark fermentative biohydrogen production. In *Microbial cell factories* (Vol. 11). https://doi.org/10.1186/1475-2859-11-115

Rotaru, A. E., Woodard, T. L., Nevin, K. P., & Lovley, D. R. (2015). Link between capacity for current production and syntrophic growth in *Geobacter* species. *Frontiers in Microbiology*. https://doi.org/10.3389/fmicb.2015.00744

Rousseau, R., Délia, M. L., & Bergel, A. (2014). A theoretical model of transient cyclic voltammetry for electro-active biofilms. *Energy and Environmental Science*. https://doi.org/10.1039/c3ee42329h

Rozendal, R. A., Sleutels, T. H. J. A., Hamelers, H. V. M., & Buisman, C. J. N. (2008). Effect of the type of ion exchange membrane on performance, ion transport, and pH in biocatalyzed electrolysis of wastewater. *Water Science and Technology*. https://doi.org/10.2166/wst.2008.043

Rozendal, René A., Hamelers, H. V. M., Euverink, G. J. W., Metz, S. J., & Buisman, C. J. N. (2006). Principle and perspectives of hydrogen production through biocatalyzed electrolysis. *International Journal of Hydrogen Energy*. https://doi.org/10.1016/j.ijhydene.2005.12.006

Sanchez, D. V. P., Jacobs, D., Gregory, K., Huang, J., Hu, Y., Vidic, R., & Yun, M. (2015). Changes in carbon electrode morphology affect microbial fuel cell performance with *Shewanella oneidensis* MR-1. *Energies*. https://doi.org/10.3390/en8031817

Sayed, E. T., Saito, Y., Tsujiguchi, T., & Nakagawa, N. (2012). Catalytic activity of yeast extract in biofuel cell. *Journal of Bioscience and Bioengineering*. https://doi.org/10.1016/j.jbiosc.2012.05.021

Schröder, C., Selig, M., & Schönheit, P. (1994). Glucose fermentation to acetate, CO2 and H2 in the anaerobic hyperthermophilic eubacterium *Thermotoga maritima*: involvement of the Embden-Meyerhof pathway. *Archives of Microbiology*. https://doi.org/10.1007/BF00307766

Schröder, U. (2007). Anodic electron transfer mechanisms in microbial fuel cells and their energy efficiency. *Physical Chemistry Chemical Physics*. https://doi.org/10.1039/b703627m

Scott, K., & Murano, C. (2007). A study of a microbial fuel cell battery using manure sludge waste. *Journal of Chemical Technology and Biotechnology*. https://doi.org/10.1002/jctb.1745

Sekar, N., Wu, C.-H., Adams, M. W. W., & Ramasamy, R. P. (2016). Exploring Extracellular Electron Transfer in Hyperthermophiles for Electrochemical Energy Conversion. *ECS Transactions*, *72*(30), 1–7. https://doi.org/10.1149/07230.0001ecst

Sekar, Narendran, Wu, C. H., Adams, M. W. W., & Ramasamy, R. P. (2017). Electricity generation by *Pyrococcus furiosus* in microbial fuel cells operated at 90°C. *Biotechnology and Bioengineering*, *114*(7), 1419–1427. https://doi.org/10.1002/bit.26271

Shehab, N. A., Ortiz-Medina, J. F., Katuri, K. P., Hari, A. R., Amy, G., Logan, B. E., & Saikaly, P. E. (2017). Enrichment of extremophilic exoelectrogens in microbial electrolysis cells using Red Sea brine pools as inocula. *Bioresource Technology*, *239*, 82–86. https://doi.org/10.1016/j.biortech.2017.04.122

Shi, L., Squier, T. C., Zachara, J. M., & Fredrickson, J. K. (2007). Respiration of metal (hydr)oxides by *Shewanella* and *Geobacter*: A key role for multihaem *c*-type cytochromes. In *Molecular Microbiology*. https://doi.org/10.1111/j.1365-2958.2007.05783.x

Sleytr, U. B., Schuster, B., Egelseer, E. M., & Pum, D. (2014). S-layers: Principles

and applications. *FEMS Microbiology Reviews*. https://doi.org/10.1111/1574-6976.12063

Slobodkina, G. B., Kolganova, T. V., Querellou, J., Bonch-Osmolovskaya, E. A., & Slobodkin, A. I. (2009). *Geoglobus acetivorans sp.* nov., an iron(III)-reducing archaeon from a deep-sea hydrothermal vent. *International Journal of Systematic and Evolutionary Microbiology*. https://doi.org/10.1099/ijs.0.011080-0

Smith, J. A., Aklujkar, M., Risso, C., Leang, C., Giloteaux, L., & Holmes, D. E. (2015). Mechanisms involved in Fe(III) respiration by the hyperthermophilic archaeon *Ferroglobus placidus*. *Applied and Environmental Microbiology*, *81*(8), 2735–2744. https://doi.org/10.1128/AEM.04038-14

Steinbusch, K. J. J., Hamelers, H. V. M., Schaap, J. D., Kampman, C., & Buisman, C. J. N. (2010). Bioelectrochemical ethanol production through mediated acetate reduction by mixed cultures. *Environmental Science and Technology*. https://doi.org/10.1021/es902371e

Tenca, A., Cusick, R. D., Schievano, A., Oberti, R., & Logan, B. E. (2013). Evaluation of low cost cathode materials for treatment of industrial and food processing wastewater using microbial electrolysis cells. *International Journal of Hydrogen Energy*, *38*(4), 1859–1865. https://doi.org/10.1016/j.ijhydene.2012.11.103

Thauer, R. K., Jungermann, K., & Decker, K. (1977). Energy conservation in chemotrophic anaerobic bacteria. *Bacteriological Reviews*. https://doi.org/10.1128/mmbr.41.1.100-180.1977

Thrash, J. C., & Coates, J. D. (2008). Review: Direct and indirect electrical stimulation of microbial metabolism. In *Environmental Science and Technology*. https://doi.org/10.1021/es702668w

Vemuri, B., Xia, L., Chilkoor, G., Jawaharraj, K., Sani, R. K., Amarnath, A.,

Kilduff, J., & Gadhamshetty, V. (2021). Anaerobic wastewater treatment and reuse enabled by thermophilic bioprocessing integrated with a bioelectrochemical/ultrafiltration module. *Bioresource Technology*. https://doi.org/10.1016/j.biortech.2020.124406

Visweswaran, G. R. R., Dijkstra, B. W., & Kok, J. (2011). Murein and pseudomurein cell wall binding domains of bacteria and archaea-a comparative view. In *Applied Microbiology and Biotechnology*. https://doi.org/10.1007/s00253-011-3637-0

Wagner, A. O., Markt, R., Mutschlechner, M., Lackner, N., Prem, E. M., Praeg, N., & Illmer, P. (2019). Medium preparation for the cultivation of microorganisms under strictly anaerobic/anoxic conditions. *Journal of Visualized Experiments*. https://doi.org/10.3791/60155

Wagner, R. C., Regan, J. M., Oh, S. E., Zuo, Y., & Logan, B. E. (2009). Hydrogen and methane production from swine wastewater using microbial electrolysis cells. *Water Research*, *43*(5), 1480–1488. https://doi.org/10.1016/j.watres.2008.12.037

Wang, H., & Ren, Z. J. (2013). A comprehensive review of microbial electrochemical systems as a platform technology. *Biotechnology Advances*, *31*(8), 1796–1807. https://doi.org/10.1016/j.biotechadv.2013.10.001

Wrighton, K. C., Agbo, P., Warnecke, F., Weber, K. A., Brodie, E. L., DeSantis, T. Z., Hugenholtz, P., Andersen, G. L., & Coates, J. D. (2008). A novel ecological role of the Firmicutes identified in thermophilic microbial fuel cells. *ISME Journal*, *2*(11), 1146–1156. https://doi.org/10.1038/ismej.2008.48

Xiao, B., Yang, F., & Liu, J. (2011). Enhancing simultaneous electricity production and reduction of sewage sludge in two-chamber MFC by aerobic sludge digestion and sludge pretreatments. *Journal of Hazardous Materials*, *189*(1–2), 444–449. https://doi.org/10.1016/j.jhazmat.2011.02.058

Yilmazel, Y. D., Zhu, X., Kim, K. Y., Holmes, D. E., & Logan, B. E. (2018). Electrical current generation in microbial electrolysis cells by hyperthermophilic archaea *Ferroglobus placidus* and *Geoglobus ahangari*. *Bioelectrochemistry*, *119*, 142–149. https://doi.org/10.1016/j.bioelechem.2017.09.012

Yu, J., & Takahashi, P. (2007). Biophotolysis-based Hydrogen Production by Cyanobacteria and Green Microalgae. *Communicating Current Research and Educational Topics and Trends in Applied Microbiology*, *January 2007*, 79–89.

Yu, L., Yuan, Y., Tang, J., & Zhou, S. (2017). Thermophilic *Moorella thermoautotrophica*-immobilized cathode enhanced microbial electrosynthesis of acetate and formate from CO2. *Bioelectrochemistry*, *117*, 23–28. https://doi.org/10.1016/j.bioelechem.2017.05.001

Zavarzina, D. G., Sokolova, T. G., Tourova, T. P., Chernyh, N. A., Kostrikina, N. A., & Bonch-Osmolovskaya, E. A. (2007). *Thermincola ferriacetica sp.* nov., a new anaerobic, thermophilic, facultatively chemolithoautotrophic bacterium capable of dissimilatory Fe(III) reduction. *Extremophiles*, *11*(1), 1–7. https://doi.org/10.1007/s00792-006-0004-7

Zeng, X., Zhang, Z., Li, X., Jebbar, M., Alain, K., & Shao, Z. (2015). *Caloranaerobacter ferrireducens sp.* nov., an anaerobic, thermophilic, iron (iii)-reducing bacterium isolated from deep-sea hydrothermal sulfide deposits. *International Journal of Systematic and Evolutionary Microbiology*, *65*(6), 1714–1718. https://doi.org/10.1099/ijs.0.000165

Zhang, J., Zhang, Y., Quan, X., & Chen, S. (2013). Effects of ferric iron on the anaerobic treatment and microbial biodiversity in a coupled microbial electrolysis cell (MEC) - Anaerobic reactor. *Water Research*. https://doi.org/10.1016/j.watres.2013.06.056

Zuo, Y., Cheng, S., Call, D., & Logan, B. E. (2007). Tubular membrane cathodes for scalable power generation in microbial fuel cells. *Environmental Science and Technology*, *41*(9), 3347–3353. https://doi.org/10.1021/es0627601

Zurawski, J. V., Blumer-Schuette, S. E., Conway, J. M., & Kelly, R. M. (2014). The Extremely Thermophilic Genus *Caldicellulosiruptor*: Physiological and Genomic Characteristics for Complex Carbohydrate Conversion to Molecular Hydrogen. https://doi.org/10.1007/978-94-017-8554-9_8

APPENDICES

A. Supplementary information for the Figures in Chapter 2

Figure 2.1. In order to acquire the relevant research article numbers via SCOPUS, following query options were used for all MFC studies (1), all MEC studies (2) all MES studies (3), thermophilic/hyperthermophilic MFC studies (4)*, thermophilic/hyperthermophilic MEC studies (5)*, thermophilic/hyperthermophilic MES studies (6)*;

1. TITLE-ABS-KEY (microbial AND fuel AND cell) AND (LIMIT-TO (DOCTYPE , "ar")) AND (LIMIT-TO (EXACTKEYWORD , "Microbial Fuel Cells") OR LIMIT-TO (EXACTKEYWORD , "Microbial Fuel Cell") OR LIMIT-TO (EXACTKEYWORD , "Microbial Fuel Cells (MFCs)") OR LIMIT-TO (EXACTKEYWORD , "Microbial Fuel Cell (MFC)"))

2. TITLE-ABS-KEY (microbial AND electrolysis AND cell) AND (LIMIT-TO (DOCTYPE , "ar")) AND (LIMIT-TO (EXACTKEYWORD , "Microbial Electrolysis Cell") OR LIMIT-TO (EXACTKEYWORD , "Microbial Electrolysis Cells") OR LIMIT-TO (EXACTKEYWORD , "Microbial Electrolysis Cell (MECs)") OR LIMIT-TO (EXACTKEYWORD , "Microbial Electrolysis Cell (MEC)"))

3. TITLE-ABS-KEY (microbial AND electrosynthesis) AND (LIMIT-TO (DOCTYPE , "ar")) AND (LIMIT-TO (EXACTKEYWORD , "Microbial Electrosynthesis") OR LIMIT-TO (EXACTKEYWORD , "Microbial Electrosynthesis (MES)") OR LIMIT-TO (EXACTKEYWORD , "Microbial Electrosynthesis System"))

4. KEY (thermophilic OR hyperthermophilic AND "microbial fuel cell") AND (LIMIT-TO (DOCTYPE , "ar"))

5. KEY (thermophilic OR hyperthermophilic AND "microbial electrolysis cell") AND (LIMIT-TO (DOCTYPE , "ar"))

6. KEY (thermophilic OR hyperthermophilic AND "microbial electrosynthesis") AND (LIMIT-TO (DOCTYPE , "ar"))

*Research articles shown in query searches 4, 5 and 6 were checked one by one whether if the study is a thermophilic or hyperthermophilic bioelectrochemical system application.

Table A.1. Number of research articles investigating bioelectrochemical systems in Figure 2.1

	2004	**2005**	**2006**	**2007**	**2008**	**2009**	**2010**	**2011**	**2012**
(1) MFC	14	22	36	61	179	205	269	332	348
(2) MEC					2	11	25	39	33
(3) MES								1	2
(4) MFC	1		1		2	1		2	2
(5) MEC						1			
(6) MES									
	2013	**2014**	**2015**	**2016**	**2017**	**2018**	**2019**	**2020**	**2021**
(1) MFC	484	498	599	673	778	733	810	824	661
(2) MEC	41	52	71	60	74	58	86	79	79
(3) MES	2	7	5	12	23	29	26	35	41
(4) MFC	1		2		1		1		1
(5) MEC	2		2	1	4	3	2	2	
(6) MES					3	1		1	

Figure 2.10/Figure 2.12 The evolutionary history was inferred by using the Maximum Likelihood method and Jukes-Cantor model [1]. For Figure 2.5, the tree with the highest log likelihood (-4553.67) is shown.. The percentage of trees in which the associated taxa clustered together is shown next to the branches. Initial tree(s) for the heuristic search were obtained automatically by applying Neighbor-Join and BioNJ algorithms to a matrix of pairwise distances estimated using the Jukes-Cantor model, and then selecting the topology with superior log likelihood value. This

analysis involved 7 nucleotide sequences. There were a total of 1262 positions in the final dataset.

Selected methods and parameters are identical in both figures. Figure 2.6, the tree with the highest log likelihood (-3108.74) is shown. Analysis involved 4 nucleotide sequences. There were a total of 1394 positions in the final dataset.

Codon positions included were 1st+2nd+3rd+Noncoding. All positions with less than 95% site coverage were eliminated, i.e., fewer than 5% alignment gaps, missing data, and ambiguous bases were allowed at any position (partial deletion option). Before constructing the phylogeny tree, DNA codons were aligned using MUSCLE Multiple Sequence Aligment method with a gap opening of -400.00 and maximum iteration of 16. Evolutionary analyses were conducted in MEGA X [2].

1. Jukes T.H. and Cantor C.R. (1969). Evolution of protein molecules. In Munro HN, editor, *Mammalian Protein Metabolism*, pp. 21-132, Academic Press, New York.

2. Kumar S., Stecher G., Li M., Knyaz C., and Tamura K. (2018). MEGA X: Molecular Evolutionary Genetics Analysis across computing platforms. *Molecular Biology and Evolution* 35:1547-1549

B. Supplementary information for Figures in Chapter 4

Table B.1 Sources for the exoelectrogenic culture compared in Figure 4.5

Exoelectrogenic culture	**Reference Article**
Thermincola ferriacetica[2]	(Parameswaran et al., 2013)
Bacteroides genus	(Shehab et al., 2017)
Archaeoglobales and *Thermococcales*	(Pillot et al., 2018)
Pyrococcus furiosus	(Sekar et al., 2017)
Geoglobus acetivorans	This study
Calditerrivibrio nitroreducens related specie	(Fu et al., 2013)
Thermodesulfobacterium commune related isolate	(Fu, Kuramochi, et al., 2015)
Ferroglobus placidus	(Yilmazel et al., 2018)
Thermincola potens	(Wrighton et al., 2008)
Calditerrivibrio nitroreducens	(Fu et al., 2013)
Geoglobus ahangari	(Yilmazel et al., 2018)
Ureibacillus sp.	(Dessì et al., 2019)
Thermincola ferriacetica[1]	(Marshall & May, 2009)
Thermincola sp.	(Mathis et al., 2008)

C. Sample Calculation for Hydrogen Production Rate (Q_{H2})

Table C.1 Peak current production data for a reactor in AT set

I (mA)	t (d)	I (mA)	t (d)
0.706	37.87	0.724	37.87
0.697	37.88	0.743	37.96
0.716	37.88	0.726	37.97
0.705	37.87	0.728	37.87
0.705	37.89	0.733	37.97
0.716	37.90	0.729	37.98
0.720	37.87	0.734	37.87
0.710	37.90	0.736	37.99
0.708	37.91	0.736	37.99
0.699	37.87	0.731	37.87
0.723	37.92	0.727	38.00
0.724	37.92	0.737	38.01
0.716	37.87	0.730	37.87
0.721	37.93	0.739	38.01
0.719	37.94	0.727	38.02
0.713	37.87	0.722	37.87
0.718	37.94	0.722	37.88
0.729	37.95	0.719	37.88

$\boldsymbol{I_{avg}} = 0.722\ mA$ (over the course of 6 hours of peak current production)

$$\boldsymbol{I_V} = \frac{\boldsymbol{I_{avg}}}{\boldsymbol{V_R}} = \frac{0.722\ mA}{5 * 10^{-6}\ m^3} = 144.33 \frac{A}{m^3}$$

$r_{cat} = 0.290$

$$Q_{H_2} = \frac{43.2\ I_V\ r_{cat}}{F\ c_g(T)}\ \frac{43.2 \cdot I_V \cdot r_{cat} \cdot R\ T(K)}{F \cdot P}$$

$$= \frac{\left(86400 \frac{s}{d} \cdot 0.5\ \frac{mol\ H_2}{mol} \cdot \frac{10^{-3} L}{m^3}\right) \cdot 144.33 \frac{A}{m^3} \cdot 0.290\ \left(\frac{C}{A \cdot s^{-1}}\right) \cdot 0.082 \left(\frac{L \cdot atm}{K \cdot mol}\right) \cdot 353.15K}{96500 \frac{C}{mol} \cdot \frac{mol\ H_2}{L} \cdot 1\ atm}$$

$$Q_{H_2} = 0.54\ \frac{\mathrm{m^3 H_2}}{\mathrm{m^3\ active\ volume\ .\ day}}$$